Aus dem Pharmakologischen Institut
Geschäftsführender Direktor: Prof. Dr. Thomas Worzfeld
des Fachbereichs Medizin der Philipps-Universität Marburg

The glucocorticoid receptor regulates epithelial plasticity in the kidney

Dissertation zur Erlangung des Doktorgrades
der Naturwissenschaften
des Fachbereichs Medizin
der Philipps-Universität Marburg

vorgelegt von
Luping Zhou
aus der Provinz Sichuan,
Volksrepublik China

Marburg, 2022

Angenommen vom Fachbereich Medizin der Philipps-Universität Marburg am: 18.02.2022

Gedruckt mit Genehmigung des Fachbereichs Medizin

Dekanin: Prof. Dr. D. Hilfiker-Kleiner

Referent: Prof. Dr. T. Worzfeld

1. Koreferent: Prof. Dr. I. Grgić

2. Koreferen:

Contents

Contents **3**

1. ABBREVIATIONS **6**

2. LIST OF FIGURES **8**

3. INTRODUCTION **9**

3.1 Glucocorticoid receptor 9

3.1.1 Structural characteristics of the glucocorticoid receptor 9

3.1.2 Ligands of the glucocorticoid receptor 10

3.1.3 Activation of the glucocorticoid receptor 12

3.2 Functions of glucocorticoids and the glucocorticoid receptor in development, homeostasis and disease 15

3.2.1 Development of the nervous system 15

3.2.2 Immune system 16

3.2.3 Cardiovascular system 18

3.2.4 Respiratory system 19

3.2.5 Gastrointestinal system 20

3.2.6 Kidney development and diseases 21

3.3 Cellular plasticity after acute kidney injury 22

4. AIM OF THE THESIS **25**

5. MATERIALS AND METHODS **26**

5.1 Antibodies and reagents 26

5.2 qPCR 27

5.2.1 RNA isolation 27

5.2.2 cDNA and quantitative PCR (qPCR) 28

5.2.3 Primers for qPCR (relative quantification) 28

5.3 Western blotting 29

5.3.1 Cell lysate preparation 29

5.3.2 Western blotting materials 29

5.4 HK2 cell line 30

5.4.1 HK2 cell culture 30

5.4.2 HK2 cell transfection and transient knockdown 30

5.5 mIMCD3 cell line 31

5.5.1 mIMCD3 cell culture 31

5.5.2 mIMCD3 cell transfection and transient knockdown 31

5.6 Human 32

Human tubuloid culture 32

5.7 Mice and methods using murine kidney tissue 33
5.7.1 Mouse kidney tubuloid culture 34
5.7.1.1 Dexamethasone treatment 35
5.7.1.2 Myoglobin treatment 35
5.7.1.3 Tubuloid number and normalization 35
5.7.2 Tubuloid damage score 36
5.7.3 FACS 36
5.7.4 Sea horse analysis of tubuloids 37
5.7.4.1 Glycolytic stress assay 37
5.7.4.2 Mito stress assay 40
5.7.5 Tubuloids immunofluorescence staining 42
5.7.6 Tubuloids mitotracker staining 42
5.8 Conditioned medium 43
5.8.1 Wnt3a conditioned medium 43
5.8.2 R-sponding-1 conditioned medium 44

6 RESULTS 46
6.1 Cellular plasticity in renal tubuloids of mice 46
6.2 Dexamethasone impacts the dedifferentiation and redifferentiation of tubuloids 48
6.2.1 Dexamethasone treatment from day1 onwards suppresses the formation of cuboidal tubuloids 48
6.2.2 Dexamethasone treatment from day3 onwards has no effect on tubuloid numbers and efficiency of formation of cuboidal cells 50
6.2.3 Dexamethasone treatment affects the expression of sox9 and vimentin in tubuloids 51
6.2.4 Dexamethasone treatment affects the expression of differentiation markers in tubuloids 52
6.2.5 Dexamethasone treatment inhibits the formation of human tubuloids 54
6.3 Dexamethasone aggravates myoglobin-induced injury of tubuloids 55
6.3.1 Dexamethasone treatment aggravates damage of mouse tubuloids 55
6.3.2 Dexamethasone treatment aggravates the damage of human tubuloids 56
6.3.3 Glucocorticoid receptor deficiency promotes mitochondrial respiration of tubuloids. 57
6.3.4 Deficiency of glucocorticoid receptor promotes the expression of enzymes of respiration of tubuloids 59
6.3.5 Deficiency of glucocorticoid receptor alterates the mitochondrial membrane potential in tubuloids 61
6.3.6 Inhibition of glycolysis has no major impact on the viability of GR-deficient tubuloids 61
6.3.7 Inhibition of oxidative phosphorylation lowers viability of GR-deficient tubuloids 62
6.4 The regulation of the mTOR pathway by GR is functionally relevant for tubuloid injury 64
6.4.1 Dexamethasone potentially inhibits the mTOR pathway activity in kidney

cell lines 64
6.4.2 Glucocorticoid receptor deficiency promotes the activation of the mTOR pathway 65
6.4.3 mTOR activation in GR-deficient tubuloids is crucial for resistance to injury 66
6.5 GR signaling suppresses epithelial plasticity by inhibition of the Wnt/β-catenin pathway 68
6.5.1 Activation of the Wnt pathway rescues the suppressive effect of dexamethasone on tubuloid formation 68
6.5.2 Dexamethasone treatment suppresses the Wnt/β-catenin pathway 70
6.5.3 CHIR treatment promotes the expression of dedifferentiation marker of tubuloids 73
6.5.4 CHIR treatment promotes redifferentiation of tubuloids 74

7 DISCUSSION 77
7.1 Origin of regenerating tubular epithelial cells after acute kidney injury 77
7.1.1 Regeneration by surviving tubular epithelial cells 77
7.1.2 Regeneration by scattered progenitor epithelial cells 78
7.2 Cellular plasticity of tubuloids 80
7.3 Role of glucocorticoid receptor in acute kidney injury 81
7.4 Role of metabolism in cellular plasticity of renal epithelial cells 81
7.5 Connection between mTOR pathway and GR signaling in renal epithelial cells 83
7.6 Connection between Wnt/β-catenin pathway and GR signaling in renal epithelial cells 85

8 REFERENCES 87

9 SUMMARY 102

10 ZUSAMMENFASSUNG 104

11 CURRICULUM VITAE 106

12 LEBENSLAUF 107

13 AKADEMISCHE LEHRER 108

14 ACKNOWLEDGEMENTS 109

15 Ehrenwörtliche Erklärung 111

1. ABBREVIATIONS

2-DG	2-Deoxy-D-glucose
AKI	Acute kidney injury
ATCC	American Type Culture Collection
apo-GR	inactive glucocorticoid receptor in a ligand-unbound state
BP	blood pressure
BSA	bovine serum albumin
BrdU	bromodeoxyuridine
BLM	basolateral membrane
CHIR	CHIR99021
CTL	control
DBD	DNA-binding domain
dex	dexamethasone
ECM	extracellular matrix
EGFR	epidermal growth factor receptor
ECAR	extracellular acidification rate
g	gram
GRE	glucocorticoid response element
GILZ	glucocorticoid-induced leucine zipper
GR	glucocorticoid receptor
GCs	glucocorticoids
HK2 cell line	human kidney proximal tubular epithelial cell line
HSP	heat-shock protein
HC	hydrocortisone
HPA	hypothalamic–pituitary–adrenal
hk2	hexokinase 2
IF	immune fluorescence
ICAM-1	intercellular adhesion molecule-1
IRI	ischemia-reperfusion injury
KO	knockout
Klf	Krüppel-like factor
l	liter
LFA1	lymphocyte function-associated antigen 1
LTL	lotus tetragonolobus lectin
LBD	ligand-binding domain
MAPK	mitogen-activated protein kinase
mIMCD-3 cell line	mouse inner medullary collecting duct-3 cell line
ml	milliliter
min	minutes

myo	myoglobin
Ncam-1	neural cell adhesion molecule 1
Nr3c1	nuclear receptor subfamily 3, group C, member 1
NF-κB	nuclear factor kappa-light-chain-enhancer of activated B cells
NDUFB6	oxidoreductase subunit B6
OCR	oxygen consumption rate
OXPHOS	oxidative phosphorylation
oligo	Oligomycin A
PFA	paraformaldehyde
PCR	polymerase chain reaction
PCNA	proliferating cell nuclear antigen
pfkp	phosphofructokinase, platelet
pfkfb3	6-phosphofructo-2-kinase/fructose-2,6-biphosphatase 3
PGC-1	peroxisome proliferator-activated receptor, gamma (PPARG), coactivator 1
qPCR	quantitative polymerase chain reaction
rTECs	renal tubular epithelial cells
RT	Room temperature
Rapa	rapamycin
Sox9	transcription factor SOX-9
$Sox9^{IE}$ mice	$Sox9^{IRES\text{-}EGFP}$ mice
TECs	tubular epithelial cells
TLR	Toll-like receptor
TNF	Tumor necrosis factor
VCAM-1	vascular cell adhesion molecule-1
tfam	transcription factor A, mitochondrial
vim	vimentin
vim-EGFP mice	Tg (Vim-EGFP) GM158Gsat/Mmucd mice
VSMC	vascular smooth muscle cells
WB	western blot
°C	degree Celsius
µ	micro

2. LIST OF FIGURES

Fig. 1	Synthesis and activation of endogenous glucocorticoids……...11
Fig. 2	Structure and genomic signaling of glucocorticoid receptor (GR)…….14
Fig. 3	Interaction of immune systerm and hypothalamic–pituitary–adrenal (HPA) axis……..17
Fig. 4	Dedifferentiation in the repair process of the renal tubular epithelium after acute kidney injury……23
Fig. 5	Cellular plasticity in renal tubuloids of mice……..47
Fig. 6	Dexamethasone treatment from day1 onwards suppresses the formation of cuboidal tubuloids……49
Fig. 7	Dexamethasone treatment from day3 onwards has no effect to the tubuloid numbers and efficiency of formation of cuboidal tubuloids…….50
Fig. 8	Dexamethasone treatment affects the expression of sox9 and vimentin in tubuloids……..52
Fig. 9	Dexamethasone treatment affects the expression of differentiation markers in tubuloids…….53
Fig. 10	Dexamethasone treatment inhibits the formation of human tubuloids….54
Fig. 11	Dexamethasone treatment aggravates the damage of mouse tubuloids.56
Fig. 12	Dexamethasone treatment aggravates the damage of human tubuloids.57
Fig. 13	Knockout of the glucocorticoid receptor promotes mitochondrial respiration of tubuloids …….....59
Fig. 14	Deficiency of glucocorticoid receptor promotes the expression of enzymes of respiration of tubuloids…….....60
Fig. 15	Knockout of glucocorticoid receptor alters the mitochondrial membrane potential in tubuloids……61
Fig. 16	Inhibition of glycolysis has no major impact on the viability of GR-deficient tubuloids……62
Fig. 17	Inhibition of oxidative phosphorylation lowers viability of GR-deficient tubuloids……63
Fig. 18	Dexamethasone potentially inhibits mTOR pathway activity in kidney cell lines……65
Fig. 19	Deficiency of glucocorticoid receptor promotes the activation of the mTOR pathway……..66

Fig. 20	mTOR activation in GR-deficient tubuloids is crucial for resistance to injury……67
Fig. 21	Activation of the Wnt pathway rescues the suppressive effect of dexamethasone on tubuloid formation……..69
Fig. 22	Dexamethasone treatment partially inhibits CHIR-induced activation of the Wnt/β-catenin pathway……71
Fig. 23	Dexamethasone treatment partially suppresses Wnt3a-induced activation of the Wnt/β-catenin pathway……72
Fig. 24	Dexamethasone treatment might reduce protein expression of β-catenin……73
Fig. 25	CHIR treatment promotes the expression of dedifferentiation marker of tubuloids……74
Fig. 26	CHIR treatment from day 1 onwards promotes redifferentiation of tubuloids……75
Fig. 27	CHIR treatment from day3 increases redifferentiation of tubuloids……..76
Fig. 28	Binding of glucocorticoid receptors to the regulatory element next to Havcr1 is modulated by injury……..82

3. INTRODUCTION

3.1 Glucocorticoid receptor

3.1.1 Structural characteristics of the glucocorticoid receptor

The glucocorticoid receptor (GR) is encoded by the gene “nuclear receptor subfamily 3 group C member 1” (NR3C1), which consists of nine exons (Hollenberg et al., 1985). Exon 1 is an untranslated region, exon 2 encodes for the amino-terminal domain (NTD), exon 3 and 4 for the DNA-binding domain (DBD), and exons 5-9 for the hinge region and the ligand binding domain (LDB) (Nicolaides et al., 2000).The alternative splicing of exon 9 leads to two isoforms, termed GRα and GRβ (R. H. Oakley et al., 1996).

The NTD of human GRα corresponds to amino acids 77 to 262 and contains the major transactivation domain, termed activation function (AF)-1 (also called τ1) domain (Fig. 2) (Almlöf et al., 1997; Almlöf et al., 1998). The AF-1 domain has been shown to play an important role in the interaction between the receptor and other proteins necessary for the initiation of transcription, including coactivators, chromatin modulators and transcription factors (Wärnmark et al., 2000). The AF-1 domain of GRα forms α-helices to interact with other transcription factors, including the TATA box binding protein (TBP) (Kumar et al., 2004) and p160 coactivator TIF2 (Khan et al., 2012), in response to ligand binding. TBP-induced conformational changes in AF-1 form the basis for the multiprotein transcription initiation complex (Khan et al., 2012). All of the phosphorylation sites of GRα are located

in the NTD (Chrousos et al., 2005; Ismaili et al., 2004). Classically, GRa is phosphorylated after binding to its ligand and this may determine target promoter specificity, cofactor interaction, strength and duration of receptor signaling and receptor stability (Ismaili et al., 2004; Ortí et al., 1993).

The DBD of human GRα corresponds to amino acids 420 to 480 and contains two cysteine 4 -type zinc finger (Fig. 2); it helps GRα to bind to specific glucocorticoid-responsive elements (GREs) (Nicolaides et al., 2000).

The LBD of human GRa corresponds to amino acids 527-777 and contains 11 α-helices and 4 small β-strands that fold into a three-layer helical domain with an overall organization (Fig. 2) (Bledsoe et al., 2002). Without ligand, interaction of the LBD with the heat shock protein (HSP) 90 contributes to the maintenance of the protein structure that allows LBD to bind with ligand (Nicolaides et al., 2000). Induced by ligand binding, two GR monomers are arranged in a unique dimer configuration (Bledsoe et al., 2002). In addition, dimer configuration in the LBD allows GRα to interact with several molecules, such as chaperones, coregulators, and other transcription factors that mediate the ligand-dependent actions of GRα (Nicolaides et al., 2000). (Mcmaster et al., 2008). The LBD of human GRα contains two ligand-dependent transactivation domains, including the AF-2 and tau2 (τ2) (Vandevyver et al., 2014; L. Yang et al., 2000). AF-2 is located near the C terminus of of human GRα and interacts with nuclear receptor coactivators, such as TIF2, which can also bind to and transactivate the N-terminal AF1 (Benecke et al., 2000; Weikum et al., 2017). Interaction of τ2 and coactivator hydrogen peroxide–inducible clone-5 (Hic-5), which is located at both focal adhesions and the nuclear matrix, may transmit signals from cell attachment sites to nuclei and modulate transcriptional responses (L. Yang et al., 2000).

3.1.2 Ligands of the glucocorticoid receptor

The ligands of the GR include endogenous glucocorticoids (GCs) and synthetic GCs. Endogenous GCs (such as cortisol in man and corticosterone in rodents) are mainly synthesized and secreted by the adrenal gland based on the hypothalamic-pituitary-adrenal (HPA) axis (Fig. 1) (Henrik et al., 2017; Wepler et al., 2020). Interestingly, local production of GCs has also been reported in the thymus, intestine and skin (Talabér et al., 2013). Activation of the HPA axis induces the synthesis and secretion of endogenous GCs, while increased blood concentrations of endogenous GCs would inhibit the activation of the HPA axis and decrease the synthesis and secration of endogenous GCs. Physiologically, activation of the HPA axis is modulated by the circadian rhythm (light-dark stimulation received by the hypothalamus), which promotes adaptation to the external

environment with changes of behavior rhythms, including the sleep-wake and feeding cycles (Henrik et al., 2017). Stimulation of stress and cytokines can also induce the activation of the HPA axis and promote the production of endogenous GCs (Quatrini et al., 2021). The local availability of endogenous GCs is modulated by two isozymes of 11beta-hydroxysteroid dehydrogenase (11-β HSD), including type 1 of 11beta-HSD (11-β HSD1) and type 2 of 11beta-HSD (11-β HSD2) (Fig. 1) (Draper et al., 2005; Stewart et al., 1999; H. Zhou et al., 2013). As studies have shown, cellular 11-β HSD1 catalyzes the inactive cortisone and 11-dehydrocorticosterone into active cortisol and corticosterone, in human and rodents respectively (Wepler et al., 2020; H. Zhou et al., 2013). Local cytokines promotes the activity of cellular 11-β HSD1 and increases the local availability of endogenous GCs (Webster et al., 2001). However, dysfunction of 11-β HSD1 may be involved in the resistance to GCs. Contrary to 11-β HSD1, cellular 11-β HSD2 promotes the conversion of active GCs into inactive metabolites (Wepler et al., 2020; H. Zhou et al., 2013).

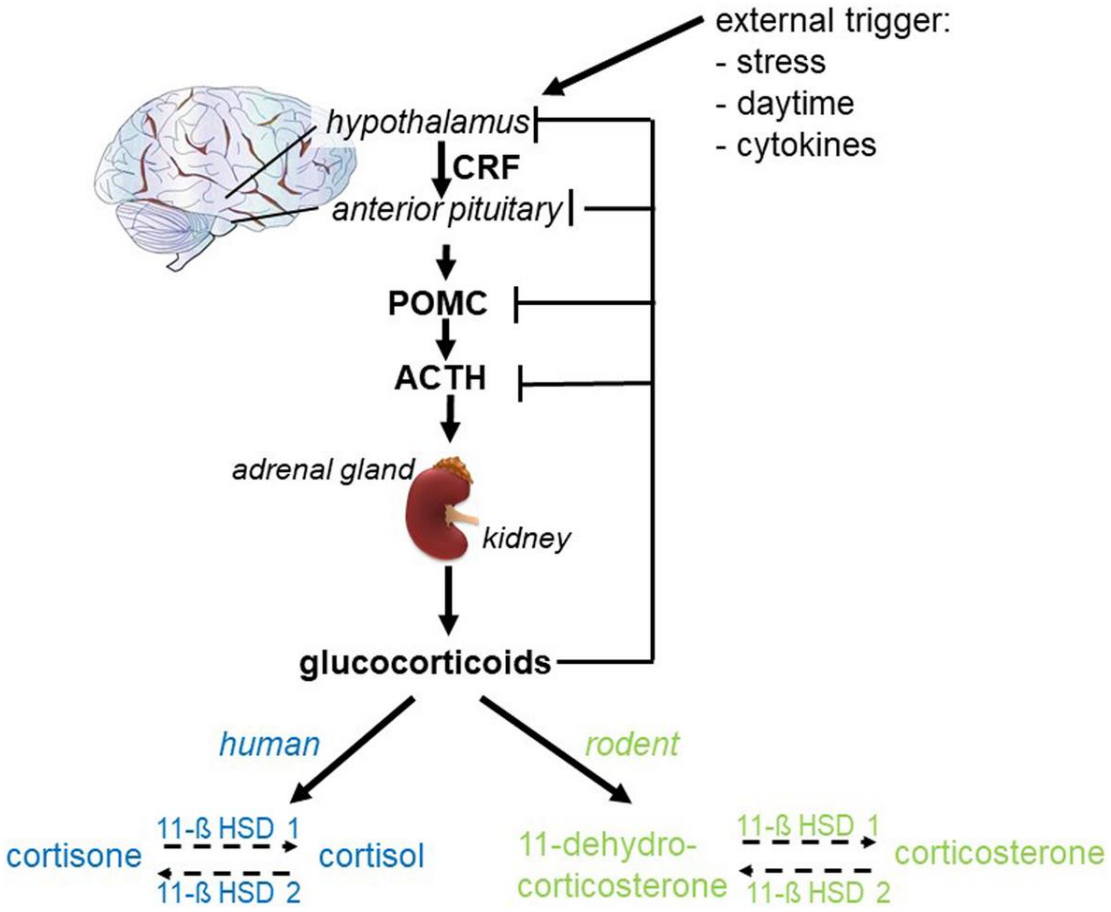

Fig. 1. Synthesis and activation of endogenous glucocorticoids. Stimulation of external triggers (including stress, light-dark, and cytokines) induces the activation of the hypothalamic-pituitary-

adrenal (HPA) axis. Correspondingly, the hypothalamus secretes more corticotropin-releasing factor (CRF), which acts on the anterior pituitary and promotes the secretion of proopiomelanocortin (POMC), which is proteolytically cleaved into adrenocorticotropic hormone (ACTH). ACTH acts on adrenal glands to promote the synthesis and secretion of endogenous glucocorticoids (GCs). Increased circulating GCs inhibit the continuous activation of the HPA axis in a negative feedback mode. Within particular tissues, 11beta-hydroxysteroid dehydrogenase type 1 (11-β HSD1) catalyzes the formation of active cortisol and corticosterone from inactive cortisone and 11-dehydrocorticosterone, in human and rodents respectively. Conversely, 11-β HSD2 promotes the metabolization of active cortisol and corticosterone into inactive metabolites, in human and rodents respectively. (Wepler et al., 2020)

Because of the close phylogenetic homology between steroid receptors, such as the GR and the mineralocorticoid receptor, endogenous glucocorticoids can bind to and activate both receptors, which contributes to side effects and adverse reactions of chronic therapy (e.g. hypertension) (Mcmaster et al., 2008). To optimize the therapeutic potential and to minimize adverse reactions, synthetic glucocorticoids have been synthesized, which bind selectively to the GR only (Mcmaster et al., 2008), e.g. beclomethasone and fluticasone (Patrick, 2013). Nevertheless, long-term regular use of GCs above a threshold dose typically results in pleiotropic side effects, including fat redistribution and osteoporosis.

3.1.3 Activation of the glucocorticoid receptor

GRα represents the classic GR, which is located in the cytoplasm when not bound to ligands; when activated by ligands, it translocates into the nucleus to act as a ligand-dependent transcription factor (R. H. Oakley et al., 1996). Human GRβ, in contrast, does not bind glucocorticoids and competes at the glucocorticoid response element (GRE) sites with GRα (Bamberger et al., 1995). In the absence of ligands, GRα is predominantly monomeric (also called apo-GRα) and forms complexes with molecular chaperones, such as HSP90 in the cytoplasm (Picard et al., 1990). The interaction of HSP90 and apo-GRα promotes a high affinity of apo-GRα to GCs (Picard et al., 1990; Weikum et al., 2017). Binding of GCs to GRα promotes allosteric changes of GRα, which in turn trigger the release of HSPs, the formation of GRα homodimers and the translocation of GR from the cytoplasm to the nucleus (Fig. 2) (R. H. Oakley et al., 2013; Weikum et al., 2017). Within the nucleus, binding of GRα to different GREs induces multiple transcriptional effects. For example, binding of the GR to the promoter/enhancer of specific genes, such as mitogen-activated kinase phosphatase (MAPK)-1(Lasa et al., 2002) and secretory leukocyte proteinase inhibitor (Abbinante-Nissen et al., 1995), induces the transactivation of these genes. Binding of GRα to transrepression GREs of genes, such as in genes encoding pro-

inflammatory transcription factors (Ito et al., 2006), triggers the repression of these genes. Moreover, the GR can repress transcription by tethering itself to other transcription factors, such as NF-κB (Kadmiel et al., 2013). Interestingly, multiple nuclear receptor co-regulator proteins determine the precise regulation of GRα genomic signaling. For example, the interaction of GR and the coactivator Hic-5 can transmit signals from the cell membrane to nuclei and control GR signal responses to the specific environment of the cell (L. Yang et al., 2000). Another nuclear receptor coactivator, TIF2, can bind both N-terminal AF1 and C-terminal AF2, and controls GRE binding of the GR (Benecke et al., 2000) (Weikum et al., 2017). In addition to translocating into the nucleus, ligand-bound GRα has been reported to translocate into mitochondria to have a direct action on mitochondrial transcription (Psarra et al., 2011). Interestingly, translocation of GRα into lysosomes triggers the negative regulation of its transcriptional activity (Nicolaides et al., 2000).

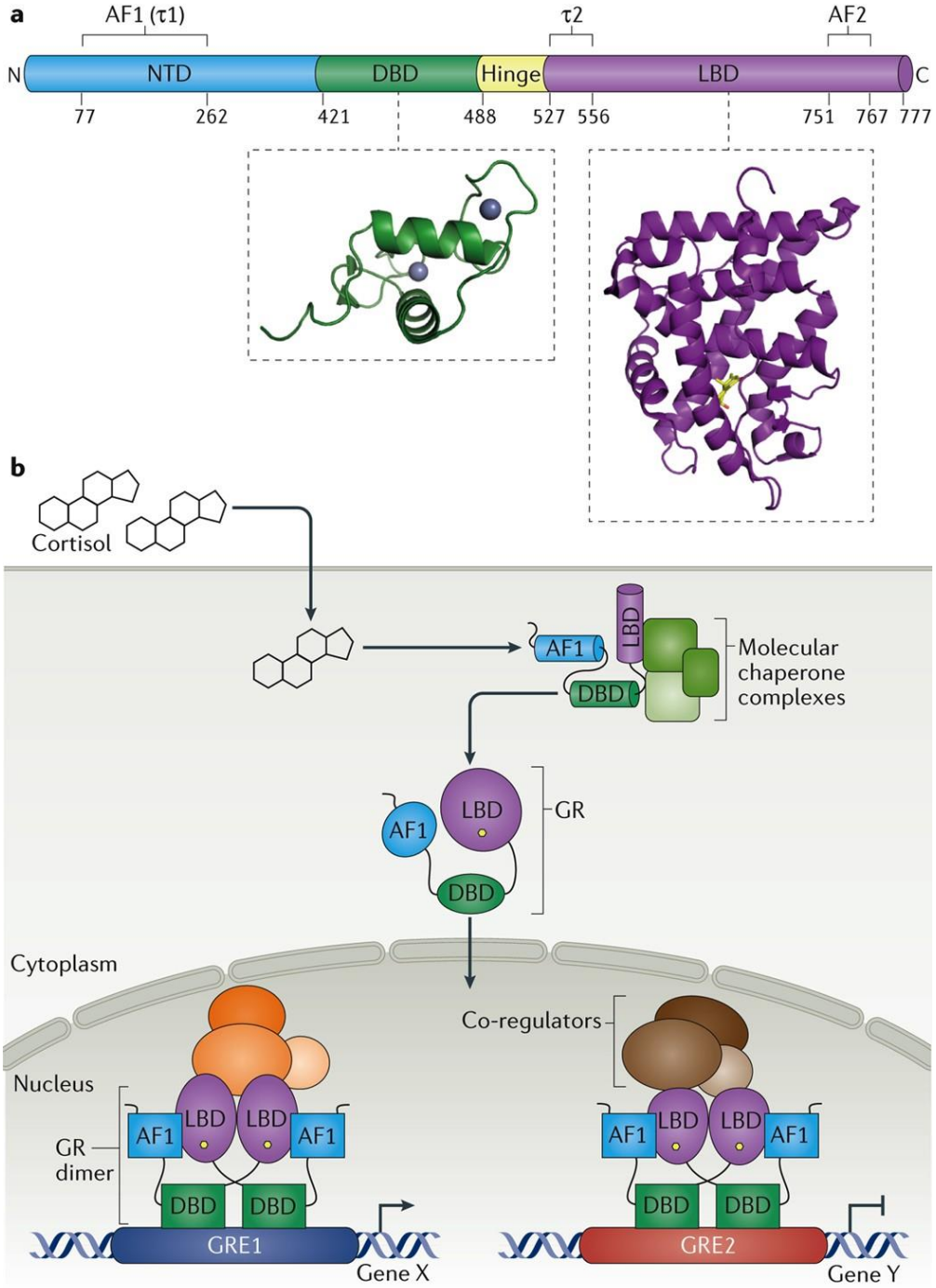

Fig. 2. Structure and genomic signaling of the glucocorticoid receptor (GR). a. The functional domains of the GR comprise the amino-terminal domain (NTD), DNA-binding domain (DBD), hinge region and the ligand binding domain (LDB). Special regions within the domains, including activation function domain 1 (AF1, τ1), tau2 (τ2) and AF2, are responsible for transcriptional regulation. Inserts: A single DBD is shown by green crystal structures, with coordinated zinc ions shown as grey spheres. Cortisol (shown by yellow spheres) binds to LBD (shown by purple crystal structure) region. b. Interaction between activated ligands, monomeric GR and associated molecular chaperone complexes promotes the allosteric changes of GR, which in turn triggers the translocation of GR from cytoplasm to nucleus. Within the nucleus, binding of GR dimers and different glucocorticoid

response elements (GREs) induces activation or repression of transcription of target genes. (Weikum et al., 2017)

3.2 Functions of glucocorticoids and the glucocorticoid receptor in development, homeostasis and disease

As a ubiquitously expressed transcription factor, GR controls many different gene networks, each uniquely determined by the particular cell type and physiological state (Weikum et al., 2017). For example, in adipocytes, activation of the GR by GCs increases the differentiation, adipogenesis and lipolysis (Patel et al., 2014). In mice, global GR deficiency leads to rapid neonatal death, which indicates the crucial role of GR in the development of organs (Cole et al., 1995). GR target genes are involved in major physiological processes, including metabolic, cognitive and immune processes, and these pathways are necessary for life after birth (Cole et al., 1995). Here, I would like to summarize the functions of GCs and GR in selected main organ systems.

3.2.1 Development of the nervous system

Abundant evidence has shown that GCs are crucial to neural tissues and affect brain development, behavior, and the HPA axis (Gould, 1994; Gould et al., 1991; Kapoor et al., 2006; Matthews, 2000; Vielkind et al., 1990). In rats, fetal exposure to synthetic GCs results in hyperactivity of the HPA axis in adult offspring, which may directly or indirectely lead to altered hippocampal development (Matthews, 2000). Prenatal corticosterone treatment results in sex- and age-specific alterations in behavior in adult offspring (Diaz et al., 1997). Daily dex treatment (0.1 mg/kg) of pregnant rats during the last week of gestation can significantly change sexual behavior of the offspring, such that male offspring became demasculinized and feminized (Holson et al., 1995). In mice, prenatal prednisone exposure results in delayed development of behaviors and actions associated with neurodevelopment, including eye opening, lifting, walking, and gripping in offspring (Gandelman et al., 1981). On gestational day 14 of pregnant mice, even one dose of betamethasone (0.10 mg) induces decreased anxiety of offspring, while one dose dex (0.10 mg) increases separation anxiety in the perinatal period of the offspring (Rayburn et al., 1997). In the brain of rodents, GR is detected in neurons and glial cells (de Kloet et al., 2005; Reul et al., 1985). Aberrant GR expression in the brain has been implicated in stress resistance, anxiety, and depressive disorder (Alt et al., 2010; de Kloet et al., 2005; Ridder et al., 2005; Wang et al., 2012; Wei et al., 2007). Knockdown of GR expression in mice (GR-heterozygous mutant mice, which have 50% GR gene expression reduction) results in increased helplessness after stress exposure, while overexpression of the GR partially

rescues this phenotype and enhances secretion of endogenous GCs when facing to stressors (Ridder et al., 2005).

In pregnant rhesus monkeys, intramuscular administration of dex induces dose-dependent degeneration of the hippocampal structure (Uno et al., 1990). In humans, a number of studies have established the long-term effects of GC exposure in children born before term on learning, behavior, and intelligence (MacArthur et al., 1981, 1982; Salokorpi et al., 1997; Smolders-de Haas et al., 1990). For these premature babies who are already at risk of varying degrees of delayed neurologic development (Breslau et al., 1996; Dammann et al., 1996; Goldenberg et al., 1996; McCarton et al., 1996), administration of synthetic GCs has no overall neurologic delay or impairment in late gestation (MacArthur et al., 1981, 1982; Salokorpi et al., 1997; Smolders-de Haas et al., 1990). However, reduced visual closure and visual memory was observed in 6-year-old children who had been exposed to antenatal GC administration (MacArthur et al., 1982). All of these studies indicate the exposure of GCs at early stages has profound effects on the development of the nervous system.

3.2.2 Immune system

Studies have shown that not only circadian cues (also called dark-light cues) and stress, but also pro-inflammatory cytokines, such as Interleukin (IL)-1, IL-6 and tumor necrosis factor (TNF)α, can trigger the activation of the HPA axis and promote the biosynthesis of glucocorticoids in the adrenal gland (Fig. 3) (Cain et al., 2017). GCs, in turn, can surpress an overraction of the immune systerm (Fig. 3) (Cain et al., 2017). A homeostatic balance between the immune system and the HPA axis is therefore of crucial importance. For example, Cushing's syndrome, or chronic hypercortisolism, induces a variety of alterations in the immune system, sometimes leading to severe clinical complications such as sepsis and opportunistic infections (Hasenmajer et al., 2020). In Addison disease, or chronic GC deficiency, patients also suffer from an immune system defect, which makes them prone to potentially deadly infections (Bancos et al., 2017).

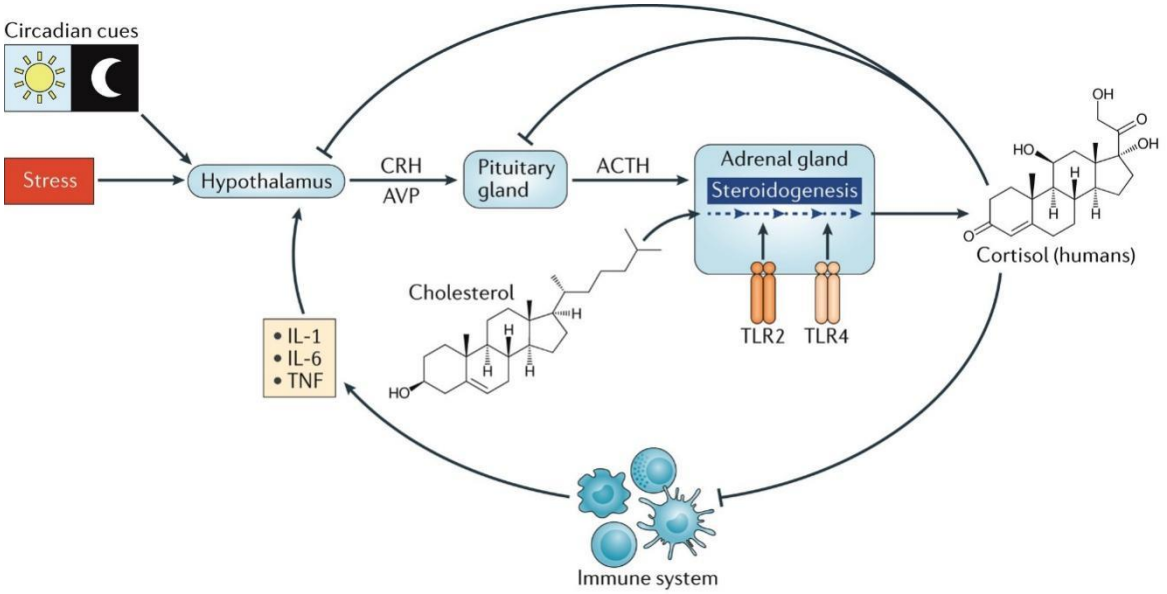

Fig. 3. Interaction of the immune systerm and the hypothalamic–pituitary–adrenal (HPA) axis. In humans, activation of the immune system (infection) triggers the release of pro-inflammatory cytockines, such as interleukin-1 (IL-1), IL-6 and tumor necrosis factor α (TNFα), which can activate the hypothalamic–pituitary–adrenal (HPA) axis, and promote the steroidogenesis in the adrenal gland. Glucocrticoids, can in turn surpress an overraction of the immune system. (Cain et al., 2017)

After the potent anti-inflammatory effects were revealed, GCs were widely used in the clinic to treat inflammatory conditions, e.g. in the skin or the lung (Busillo et al., 2013). An abundant number of studies have focused on the mechanisms through which GCs regulate inflammation (Beck et al., 2009; A. R. Clark et al., 2012; Quax et al., 2013), including the dilation of local blood vessels, vascular permeability and the leakage of plasma into tissue (Cain et al., 2017). In the alarm phase of the inflammatory response, GCs inhibit transmission of 'danger' signals and release of inflammatory mediators (Cain et al., 2017) by suppressing the activity of NF-κB (Cain et al., 2017; Scheinman et al., 1995) and activator protein 1 (Busillo et al., 2013). Importantly, many of the signaling pathways of proinflammatory regulators are targeted by GCs. For example, GC treatment attenuates the release of histamine of mast cells via inhibition of the signal transduction of Fcε receptors (Oppong et al., 2013). In addition, binding of GCs to the GR increases the expression of annexin A1, which interferes with the release of arachidonic acid, a fatty-acid intermediate of eicosanoid biosynthesis (S.-W. Kim et al., 2001). GC treatment can increase the expression of angiotensin-converting enzyme and endothelin, rendering endothelial cells more sensitive to vasoconstrictors and suppressing the release of vasodilators to reduce blood flow to inflammatory sites (PERRETTI et al., 2000). In addition, GC treatment markedly attenuates the subsequent adherence of leukocytes to

endothelial cells via surpression of the expression of adhesion molecules, such as vascular cell adension molecule-1 (VCAM-1) and intercellular adhesion molecule-1 (ICAM-1) (Atsuta et al., 1999; Cronstein et al., 1992). In mouse models of multiple sclerosis, GR deficiency in T cells, but not in myeloid cells, results in resistance to dex treatment, indicating that the main effects of GCs are on T cells (Wüst et al., 2008). Furthermore, GC administration reduces the adhesion of T cells and endothelial cells via decreasing the expression of cell adhesion molecules (such as lymphocyte function-associated antigen 1 and very late antigen 4) in T cells (Wüst et al., 2008), and impedes neutrophil recruitment via an induction of annexin A1 (Perretti et al., 2004). Besides of that, ligand-bound GR can directly bind to chemokine-encoding mRNA transcripts, and promote the decay of chemokines (Ishmael et al., 2011). In the resolution phase of the inflammatory response, GCs along with lipoxins, resolvins, collectins and protectins, modulate the clearance of cellular debris and the production of anti-inflammatory factors (Serhan et al., 2005). GCs initiate gene programmes in monocytes and macrophages and promote the phagocytosis of apoptotic cells and debris (Ehrchen et al., 2006; Giles et al., 2001; Liu et al., 1999; Martinez et al., 2008). GCs can also sensitize cells to other pro-resolving factors through the upregulation of the lipoxin A4 receptor (Perretti et al., 2002).

3.2.3 Cardiovascular system

It has been established that GCs promote the maturation of the cardiovascular system. For example, GCs improve the contractility and maturation of primary mouse foetal cardiomyocytes via proliferator-activated receptor gamma coactivator 1-alpha (PGC-1α), a critical regulator of cardiac mitochondrial capacity (E. A. Rog-Zielinska et al., 2015). Maternal treatment with GCs leads to increased myocardial maturation and improved cardiac function of preterm piglets (Eiby et al., 2012; M. Y. Kim et al., 2014). However, excessive prenatal exposure to GCs could potentially result in a delay of cardiac maturation and even cause cardiovascular problems in adult life (Gay et al., 2015; Xiong et al., 2016). Abundant evidence has shown the connection between the GR and the development of the cardiovascular system. In mice, conditional disruption of GR in cardiomyocytes and vascular smooth muscle cells (VSMC) leads to impaired heart function and generalized edema in the embryo (Eva A. Rog-Zielinska et al., 2013), and pathological consequences in the adult heart, such as cardiac hypertrophy and left ventricular systolic dysfunction (Robert H. Oakley et al., 2019; Robert H. Oakley et al., 2013; Richardson et al., 2014). The cardiomyocyte-specific GR KO results in supression of genes important for maintaining cardiac contractility (such as ryanodine receptors 2), promoting cardiomyocyte survival (such as prostaglandin D2 synthase), and inhibiting inflammation (such as lipocalin 2)

(Robert H. Oakley et al., 2013). The cardiomyocyte-specific GR KO also leads to the suppression of genes involved in calcium handling, especially L-type calcium channels in hearts and leads to premature death (median survival approximately 7 months) of mice from spontaneous cardiovascular disease (Cruz-Topete et al., 2016; Robert H. Oakley et al., 2019). GR signaling may directly control cardiovascular pathophysiology. In mice, overexpression of the GR solely in cardiomyocytes induces atrio-ventricular block (Sainte-Marie et al., 2007), strongly suggesting a direct effect of the GR on the heart rhythm.

GR is widely expressed in tissues relevant to blood pressure (BP) regulation, including the heart, blood vessels, and the kidney (Goodwin et al., 2012; Kornel et al., 1993; Provencher et al., 1995; Tsugita et al., 2008). Recently, abundant studies have shown the potent role of GR in cardiovascular pathophysiology, including hypertension and atherosclerosis. In rats, oral administration of dex (0.1 mg/day) significantly elevates BP potentially via increasing the expression of angiotensin II type 1 (AT1) receptor, which has been established to control blood volume and pressure in the cardiovascular system via modulating the secretion of aldosterone, in VSMC (Sato et al., 1994; S. Yang et al., 2004). However, GR deficiency in VSMC in mice results in attenuated acute and chronic hypertension responses (Goodwin et al., 2008). Consistent with that, GR KO in the vascular endothelium leads to resistance to hypertension, highlighting the importance of GR in vascular endothelial cells in the adjustment of BP in vivo (Goodwin et al., 2011). Interestingly, a conditional GR KO in vascular endothelial cells leads to a more severe vascular inflammation and atherosclerotic phenotype in mouse models, indicating the important role of GR in the onset and development of atherosclerosis (Goodwin et al., 2015).

3.2.4 Respiratory system

GCs have been established to play a vital role in the development of the lung, particularly in enhancing surfactant biosynthesis and promoting distal alveolar development (Bird et al., 2007; Flecknoe et al., 2004). Antepartum GC treatment is performed to promote the maturation of the respiratory system and to prevent the acute respiratory distress syndrome (M. Hallman et al., 2010; Jobe et al., 2004; Liggins et al., 1972; Lyons et al., 2002) However, long-term and high doses of fetal exposure to GCs may lead to side-effects, such as supression of physical growth, disrupted immune cell proliferation and perturbed central nervous system development (Coe et al., 2005). On a pure 129sv or C57BL/6 genetic background, all GR-deficient mice die at birth, due to severe atelectasis (Brewer et al., 2002; Cole et al., 1995). The lungs of global GR-deficient fetal mice have increased lung weight and increased airway to capillary diffusion distance, accompanied by an increased

number of type II cells and and undifferentiated alveolar epithelial cells as well as a markedly reduced number of type I cells (Cole et al., 2004). These findings suggest that the GR participates in modulating the differentiation of alveolar epithelial cells into type I cells, but not type II cells, and the development of the lung structure. A GR KO specifically in airway epithelial cells induces a reduction of surfactant proteins in lungs and a reduced survival rate of newborn mice (Manwani et al., 2010). This study demonstrates the important role of the GR in lung epithelial cells for lung development and maturation.

Abundant studies have demonstrated the therapeutic effects of GCs, especially inhaled corticosteroids (ICS), in treating asthma and chronic obstructive pulmonary disease (COPD)(Brown et al., 1972; T. J. Clark, 1972; Gelfand, 1951). The local application of GCs through inhalation results in less side effects and less adrenal suppression in comparison to systemic GCs (Barnes, 2011). Consequently, administration of ICSs is now the standard of care for treating the majority of asthma patients (Stoloff et al., 2011). From a mechanistic view, it has been established that GCs surpress the expression of cytokines in airway epithelial cells via modulating the transcriptional activity of proinflammatory factors, such as NF-κB. In addition, activation of the GR promotes the expression of negative regulators of inflammation, such as DUSP1 (Shipp et al., 2010).

3.2.5 Gastrointestinal system

Abundant evidence has shown that treatment with GCs can promote the maturation of the gastrointestinal epithelium and the formation of the gastrointestinal barrier. For example, treatment of suckling rat with hydrocortisone (HC) promotes the maturation of glycoprotein galactosylation and fucosylation processes in the small intestine (Biol-N'garagba M et al., 2003). Prenatal corticosteroid treatment of mothers at risk for premature delivery or to preterm infants during the first week of life has been shown to prevent or significantly decrease the severity of necrotizing enterocolitis and increase the surviving rate of suckling mice (Bauer et al., 1984; Halac et al., 1990). Conversely, the suppression of GC metabolism by carbenoxolone, an inhibitor of 11betaHSD, leads to the dysfunction of the gastrointestinal barrier and increases the mortality of suckling mice (Pácha et al., 2003). In addition, suppressing the secretion of endogenous GCs via adrenalectomy during the weaning period in rats reduces the level of glycosylation in the small intestine (Miyata et al., 2008). Mechanistically, HC treatment of cultured enterocytes has been shown to promote tight junction formation, microvilli maturation, and reorganization of the endoplasmic reticulum and trans-Golgi network (Quaroni et al., 1999). HC administration to cultured human fetal intestinal organoids, interestingly, promotes brush border hydrolytic activities and epithelial cell proliferation (Arsenault et al., 1985).

As potent anti-inflammatory agents, GCs are recommended as therapeutics for inflammatory bowel diseases (Baumgart et al., 2007). For example, administration of prednisone significantly restores intestinal epithelial integrity (lactulose/mannitol ratio]) in Crohn's disease (Wild et al., 2003), potentially via promoting tight junction sealing (Felinski et al., 2008; Fischer et al., 2007; Romero et al., 2003; Zettl et al., 1992). Interestingly, "GRdim mice", which express a mutant form of the GR with strongly reduced dimerization and DNA-binding abilities, show more severe TNF-induced intestinal inflammation in comparison with control mice, indicating that GR protein dimerization is important for the protective effects of GCs in the intestine (Ballegeer et al., 2018).

3.2.6 Kidney development and diseases

Some studies have shown an effect of GC treatment and renal development. For example, treating pregnant rats with dex (0.2 mg/kg) results in offspring with lower body and kidney weight, accompanied by a lower number of glomeruli, lower glomerular filtration rate, higher BP, and albuminuria than control mice (Celsi et al., 1998). In addition, a targeted deletion of 11-β HSD2, which promotes the inactivation of GCs, leads to abnormal development of the distal renal tubule and also triggers the onset of hypertension, accompanied by hypotonic polyuria, hypokalemia and hypochloremia (Holmes et al., 2001). In terms of mechanism, studies have shown that dex treatment can lead to hyperglycaemia, which can impair nephrogenesis by increasing the expression of the IGF-II/mannose-6-phosphate receptor (Bertram et al., 2001). In addition, dex treatment induces the production and release of aldosterone, which promotes the reabsorption of sodium and water in kidney, and increases the BP (Sato et al., 1994; S. Yang et al., 2004).

For their anti-inflammatory effects, GCs are widely used in acute and chronic renal diseases, such as septic AKI and necrotizing glomerulonephritis. In a cecal ligation and puncture-induced septic AKI mouse model, dex treatment (2.5mg/mL) significantly attenuates the renal dysfunction partially via reducing mitochondrial damage and apoptosis (H. M. Choi et al., 2013). In a nephrotoxic serum-induced crescentic nephritis mouse model, high-dose prednisolone treatment (2.5mg/kg) partially rescues the albuminuria and cellular crescent formation (Kuppe et al., 2017). Interestingly, a similar kidney-protective phenotype is observed in mice with a TEC-specific deletion of the GR and in mifepristone (GR antagonist)-treated mice, but without the immunosuppressive effects observed after prednisolone treatment (Kuppe et al., 2017). These studies suggest the using of GCs antagonism for the treatment of glomerulonephritis. However, the mechanism of how GR deficiency or GCs antagonism protect TECs against nephrotoxic factors is still an open question.

3.3 Cellular plasticity after acute kidney injury

Acute kidney injury (AKI), also called acute kidney failure (ARF) is defined by a rapid loss of kidney function, with a sudden reduction of urinary output and increased serum creatinine levels (Kellum et al., 2021). While being largely mitotically quiescent under homeostatic conditions, the kidney is equipped with enormous regenerative abilities after injury. The dynamic processes in the kidney after AKI are characterized by hemodynamic alterations, inflammation, and endothelial and epithelial cell injury, followed by adaptive repair to restore epithelial integrity or maladaptive repair, which leads to chronic kidney disease (Bonventre et al., 2011). After injury, surviving tubular epithelial cells possess the capacity to become proliferative (Berger et al., 2014). The surviving tubular epithelium displays morphological changes, such as flatteningand microvilli loss (Lan et al., 2012; Lan et al., 2016) along with a strong up-regulation of the expression of progenitor markers such as vimentin (Gröne et al., 1987; Kitamura et al., 2015; Kitamura et al., 2005; Maeshima et al., 2006; Maeshima et al., 2003; Witzgall et al., 1994) and sox9 (Chang-Panesso et al., 2019; Kang et al., 2016) for a short period. Interestingly, after surviving TECs restored mature morphology and function of the tubule, the expression of these progenitor markers largely disappears.

A mature differentiated cell can be converted or reprogrammed to a progenitor cell (termed dedifferentiation) or directly to another differentiated cell type (termed transdifferentiation). This phenomenon is termed cellular plasticity (Bonventre et al., 2011; Tata et al., 2016). Cellular plasticity contributes to regenerative responses to injury in various organs, including the gastric epithelium (Stange et al., 2013), the intestine (van Es et al., 2012), skin follicles (Rompolas et al., 2013), the airway (Tata et al., 2013) and the nervous system (Johnston et al., 2016). As already mentioned above, the adult kidney epithelium exhibits low physiological turnover; however, it has an efficient regenerative ability upon damage (Little et al., 2017). Importantly, what exact cell type(s) is/are responsible for the regeneration of the injured tubular epithelium is still controversial (Huling et al., 2017). Using genetic lineage analysis, researchers revealed that the origin of the repairing cells resides within the tubule rather than arising from an extratubular source (Chang-Panesso et al., 2017; Humphreys et al., 2008). Moreover, several studies suggest that the regenerative potential in the kidney tubular epithelium either depends on scattered progenitor/stem cells in the kidney tubular epithelium or on the dedifferentiation of surviving differentiated renal tubular epithelial cells (rTECs) after AKI (Fig. 3) (Eymael et al., 2016).

Studies have been undertaken to identify renal stem cells that repeatedly divide in response to injury. One of these studies characterized $CD133^{+}CD24^{+}$ scattered tubular cells (STCs) on the basis of their expression of the surface marker CD106, also known as

VCAM-1 (Angelotti et al., 2012); Two subpopulations of STCs were identified. The CD133+CD24+CD106− subpopulation, localized in the proximal and distal tubules, has low proliferative capacity and unipotent potential towards TECs; the CD133+CD24+CD106+ subpopulation was localized in the urinary pole of the Bowman capsule and showed a high proliferative rate and multipotent differentiation capability towards tubular epithelium and podocytes (Angelotti et al., 2012). This study established that a distinct group of intratubular epithelial cells might function as fixed progenitors (Chang-Panesso et al., 2017). However, no consensus on the nature of renal stem cells has been reached till now (see below).

Lineage tracing approaches indicate a dominant role of dedifferentiation in the repair process of the renal epithelium after AKI (Fig. 4) (Humphreys et al., 2011; Humphreys et al., 2008; Kusaba & Humphreys, 2014; Kusaba, Lalli, et al., 2014). In addition, cell division of the surviving TECs during repair has been shown to be stochastic (Kusaba, Lalli, et al., 2014). According to these reports, following injury, all surviving differentiated TECs have equal chances to rapidly re-enter the cell cycle to divide again (Chang-Panesso et al., 2017) (Humphreys et al., 2011; Vogetseder et al., 2005; Vogetseder et al., 2008). These observations suggest that the regeneration of kidney TECs after AKI crucially relies on the surviving differentiated epithelial cells to dedifferentiate to a progenitor-like phenotype; these newly formed progenitor cells then proliferate and redifferentiate to replace the damaged cells, thereby resulting in restoration of the functional integrity of the nephron.

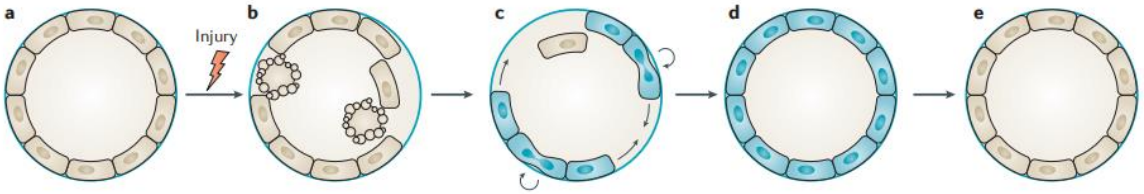

Fig. 4. Dedifferentiation in the repair process of the renal tubular epithelium after acute kidney injury. After injury, damaged epithelial cells die via apoptosis or necrosis (a, b), while the surviving epithelial cells regain proliferation capacity via dedifferentiation, and then proliferate (c) and re-differentiate (d) to replace the dead epithelial cells to promote renal epithelial repair (e). (Chang-Panesso et al., 2017)

The mechanisms of dedifferentiation of TECs after AKI are unclear. Morphologically, dedifferentiated TECs lose their polarity and become flattened and elongated (Bonventre, 2003). During dedifferentiation, differentiation markers, such as villin and SLC34a1, expressed by mature differentiated TECs decreases, while several dedifferentiation genes, including vimentin (Gröne et al., 1987; Kitamura et al., 2015; Kitamura et al., 2005;

Maeshima et al., 2006; Maeshima et al., 2003; Witzgall et al., 1994), sox9 (Chang-Panesso et al., 2019; Kang et al., 2016), CD24, CD133, kidney injury molecule 1 (KIM-1) and neural cell adhesion molecule 1 (Ncam-1) (Abbate et al., 1999; Kusaba & Humphreys, 2014; Kusaba, Lalli, et al., 2014; Lombardi et al., 2016; Witzgall et al., 1994) are re-expressed. The modulators of dedifferentiation have not been fully understood; only two publications have shown in vitro, that dedifferentiation may be driven in part by epidermal growth factor receptor (EGFR) and inhibitor of differentiation-1 (Id1) transcription factor activation at the tubular sites of injury (M. A. Hallman et al., 2008; Li et al., 2007).

4. AIM OF THE THESIS

The glucocorticoid receptor (GR) is a ubiquitously expressed transcription factor, which controls central cellular functions. Synthetic ligands of the GR, i.e. synthetic glucocorticoids (GCs), are widely used in the clinic, primarily for their immunosuppressive effects. Also in patients with acute kidney injury (AKI), GCs are often applied as therapeutics. However, the role of the GR in renal tubular epithelial cells, particularly during epithelial repair after AKI, is unclear. The aim of this thesis was to unravel the functional significance of the GR for epithelial plasticity during kidney regeneration.

5. MATERIALS AND METHODS

5.1 Antibodies and reagents

Primary antibodies

Name	Source	Cat. No.	Application
GR	monoclonal rabbit	Cell Signaling cat.# 12041s	WB 1:1000
Ki67	polyclonal rabbit	Abcam cat.# ab15580	IF 1:200
mTOR	polyclonal rabbit	Cell Signaling cat.# 2972	WB 1:1000
p-mTOR	polyclonal rabbit	Cell Signaling cat.# 2971	WB 1:1000
tubulin	monoclonal rabbit	Cell Signaling cat.# 2125	WB 1:2000
villin	monoclonal mouse	Santa cruz cat.# sc-58897	IF 1:100
Vimentin	monoclonal rabbit	Abcam Cat.# ab92547	IF 1:200
β-catenin	monoclonal mouse	BD cat.# 610153	WB 1:500

Secondary antibodies

Name	Conjugation	Cat. No.	Application
anti-mouse	AlexaFluor 647	Invitrogen cat.# A-32728	IF 1:200
anti-rabbit	AlexaFluor 647	Invitrogen cat.# A-48285	IF 1:200
anti-rabbit	HRP	Cell Signaling cat.# 7074	WB 1:3000
anti-mouse	HRP	Cell Signaling cat.# 7076	WB 1:3000

Reagents

Product	Cat. No.	Concentration
2-DG	Tocris Bioscience cat.# 4515	10 μM
CHIR	Tocris Bioscience cat.# 4423	2 μM
dexamethasone	Sigma-Aldrich cat.# D4902	100 nM, 1 μM
myoglobin	Sigma-Aldrich cat.# M0630	20 mg/ml, 30 mg/ml
Oligomycin A	Tocris Bioscience cat.# 4110/5	0.1 μg/ml, 1 μg/ml
rapamycin	Tocris Bioscience cat.# 1292/1	10 μM

5.2 qPCR

5.2.1 RNA isolation

a) Add 400 μl/well ice-cold trizol (SimaAldrich, cat.# T9424) to cells in 24-well-plate.

b) Scratch the cells down with pipette tips and collect the lysates in 1.5 ml eppendorf tubes. (The lysate at this stage can be kept for days at -80ºC.)

c) Add 400 μl/well ethonal (95%-100%) to the 1.5 ml eppendorf tubes;

d) Tansfer the mixtures (totally 800 μl) into columns from Direct-zol RNA miniprep (Zymo Research, cat.# R2052).

e) Centrifuge the samples at 15000 rpm for 10 minutes at 4ºC.

f) Transfer the columns into new collection tubes.

g) Add 400 μl RNA wash bufferr from the kit to the columns.

h) Centrifuge the samples at 8000 rpm for 1 minute at 4ºC.

i) Add 5 μl DNAse I (6 U/μl) to each column and keep it for 15 minutes at RT.

j) Add 400 μl RNA pre-wash bufferr from the kit and centrifuge at 8000 rpm for 1 minute at RT, discard wash through.

k) Add 700 μl RNA wash buffer from the kit, centrifuge again to discard flow, repeat this step again.

l) Centrifuge in a clean collection tube at 15000 rpm for 2 min to remove the ethanol completely.

m) Elute RNA with 30~500 μl RNAase-free water.

n) Process immediately or store at -80°C.

5.2.2 cDNA and quantitative PCR (qPCR)

cDNA was synthesized by reverse transcription using the Transcriptor high fidelity cDNA synthesis kit according to the manufacturer's instructions (Roche, cat. No. 04379012001). Quantitative PCR reaction was performed using SYBR green (FastStart SYBR Green Master, Sigma Aldrich, cat# 4673484001) according to standard protocols. Primers were designed by the online tool Primer-BLAST (NCBI), or followed the harvard primer bank (https://pga.mgh.harvard.edu/primerbank/).

5.2.3 Primers for qPCR (relative quantification)

Gene	**Used for**	**Sequence (5' to 3')**
AXIN2	HK2 cell line	TACACTCCTTATTGGGCGATCA
		TTGGCTACTCGTAAAGTTTTGGT
BCL9L	HK2 cell line	TGAACCTGAACGTGCAGATGA
		CCCTGGTTGGGAAACTGTG
CCND1	HK2 cell line	GCTGCGAAGTGGAAACCATC
		CCTCCTTCTGCACACATTTGAA
CDH1	HK2 cell line	CGAGAGCTACACGTTCACGG
		GGGTGTCGAGGGAAAAATAGG
CD44	HK2 cell line	CTGCCGCTTTGCAGGTGTA
		CATTGTGGGCAAGGTGCTATT
Hk2	Mouse tubuloids	CTAAGGGGTTCAAGTCCAGTGG
		AGACCAATCTCGCAGTTCTGA
Nr3c1	Mouse tubuloids	GGACCACCTCCCAAACTCTG
		GTGCTGTCCTTCCACTGCTC
NDUFB6	Mouse tubuloids	TGGAAGAACATGGTCTTTAAGGC
		TTCGAGCTAACAATGGTGTATGG
NDUFB8	Mouse tubuloids	GATGCTCCCCAACCGATCAC
		TGTCCACACGATTCCTGATGT
pfkp	Mouse tubuloids	TCAACGTGGTGGGTATGGTG
		GGCTGAATCTGTACCAATGGTC
Pfkfb3	Mouse tubuloids	TATCGGCGTGAGGCTGTGA
		GTTTTCGGACTCTCATGGCTT
PGC-1a	Mouse tubuloids	TATGGAGTGACATAGAGTGTGCT
		GTCGCTACACCACTTCAATCC
PGC-1β	Mouse tubuloids	TCCTGTAAAAGCCCGGAGTAT
		GCTCTGGTAGGGGCAGTGA
tfam	Mouse tubuloids	AACACCCAGATGCAAAACTTTCA
		GACTTGGAGTTAGCTGCTCTTT
TCF4	HK2 cell line	TGCAAAGCCGAATTGAAGATCG

		AGAAGGTCCAATGATTCCATGC
Vimentin	Mouse tubuloids	TCCACACGCACCTACAGTCT
		CCGAGGACCGGGTCACATA
β-actin	Mouse tubuloids	GGCTGTATTCCCCTCCATCG
		CCAGTTGGTAACAATGCCATGT
β-Actin	HK2 cell line	CATGTACGTTGCTATCCAGGC
		CTCCTTAATGTCACGCACGAT

5.3 Western blotting

5.3.1 Cell lysate preparation

500 µl of 1X RIPA buffer was added to cells per well of a 6-well-plate. Then, cells lysates were collected in 1.5 ml eppendorf tubes, and rotated for 5 minutes at 4°C. Afterwards, cells lysates were centrifuged, and supernatants were used for Western blotting according to standard laboratory protocols.

4x Cell lysis buffer (RIPA buffer)

5M NaCl	12 ml
2M Tris-HCl (pH7.4)	10 ml
0.5M EDTA (pH8.0)	4 ml
20% SDS	2 ml
10% Na-DOC (sodium deoxycholate)	20 ml
Triton X-100	4 ml
H_2O	Add up to 100ml

5.3.2 Western blotting materials

Western blotting Product	**Company**	**Cat. No.**
Acrylamide/Bis	Serva	10687.03
TEMED	Applichem:	A1148,0100
Nitrocellulose transfer membrane	GE Healthcare	10401196
Pageruler plus protein ladder	Thermo scientific	SM1812
Pageruler protein ladder	Thermo scientific	SM0672
FUJIFILM super RX	FUJIFILM	4741008389
SuperSignal Chemiluminescent	Thermo scientific	34094
Glass plates- short plates	BioRad	1653308

Protein transfer buffer (10x) Stock	
Tris base	30 g
Glycine	144 g
ddH2O	added up to 1 l

Protein transfer buffer (1x)	
Protein transfer buffer (10x) Stock	1 ml
methonal	2 ml
ddH20	added up to 10 ml

Electrophoresis buffer (5x) Stock	
Tris base	15.1 g
Glycine	94 g
SDS	5 g
ddH2O	added up to 1 l

Washing buffer: PBS-Tween (PBST)	
1x PBS	
0.1% Tween®20	
Solution was kept at RT.	

Blocking solution	
Skim milk (5%)	5 g
H2O	100 ml
Solution was prepared freshly before use.	

Stripping buffer	
Sodium Phosphate buffer (pH 7-7.4)	5 mM
SDS	2%
Before use, 10 µl of β-Mercaptoethanol was added to 50 ml buffer.	

5.4 HK2 cell line

The HK2 cell line (human kidney proximal tubular epithelial cell line, CRL-2190) was obtained from the American Type Culture Collection (ATCC).

5.4.1 HK2 cell culture

HK2 cells were cultured in Keratinocyte Serum Free Medium (K-SFM), supplemented with 0.05 mg/ml (bovine pituitary extract (BPE) and 5 ng/ml human recombinant epidermal growth factor (EGF). BPE and EGF were supplied in the K-SFM kit (Gibco, cat.# 17005-042). Cells were split by adding 0.05% trypsin+EDTA whenever necessary so that cells were kept in a sub-confluent state.

5.4.2 HK2 cell transfection and transient knockdown

To generate a transient knockdown of GR (encoded by NR3C1), HK2 cells were transfected with siRNA using lipofectamine RNAiMax (Invitrogen, Cat. No. 13778150) according to the following process.

a) The lyophilized siRNA (1nmol) was diluted with RNase-free water (50 µl) to obtain a 20 µM stock solution.

b) The day before the transfection, the cells were seeded in 6-weel-plate ($5x10^4$ cells per well).

c) The day of transfection, the stock solution of Nr3c1 and scrambled (Qiagen, Cat. No. 1027310) siRNA was refreeze on ice.

d) Prepare the transfection mixture: 250 µl Opti MEM (Gibco, Cat. No. 31985062) + 2 µl siRNA + 5 µl lipofectamine RNAiMax.

e) Vortex the transfection mixture for 10 seconds and incubate it in the RT for 5 to 20 minutes.

f) Add culture medium to the 6-weel-plate (1750 µl/well).

g) Add the transfection mixture into the wells (254 µl/well).

h) cells were kept in the solution of siRNA for 48 hours and then used for western blot and qPCR analyses.

siRNA for human glucocorticoid receptor

Product name	**Cat. No.**	**Target sequence**	**Final conc.**
Hs-NR3C1-3	Qiagen SI00003759	AAGGACGGTCTGAAGAGCCAA	20 nM
Hs-NR3C1-4	Qiagen SI00003766	CGGTGGCAATGTGAAATTGTA	20 nM

5.5 mIMCD3 cell line

The mIMCD3 cell line (a mouse kidney collecting tubular epithelial cell line) was obtained from ATCC.

5.5.1 mIMCD3 cell culture

mIMCD-3 cells were cultured in DMEM/F12 medium (Gibco, cat.# 11320033) supplemented with 10% fetal bovine serum (FBS). Cells were split by adding 0.05% trypsin+EDTA whenever necessary so that cells were kept in a sub-confluent state.

5.5.2 mIMCD3 cell transfection and transient knockdown

miMCD-3 cells were transfected with siRNA according to the manufacturer's instructions (see 5.4.2).

siRNA for mouse glucocorticoid receptor

Product name	**Cat. No.**	**Target sequence**	**Final con.**
Mm-NR3C1-3	Qiagen SI01330721	CAGACTCAGCATGGAGAATTA	20 nM
Mm-NR3C1-4	Qiagen SI01330728	AAGCGTGATGGACTTGTATAA	20 nM

5.6 Human

Human tubuloid culture

Patient-derived kidney tissue obtained from tumor nephrectomy samples (Ethikvotum 22-21) was used to establish renal tubuloid cultures following published protocols (Kuppe et al., 2021; Schutgens et al., 2019). Cortical kidney tissue was taken distant from the tumor, dissected and minced using a sterile scalpel in cold Ca^{2+}- and Mg^{2+}-free PBS. The fragments were digested by digestion buffer for 45 minutes at 37°C. Then, the digested fragments were passed through a 70 µm cell strainer (MACS, cat.# 130-098-462) to achieve a tubule fragment suspension. Fragments were then seeded in growth factor-reduced Matrigel (Corning, cat.# 354230) and cultured in human tubuloids culture medium.

Digestion buffer (10 ml)

Product	**Cat. No.**	**Final Conc.**
collagenase	Sigma Aldrich cat.# C4-22	1 mg/ml
DNase I	Sigma cat.# D5025	60 units/ml
Liberase TL	Roche cat.# 540102001	0.2 mg/ml

Preparation of these reagent: Liberase TL, 5mg (-20°C), dilute in 1ml of sterile water for 5mg/ml stock Solution, then add 400 µl 5mg/ml LiberaseTL in 10ml DMEM (no FCS) to final concentration of 0,2 mg/ml. DNase I (Qiagen: 10000U in 100 µl), add 6 µl 100 units/µl of DNase I in 10ml of DMEM. Prepare the digestion buffer freshly for the experiment.

Human tubuloids culture medium (10 ml)

Product	**Cat. No.**	**Final conc.**

ADMEM/F12 medium	Gibco cat.# 12634028	-
penicillin/streptomycin	Gibco cat.# 15140122	1%
HEPES	Capricorn cat.# HEP-B	10 mM
GlutaMAX	Gibco cat.# 35050061	1X
B27 supplement	Gibco cat.# 17504044	1.5%
Rspo1-conditioned medium	-	10%
EGF	Invitrogen cat.# RP-8661	50 ng/ml
N-acetylcysteine	Sigma Aldrich Caat# 616-91-1	1 mM
A8301	Tocris Bioscience cat.# 2939	5 µM
FGF-10	Peprotech cat.# 400-42	100 ng/ml
primocine	Invivogen cat.# ant-pm-1	0.1 mg/ml
Rho-kinase inhibitor Y-27632	Abcam cat.# ab228551	10 µM

5.7 Mice and methods using murine kidney tissue

Mice were permanently housed in temperature-, humidity-, and light-cycle (12 h) controlled rooms. Food and water were provided ad libitum. Female and male mice (age ≥ 12 weeks) were used for obtaining kidney tissue.

C57BL/6J mice were obtained from The Jackson Laboratory, and bred at the animal facility of the Philipps-University, Marburg.

To generate mice constitutively lacking GR specifically in rTECs, mice carrying loxP sites flanking exon 3 of the Nr3c1 gene (nr3c1$^{flox/flox}$) (Mittelstadt et al., 2012) were crossed with mice expressing Cre constitutively under the control of the Pax8 promoter (Pax8-Cre) (Bouchard et al., 2002). The Sox9^{IE} (= Sox9$^{IRES-EGFP}$) knock-in strain (stain name: B6;129S4-*Sox9*$^{tm1.1Tlu}$/J; stock no.030137) expressing EGFP from the endogenous Sox9

locus was obtained from The Jackson Laboratory. The mice used in the experiments reported here were bred at the animal facilities of the Philipps University, Marburg. The Vim-EGFP BAC transgene mouse strain (strain name: STOCK Tg(Vim-EGFP)GM158Gsat/Mmucd; stock no. 016856-UCD) was obtained from the Mutant Mouse Resource & Research Centers (MMRRC) (Gong et al., 2003).

5.7.1 Mouse kidney tubuloid culture

Kidneys of sacrificed mice were immediately taken out and placed in ice-cold Ca^{2+}- and Mg^{2+}-free PBS. The kidney cortex was separated using a razor blade, and only the cortex was used to continue with the following process. The tissue was dissected and minced using a sterile scalpel in Ca^{2+}- and Mg^{2+}- free PBS. The fragments were digested by digestion buffer (sesion 5.6) for 15 min. Then, the digested fragments were passed through a 70 µm cell strainer (MACS, 130-098-462)) to obtain a tubule fragment suspension. Fragments were seeded in growth factor-reduced Matrigel (Corning, cat.# 354230) and cultured in mouse tubuloids culture medium as described previously (Kuppe et al., 2021; Schutgens et al., 2019).

Mouse tubuloids culture medium (10 ml)

Product	**Cat. No.**	**Final Conc.**
ADMEM/F12 medium	Gibco cat.# 12634028	-
penicillin/streptomycin	Gibco cat.# 15140122	1%
HEPES	Capricorn cat.# HEP-B	10 mM
GlutaMAX	Gibco cat.# 35050061	1X
B27 supplement	Gibco cat.# 17504044	1.5%
Wnt3a-conditioned medium	-	10%
EGF	Invitrogen cat.# RP-8661	50 ng/ml
N-acetylcysteine	Sigma Aldrich Caat# 616-91-1	1 mM

A8301	Tocris Bioscience cat.# 2939	5 µM
FGF-10	Peprotech cat.# 400-42	100 ng/ml
primocine	Invivogen cat.# ant-pm-1	0.1 mg/ml
Noggin	Peprotech cat.# 250-38	50 ng/ml

Fragments density in matrigel

Plate size	number of fragments	matrigel/well (µl)	medium/well (µl)
8-well ibidi	$2x10^4$	20	200
12-well plate	$1.26x10^5$	100	1000
24-well plate	$6x10^4$	50	500
48-well plate	$3x10^4$	25	250
96-well plate	$1.5x10^4$	10-15	100

5.7.1.1 Dexamethasone treatment

One day after seeding the tubular fragments or passaged tubuloids in matrigel, dex (sigma, cat. # D4902) was added to culture medium (without FCS) in final concentration of 100 nM or 1 µM. Dex was diluted with ethanol according to the manufacturer's instructions (sigma).

5.7.1.2 Myoglobin treatment

One day after seeding the passaged tubuloids in the matrigel, horse skeletal muscle myoglobin (M-0630; sigma; USA; cat.# SLCC0370) was added to tubuloids at a final concentration of 20 mg/ml or 30 mg/ml. A 40 mg/ml stock myoglobin solution was prepared in mouse tubuloids culture medium (see section 5.7.1) sonication. Since only reduced myoglobin (Fe^{2+}) is cytotoxic (Bywaters et al., 1942), 12 mM vitamin C (L-ascorbic acid 2-phophate, Sigma, A8960, cat.# SLCC4554, pH7.4) was added to the stock solution to get a metmyoglobin (Fe^{3+}) to myoglobin conversion (Zager et al., 1997; Zager et al., 1992). After 1 h incubation at room temperature (protected from light), myoglobin was added to the tubuloids (final concentration, 20 mg/ml or 30 mg/ml—3 mM vitamin C). Tubuloids were then incubated under this condition for 72 hours.

5.7.1.3 Tubuloid number and normalization

To compare the formation of tubuloids in different experimental groups, tubuloid numbers were calculated as follows: The tubuloid number given in the figures is the tubuloid number

on the day of analysis minus the tubuloid number on day1 (expressed as "Δ").

5.7.2 Tubuloid damage score

To assess the damage severity of tubuloids, they were stained with propidium iodide (PI) (Abcam; cat.# ab139418) and Hoechst (Hoechst 33342 Solution (20 mM); Thermofisher; cat.# 62249) after proper treatment. Tubuloids were imaged using a Leica Thunder microscope, the total number of the cells and PI-positive cells were counted, and the percentage of PI-positive cells was calculated. The tubuloid damage score was defined as follows: Score 0 = PI-negative tubuloids; score 1: ＜30% of cells are PI-positive; score 2: 30-60% of cells are PI-positive; score 3: >60% are PI-positive; score 4: tubuloids are destroyed. At least 20 randomly selected tubuloids were analyzed for each experimental group per independent experiment, and an average score was calculated. Two days and four days after removing myoglobin from the culture medium, images were taken again to observe and calculate the percentage of surviving tubuloids.

5.7.3 FACS

To assess the percentage of Sox9- and Vim-positive TECs in renal tubuloids from $Sox9^{IE}$ and Vim-EGFP mice, FACS was performed with tubular fragments seeded in 24-well-plates. The supernatant of tubuloid cultures was removed away and 1 ml pre-warmed PBS was added to wash once. Then, 1 ml of digestion buffer (sesion 5.6) was directly added to wells, and matrigel was mechanically damaged directly in the wells. After pipetting up and down, the tubuloid suspension was collected to a 50 ml centrifuge tube. To isolate single cells from tubuloids, the tubuloid suspension was placed in a water bath (37 °C) for 30 minutes, and was then pipetted up and down for 60 times, passed through 70 μm (MACS, 130-098-462) and 30 μm cell strainers (MACS, cat.# 130-098-458). Then, the tubuloid suspension was centrifuged at 1200 rpm for 10 min to harvest the single cells. Next, the single cells were resuspended with FACS working buffer, and the single-cell-suspension was incubated with CD31, CD45, CD11b and CD326 antibodies for 30 min on ice. Finally, the percentage of Sox9 or Vim positive (GFP^+) cells from all cells that were blood cell markers negative ($CD31^-CD45^-CD11b^-$) and epithelial marker positive ($CD326^+$) was analyzed with a Flow cytometer (BD Biosciences, BD Aria III).

FACS working buffer (10ml)

Products	Cat. No.	Final Conc.

PBS	Capricorn cat.# PBS-10XA	-
B27 supplement	Gibco cat.# 17504044	1.5%
Rho-kinase inhibitor Y-27632	Abcam cat.# ab228551	10 µM

Materials for FACS of tubuloids

products	**Cat. No.**	**Final con.**
APC/Fire 750™ anti-mouse CD326 (Ep-CAM) Antibody	Biolegend cat.# 118229	1:200
Brilliant Violet 421™ anti-mouse CD31 Antibody	Biolegend cat.# 102423	1:200
Brilliant Violet 421™ anti-mouse CD45 Antibody	Biolegend cat.# 103133	1:200
Brilliant Violet 421™ anti-mouse/human CD11b Antibody	Biolegend cat.# 101235	1:200

5.7.4 Sea horse analysis of tubuloids

5.7.4.1 Glycolytic stress assay

Preparation

a) Seed passaged tubuloids in Seahorse XF96 V3 PS Cell Culture Microplates: To purify tubuloids from other kind of cells, such as blood cells and immune cells, passaged tubuloids were used for sea horse analysis. As recommeded by the lab of Hans Clevers, et al. (Schutgens et al., 2019), the tubuloids can be expanded for at least 20 passages. Here, tubuloids of passage 2 to 6 were used in the sea horse analysis. One day before the extracellular flux assays, 50 to 100 tubuloids were seeded in Seahorse XF96 V3 PS Cell Culture Microplates with 5 µl matrigel per well, and 6 replicates of each group. The tubuloids were cultured with 100 µl mouse tubuloid culture medium (session 5.7.1) in a 37°C, 5% CO_2 incubator.

b) One day before the extracellular flux assays, do the hydration of the sensor cartridge: lift the sensor cartridge, fill each well of the plate with 200 µl of a calibration solution, and carefully load the cartridge back to submerge the sensors in the calibration solution. Place the cartridge in a 37°C, CO_2-free incubator for overnight prior to use.

c) Prepare 2 tubes of 40ml XF DMEM Medium in a 37°C, CO_2-free incubator for overnight prior to use.

Materials of glycolysis stress assay

products	**Company**	**Cat. No.**
Seahorse XF96 V3 PS Cell Culture Microplates	Agilent	101085-004
Seahorse XFe96 Analyzer	Agilent	-
Seahorse XF Glycolysis Stress Test Kit	Agilent	103020-100
QIAamp DNA Micro Kit (50)	Qiagen	56304
Seahorse XFe96 FluxPak mini	Agilent	102601-100
calibration solution	Agilent	4690008

On the day of the sea horse analysis

a) Prepare the working solution:

Products	**Reagent & Cat. No.**	**Final conc.**	**40 ml x 2**
Recommended Medium	Seahorse XF DMEM Medium, pH 7.4, Cat#103575-100	-	40 ml
Required supplements	Seahorse XF Pyruvate (100mM solution), cat.# 103578-100	1 mM	400 µl
	Seahorse XF L-Glutamine (200mM solution), cat.# 103579-100	2 mM	400 µl

b) Remove the culture medium, wash twice with 180 µl working solution, and incubate the plates in a 37 °C, CO_2-free incubator for 40 min to one hour.

c) Prepare the stock solution of compounds of Glycolysis Stress Test Kit:

Compound	**Volume of working solution**	**Final conc.**
Oligomycin	630 µl	100 µM
2-DG (0.3g)	360 µl	5 M

d) Dilute the compounds with working solution:

Glucose: 300 µl Stock + 2700 µl working solution

10X Oligomycin (20 µM): 600 µl Stock (100 µM) + 2400 µl working solution

2-DG: 300 µl Stock (100 µM) + 2700 µl XF DMEM Assay Medium

e) Load the cartridge ports with the following compounds:

Port A: 20 µl Glucose

Port B: 22 µl Oligomycin

Port C: 25 µl 2-DG

f) Incubate the cartridge in a 37°C CO_2-free incubator for 10 min.

g) Turn on the extracellular flux analyzer and the controller.

h) Open the Analyzer Software and input the following protocol: Choose glycolysis stress Assay and lable the samples. Under the protocol tab, set the following mix and measure cycles of calibrate, inject port A, B and C as： mix for 2 min, wait for 2 min, and measure for 3 min (repeat this cycle 3 times). Press start to begin the calibration. Remember to remove the cover of the calibration plate. After the calibration step, press the prompt command to change the cartridge plate to the cell culture plate and continue the run. When the run is completed, transfer the data, and remove away the 96-well plate. Meassure the DNA concentration of each well of the 96-well-plate with DNA Micro Kit, and normalize the ECAR data to DNA concentration.

Analysis of glycolysis stress assay

The calculation of glycolysis and glycolytic capacity of glycolysis stress test were performed according to the manufacturer's instructions (Agilent).

Glycolysis = (Maximun rate measurement before oligomation injection) – (Last measurement before glucose injection)

Glycolytic capacity = (Maximun rate measurement after oligomation injection) – (Last measurement before glucose injection)

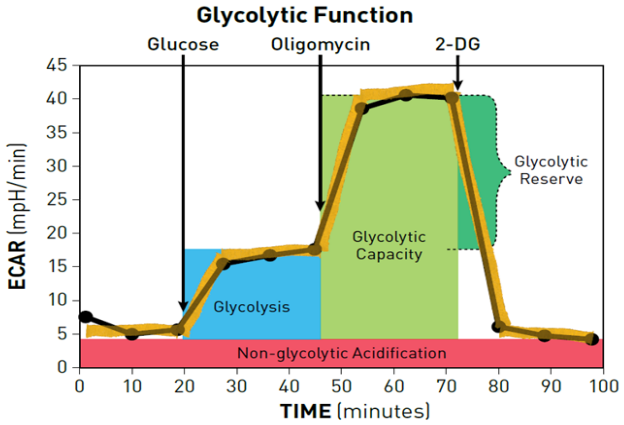

5.7.4.2 Mito stress assay

To assess the mitochondria respiratory of the tubuloids, Mito stress assay was performed with the Mito Stress Test Kit (Seahorse XF Cell Mito Stress Test Kit, Agilent, cat.# 103015-100).

One day before, the preparation of this experiment is the same with section 5.7.4.1, including tubuloids seeding, hydration of the sensor cartridge and pre-warming of the XF DMEM Medium. The day of the Mito stress assay, firstly, the working solution (see section 5.7.4.1) was prepared with pre-warmed XF DMEM Medium. Then, the tubuloids were prepared (see section 5.7.4.1) for the process of Mito stress assay. Next, do the following steps (be careful, the compounds of glycolytic and mito stress assay are different):

a) Prepare the stock solution of compounds of Mito Stress Test Kit:

Compound	**Volume of working solution**	**Final conc.**
Oligomycin	630 µl	100 µM
FCCP	720 µl	100 µM
ROT/AA	540 µl	50 µM

b) Dilute the compounds with working solution:

10X Oligomycin (20 µM): 600µl Stock (100 µM) + 2400 µl working solution

10X FCCP (1 µM): 300µl Stock (100 µM) + 2700 µl XF DMEM Assay Medium

Rot/AA (5 µM): 300µl Stock (100 µM) + 2700 µl XF DMEM Assay Medium

c) Load the cartridge ports with following compounds:

Port A: 20 µl Oligomycin (20 µM)

Port B: 22 µl FCCP (1 µM)

Port C: 25 µl Rot/AA (5 µM)

d) Incubate the cartridge in a 37 °C CO2-free incubator for 10 min.

For the following, see section 5.7.4.1.

Analysis of mito stress assay

The calculation of basal OCR and Maximal OCR of cell mito stress test were performed according to the manufacturer's instructions (Agilent).

Basal OCR = (last rate measurement before oligomation injection) – (non-mitochondrial respiration rate)

Maximal OCR = (Maximun rate measurement after FCCP injection) – (non-mitochondrial respiration rate)

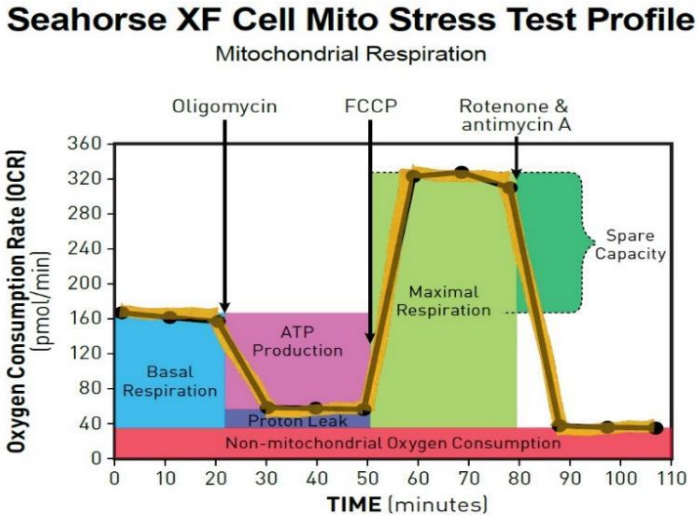

5.7.4.3 ATP rate assay

To assess the ATP production rate and total ATP production of the tubuloids, ATP rate assay was performed with the ATP Rate Assay Kit (Seahorse XF Real-Time ATP Rate Assay Kit, Agilent, 103591-100).

One day before, prepare the materials for this assay (see section 5.7.4.1), including tubuloids seeding, hydration of the sensor cartridge and pre-warming of the XF DMEM Medium. The day of the experimant, the working solution (see section 5.7.4.1) was prepared with pre-warmed XF DMEM Medium. Then, the tubuloids were prepared (see section 5.7.4.1) for the process of ATP rate assay. Next, do the following steps:

a) Prepare the stock solution of compounds of ATP Rate Assay Kit:

Compound	**Volume of working solution**	**Final conc.**
Oligomycin	630 µl	100 µM
ROT/AA	540 µl	50 µM

b) Dilute the compounds with working solution:

10X Oligomycin (20 µM): 600 µl Stock (100 µM) + 2400 µl working solution

Rot/AA (5 µM): 300µl Stock (100 µM) + 2700 µl XF DMEM Assay Medium

c) Load the cartridge ports with the following compounds:

Port A: 20µl Oligomycin (20 µM)

Port B: 25µl Rot/AA (5 µM)

For the following steps, see section 5.7.4.1.

Alalysis of real-time ATP rate assay

Original data of ATP rate assay was exported from the system of Wave 2.6.0, and load the deta to Sea horse real-time ATP rate assay report generator. The total ATP production rate was calculated automately by the report generator (Agilent).

5.7.5 Tubuloids immunofluorescence staining

Seed the tubuloids in 8-well-ibidis (Ibidi, cat. 80826), do the IF staining of tubuloids directely in the ibidis.

a) Remove the culture medium, wash once with PBS (RT).
b) Fix the tubuloids with prewarmed 4% PFA for 30 minutes (cold PFA would destroy the matrigel, and tubuloids would also be washed away).
c) Wash with PBS for 3 times.
d) 0.2% Tx-100/PBS for 10min in RT.
e) 3% BSA/PBS block for 1 hour.
f) Prepare primary antibody solution in 3% BSA/PBS, and incubate the tubuloids in the primary antibody solution for overnight in 4 ºC.
g) Wash with PBS for 3 times;
h) Prepare secondary antibody and DAPI in 3% BSA/PBS, and incubate the tubuloids in the secondary antibody solution for 1 hours in RT;
i) Wash with PBS for 3 times;
j) Fix the tubuloids with one drop of mounting medium, check the staining with confocal microscopy.

5.7.6 Tubuloids mitotracker staining

preparation

a) MitoTracker™ Deep Red FM (Invitrogen, Cat#.M22426), add 92 µl DMSO into one tube of MitoTracker™ Deep Red FM (MW: 543.58g/mol, 50 µg) to get a final concentration of 1mM as the stock package.
b) Hoechst 33342, dilute 20mM original solution to 2mM with water. Store them at -80℃ and protected from light.

process

a) Pre-warm DMEM/F12 medium (Gibco, cat.# 11320033) in 37°C water bath for 20 min before starting the experiment.
b) Dilute 1mM MitoTracker stock solution (10µl per tube) to 100 µM with DMSO (90 µl);

Reagent	Stock con.	Final con.

MitoTracker	100 μM	200 nM
Hoechst 33342	2 mM	4 μM

c) Seed tubuloids in ibidis with matrigel. Culture the tubuloids with appropriate culture medium in 37 °C, 5% CO2 incubator.

d) After corresponding treatment, remove away the supernatant, wash once with pre-warmed DMEM/F12 medium.

e) Incubate the tubuloids with staining solution containing 200nM MitoTracker and 4 μM Hoechst 33342 for 90 min in 37 °C, 5% CO2 incubator.

f) Take pictures with confocal fluorescence microscope.

5.8 Conditioned medium

5.8.1 Wnt3a conditioned medium

Media and cell line

a) Basal growth medium (550 ml)

Name	**Company**	**Cat. No.**	**Volume**
DMEM	thermofisher	31966	500 ml
FBS	sigma	F7524	50 ml
Pen/Strep	thermofisher	15140	5 ml

b) Selection growth medium (50ml)

Name	**Company**	**Cat. No.**	**Volume**
Basal growth medium	-	-	50 ml
Zeocin (100mg/ml)	Invivogen	ant-zn-5	62.5 μl

c) Conditioning medium (500mL)

Name	**Company**	**Cat. No.**	**Volume**
Advanced DMEM/F12	thermofisher	12634010	500 ml
HEPES (1M)	thermofisher	15630106	5 ml (10 mM)
GlutaMax (100X)	thermofisher	35050	5 ml
FBS	sigma	F7524	50 ml (10%)
Pen/Strep	thermofisher	15140	5 ml (1%)

d) 2X freezing medium (10mL)

Name	Company	Cat. No.	Volume
Basal growth medium	-	-	5 ml
FBS	sigma	F7524	3 ml
DMSO	sigma	67-68-5	2 ml (final: 10%)

e) Cell line: L-wnt3a cells (Schutgens et al., 2019)

Preparation protocol

a) Prewarm basal growth medium in 37 °C water bath.

b) Take one vial of L-wnt3a-cell into 37 °C water bath, shake it frequently to make it melt quickly and evenly.

c) Prepare one 10ml dish, cover the dish with 10ml prewarmed basal growth medium.

d) Transfer the cells to prepared 10 ml dish.

e) Keep the cells in 37 °C, 5% CO_2 cell incubator for overnight.

f) The other day, remove the basal growth medium (to remove away the DMSO from freezing medium) and add 10ml selection growth medium.

g) Keep the cells in 10ml selection medium for 10 ~ 12 days.

h) Split the cells every 2~3 days (as 1 to 6 ~ 8) when the cellular confluent is around 80 ~ 90 %; only keep one dish of the L-wnt3a cells, trash the leftover.

i) After the selection, change the medium to basal growth medium, freeze vials of cells at this step. (Notes: freeze as much as porrible the cells at the first time preparing the conditioned medium)

j) After 2 ~ 3 days, change to conditioning medium when the cellular confluency is around 60 ~ 70%.

k) Keep the conditioning medium with the L-wnt3a cells for 6~ 7 days. (Note: it is normal if the medium become yellow or there are some dead cells.)

l) Harvest the conditioned medium into 50 ml centrifuge tube

m) Centrifuge the conditioned medium in 2000 rpm/min for 5 min to spin down the dead cells.

n) Collect the supernatant to 250 ml bottles as wnt3a conditioned medium.

o) Filter the collected wnt3a conditioned medium with bottle top filters (Sarstedt, cat.# 83.3941-CS).

p) Keep wnt3a conditioned medium in -80°C freezer.

5.8.2 R-sponding-1 conditioned medium

Media and cell line

a) Basal growth medium (550 ml)

Name	**Company**	**Cat. No.**	**Application**
DMEM	thermofisher	31966	500 ml
FBS	sigma	F7524	50 ml
GlutaMax (100X)	thermofisher	35050	5 ml
Pen/Strep	thermofisher	15140	4 ml (1%)

b) Selection growth medium (50 ml)

Name	**Company**	**Cat. No.**	**Application**
Basal growth medium	-	-	50 ml
Zeocin (100mg/ml)	Invivogen	ant-zn-5	62.5 µl

c) Conditioning medium (500 ml)

Name	**Company**	**Cat. No.**	**Application**
Advanced DMEM/F12	thermofisher	12634010	500 ml
HEPES (1M)	thermofisher	15630106	5 ml (10 mM)
GlutaMax (100X)	thermofisher	35050	5 ml
Pen/Strep	thermofisher	15140	6 ml (1%)

d) Cell line: HA-R-Spondin1-Fc 293T cells (Schutgens et al., 2019)

The R-spondin-1-conditioned medium was prepared in analogy to the Wnt3a-conditioned medium (5.8.1)

6 RESULTS

6.1 Cellular plasticity in renal tubuloids of mice

The first aim of the thesis was to establish an in vitro model system to study the role of the GR in epithelial plasticity. To do so, kidney organoids, so-called tubuloids were cultured according to a published protocol of the research group of Hans Clevers (Schutgens et al., 2019) This protocol involves the isolation of tubular fragments from mouse kidney, followed by an embedding in matrigel as described in the Materials & Methods section. First, morphological changes during tubuloid formation were observed and assessed. For this, individual tubuloids were continuously imaged for several days using a Leica Thunder Live-Cell Imaging System. By definition, the day of seeding was termed “day 0”, the day after seeding “day 1”, and so on. Using this approach, it could be seen that epithelial cells in tubular fragments undergo phenotypical changes typical for a dedifferention-redifferentiation sequence: Early on, TECs display a flat morphology, which changes into a cuboidal shape as tubuloid formation progresses (Fig. 5 A). In order to understand wether these morphological changes are accompanied by corresponding molecular changes, immunofluorescence stainings for the dedifferentiation marker vimentin and the differentiation markers villin and Lotus tetragonolobus lectin (LTL) were performed (Fig. 5 B, C). As shown in Fig. 5 B, tubuloids at day 2 after seeding were mostly positive for vimentin. Moreover, 4 days after seeding, flat tubuloids were vimentin-positive and LTL-negative, while – on the contrary – cuboidal tubuloids were vimentin-negative and villin-positive (Fig. 5 C). These experiments have demonstrated that tubuloids undergo morphological and molecular changes consistent with dedifferention-redifferentiation processes. To investigate whether cellular plasticity could also be induced and observed in tubuloids after toxin-induced injury, mature tubuloids were treated with myoglobin (30 mg/ml) for 3 days. The damage of tubuloids was assessed by propidium iodide (PI) and Hoechst staining. Images were taken before myoglobin treatment as well as during and 2 days after myoglobin treatment. Indeed, myoglobin induced tubuloid damage with surviving epithelial cells adopting a flat morphology (Fig. 5 D, middle). 2 days after ceasing myoglobin treatment, cuboidal tubuloids reformed (Fig. 5 D, middle). Interestingly, failure to adopt a flat morphology would result in tubuloid death (Fig. 5 D, bottom).

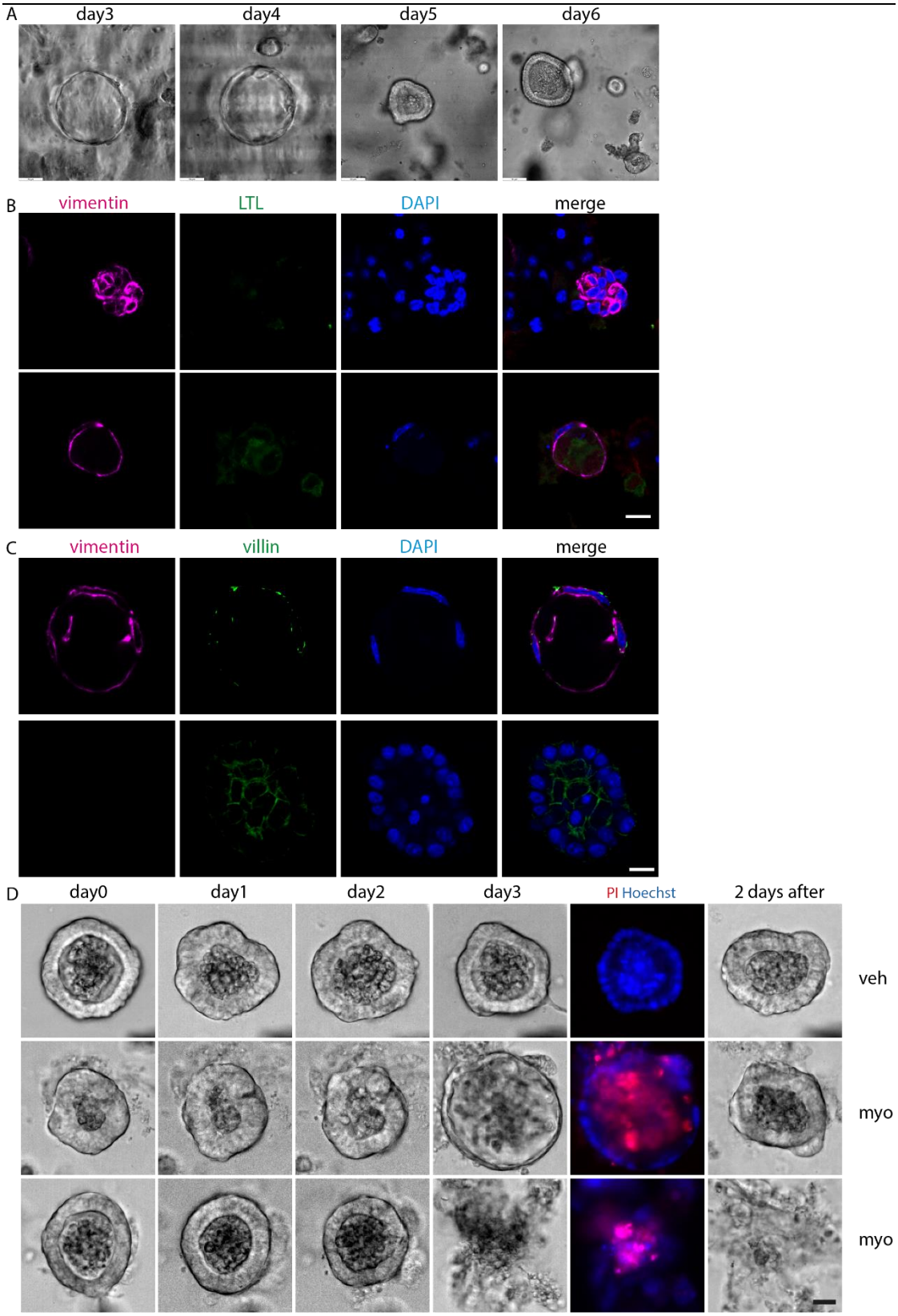

Fig. 5. Cellular plasticity in renal tubuloids of mice. A. kidney cortical fragments from wildtype ("WT") mice were grown in matrigel. Bright-field images (scale bar, 50 µm). **B.** Representative confocal images of tubuloids (day2, time scheduel follows Fig. 6 A) immunostainings using anti-Vimentin (fuchsia) and lectins LTL (green) (scale bar, 10 µm).

Blue: DAPI. **C.** Representative confocal images of immunostainings using anti-Vimentin (fuchsia), anti-Villin (green) antibodies (scale bar, 10 µm). Blue: DAPI. **D.** Representative BF and fluorescence images of vehicle and myo (30 mg/ml) treated tubuloids. Myo treatment was done for 3 days. PI/Hoechst staining was performed at day 3 of myo treatment. (scale bar, 10 µm). veh, vehicle; myo, myoglobin.

6.2 Dexamethasone impacts the dedifferentiation and redifferentiation of tubuloids

6.2.1 Dexamethasone treatment from day1 onwards suppresses the formation of cuboidal tubuloids

To test the role of GR signaling in tubuloid formation, dexamethasone ("dex") treatment was applied one day after seeding of tubule fragments (day 1) (workflow is shown in Fig. 6 A). The 100 nM and 1 µM doses of dex represent therapeutically releveant doses. Tubuloid numbers (Fig. 6 C, D) and the percentage of tubuloids with cuboidal epithelial cells were then analyzed (Fig. 6 B and Fig. 6 E-I). When tubuloids were treated with dex (100 nM or 1 µM) from day 1, tubuloid numbers at day 2 were significantly decreased (Fig. 6 B-D) and the formation of cuboidal cells was suppressed (Fig. 6 B and Fig. 6 E-I) in comparison to the vehicle group. These data suggest that activation of the GR by dex delays the formation of mouse tubuloids. However, which stage of the tubuloid formation had been affected was unclear.

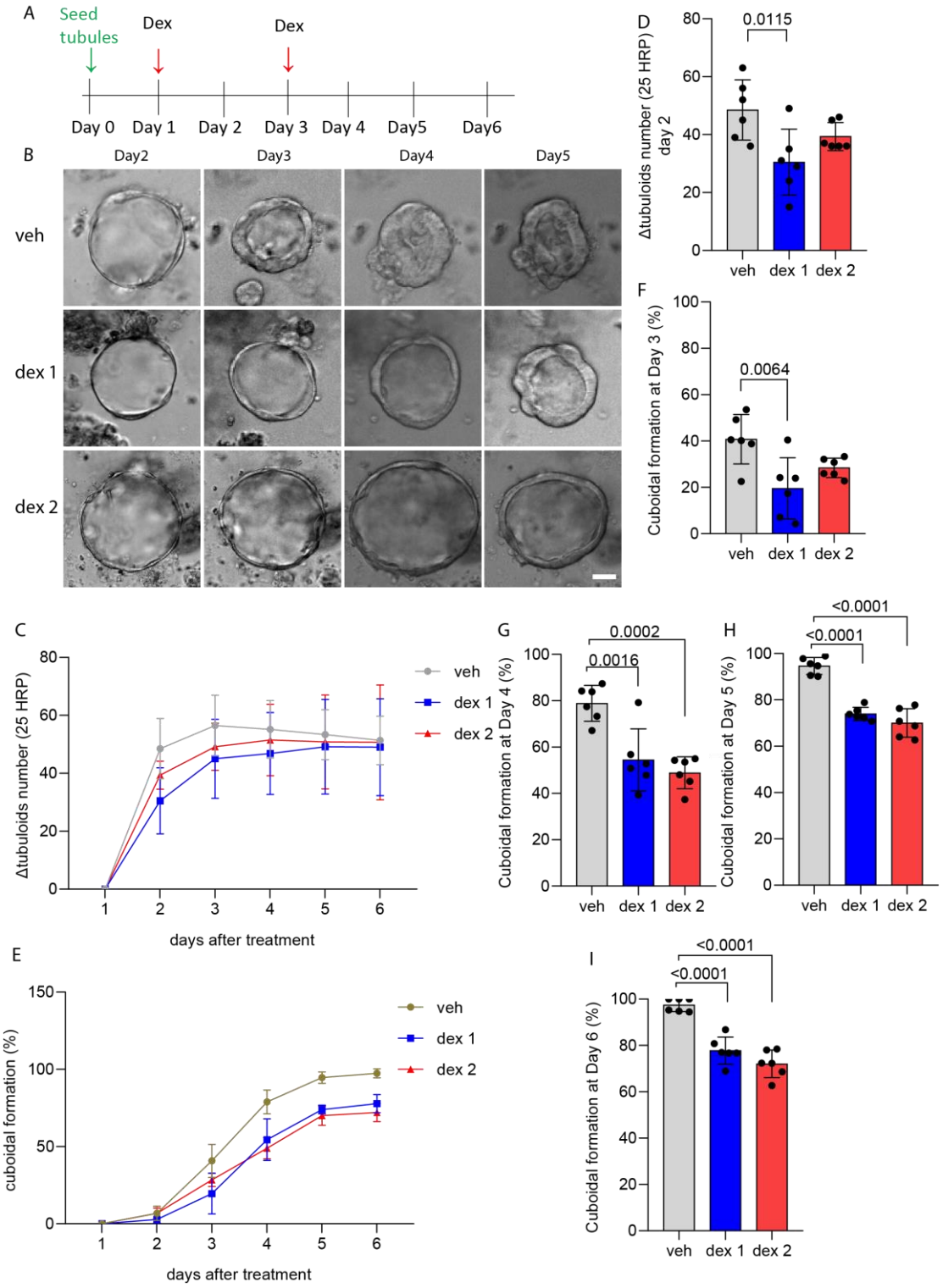

Fig. 6. Dexamethasone treatment from day1 onwards suppresses the formation of cuboidal tubuloids. A. Workflow for the treatment with dex. **B.** Bright field images of tubuloid formation. Dex (dex 1 and dex 2 represent 100nM and 1 µM of dex treatment, respectively) treatment starts from day 1. Scale bar, 10 µm. **C.** Quantification of tubuloid numbers on different days of culture (mean ± SD). Tubuloid numbers were normalized (expressed as Δ) to the number at day 1 (as described in section 5.7.1.3). **D.** Quantification results of day 2 of C in

more detail (mean ± SD; One-way ANOVA, Tukey test). For all other days, there were no significant differences. **E.** Quantification of tubuloids with cuboidal shape. Dex treatment was from day 1 (mean ± SD). **F.** Quantification results of day 3 of E in more detail (mean ± SD; One-way ANOVA, Tukey test). **G.** Quantification results of day 4 of E in more detail (mean ± SD; One-way ANOVA, Tukey test). **H.** Quantification results of day 5 of E in more detail (mean ± SD; One-way ANOVA, Tukey test). **I.** Quantification results of day 6 of E in more detail (mean ± SD; One-way ANOVA, Tukey test). veh, vehicle; dex, dexamethasone.

6.2.2 Dexamethasone treatment from day3 onwards has no effect on tubuloid numbers and efficiency of formation of cuboidal cells

To further test whether the activation of GR affects the differentiation of tubuloid formation, dex (100 nM or 1 µM) was applied from 3 days after seeding of tubule fragments (work flow is shown in Fig. 6 A). Similar to section 6.2.1, tubuloid numbers and the percentage of tubuloids with cuboidal epithelial cells were then analyzed. In contrast with dex treatment started from day1, significant differences in tubuloid number (Fig. 7 A) and efficiency of formation of cuboidal cells could not been observed (Fig. 7 B). These data suggest that activation of the GR by dex may affected the early stage (dedifferentiation) of regeneration of surviving epithelia.

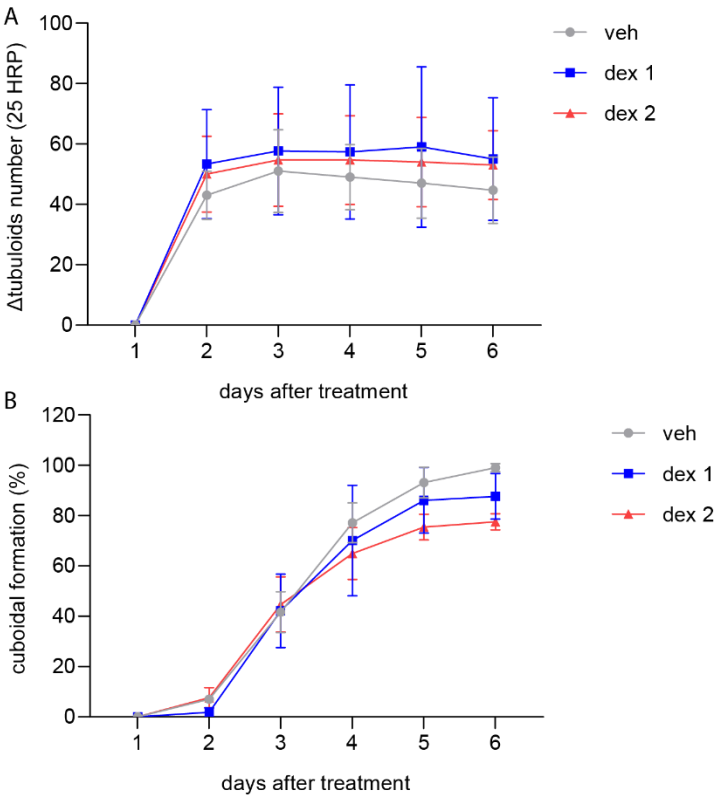

Fig 7. Dexamethasone treatment from day3 onwards has no effect to the tubuloid numbers and efficiency of formation of cuboidal tubuloids. A. Tubuloid numbers were normalized expressed as Δ, as described in section 5.7.1.3) to the number at day 1 (mean ± SD). Dex (dex 1 and dex 2 represent 100nM and 1 µM of dex treatment, respectively) treatment was from day 3. **B.** Quantification of tubuloids with cuboidal shape. Dex treatment was from day 3 (mean ± SD). veh, vehicle; dex, dexamethasone.

6.2.3 Dexamethasone treatment affects the expression of sox9 and vimentin in tubuloids

In addition to vimentin (Gröne et al., 1987; Kitamura et al., 2015; Kitamura et al., 2005; Maeshima et al., 2006; Maeshima et al., 2003; Witzgall et al., 1994), Sox9 is another marker indicating dedifferentiation (Chang-Panesso et al., 2019; Kang et al., 2016). To assess a potential connection between GR signaling and dedifferentiation, tubuloids generated from the kidneys of transgenic mice, which express GFP under the control of the vimentin ("Vim-GFP") or the Sox9 promoter ("Sox9-GFP"), respectively, were studied. To do so, tubuloids were treated with or without dex (100 nM) (workflow of Fig. 6 A). Single cells from dissociated tubuloids were then analyzed by FACS (Fig. 8 A). Interestingly, dynamic changes in the percentage of GFP-positive cells were observed in both Sox9-GFP (Fig. 8 B-D) and Vim-GFP tubuloids (Fig. 8 E, F). The percentage of GFP-positive cells in Vim-GFP tubuloids started to increase earlier but also to reduce earlier than in Sox9-GFP tubuloids (Fig. 8 B, E). At day 2, Sox9-GFP tubuloids treated with dex displayed a decrease in the percentage of GFP-positive cells (Fig. 8 C). In Sox9-GFP tubuloids, towards the end of the observation period (i.e. at day 7), the percentage of GFP-positive cells declined in control tubuloids, but was still rising in dex-treated tubuloids (Fig. 8 B). Similarly, in Vim-GFP tubuloids, the percentage of GFP-positive cells in control tubuloids started to go down at day 5, while it still increased in dex-treated tubuloids until day 6 (Fig. 8 F). In other words, dex treatment significantly increased the percentage of GFP-positive cells in both Sox9-GFP (Fig. 8 D) and Vim-GFP (Fig. 8 F) tubuloids at day 7, when veh-treated tubuloids already re-differentiated (as indicated by a decrease in GFP-positive cells).

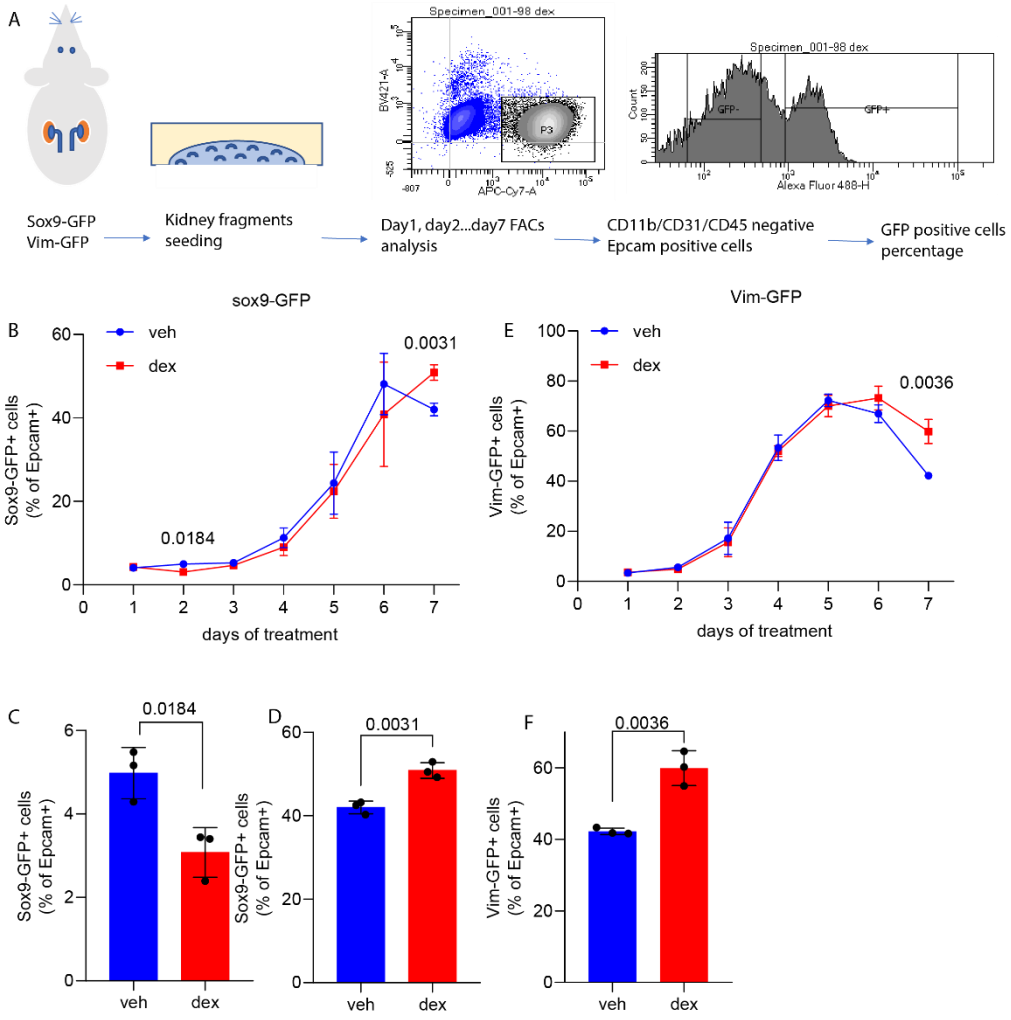

Fig. 8. Dexamethasone treatment affects the expression of sox9 and vimentin in tubuloids. A. Workflow for the FACS analysis of the percentage of GFP-positive (GFP+) cells. Dex (dex 1 and dex 2 represent 100nM and 1 µM of dex treatment, respectively) treatment was started from day 1. **B.** Quantification of GFP+ cells in renal tubuloids from Sox9-GFP mice (mean ± SD). **C.** Quantification results at day 2 of B in more detail (mean ± SD; One-way ANOVA, Tukey test). **D.** Quantification results at day 7 of B in more detail (mean ± SD; One-way ANOVA, Tukey test). **E.** Quantification of GFP+ cell percentage of renal tubuloids from Vim-GFP mice (mean ± SD). **F.** Quantification results at day 7 of E in more detail (mean ± SD; One-way ANOVA, Tukey test). Sox9-GFP, Sox9 GFP knock-in mouse strain; Vim-GFP, Vim-EGFP BAC transgene mouse strain; veh, vehicle; dex, dexamethasone.

6.2.4 Dexamethasone treatment affects the expression of differentiation markers in tubuloids

To confirm these results of 6.2.3 with an independent experimental approach, the effect of dex on differentiation of tubuloids was analyzed by fluorescence staining for

the differentiation marker LTL at day 7. In addition, proliferation was visualized by Ki67 immunostaining. Indeed, dex treatment affected the normal localization of LTL in tubuloids, independently of whether dex was applied from day 1 (Fig. 9 A, B) or day 3 (Fig. 9 C, D). Ki67 expression was not affected by dex treatment (Fig. 9 E). Taken together, these data show that activation of the GR by dex inhibits the dedifferentiation-redifferentiation sequence in tubuloids.

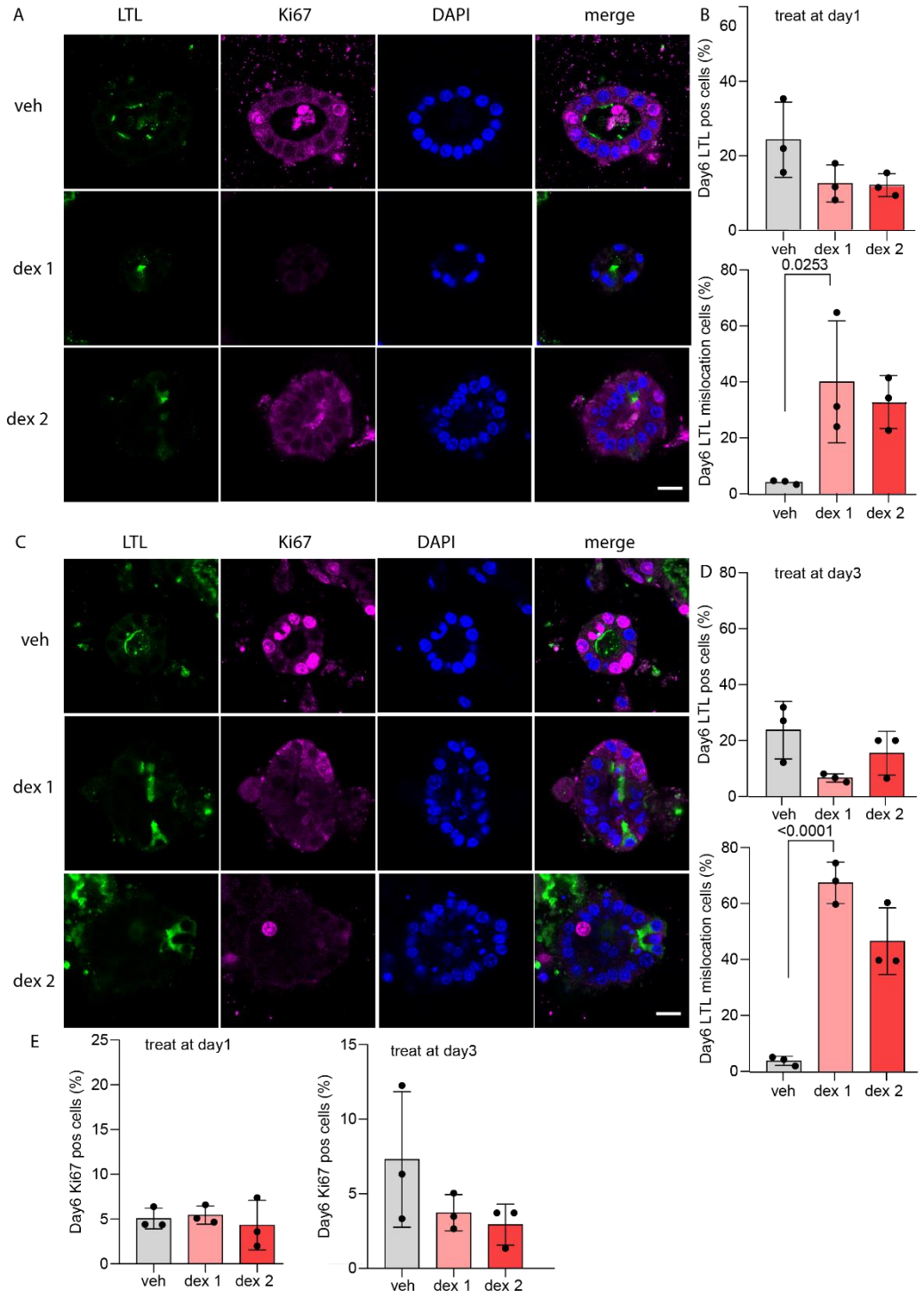

Fig. 9. Dexamethasone treatment affects the expression of differentiation markers in tubuloids. A. Confocal images of immune fluorescence (IF) stainings of tubuloids at day 7 using anti-Ki67 (fuchsia) antibody and lectins LTL (green) (scale bar, 10 µm). Blue: DAPI. Dex (dex 1 and dex 2 represent 100nM and 1 µM of dex treatment, respectively) was added from day 1. **B.** Quantification of LTL-positive cells and LTL mislocalization. Dex was added from day 1. **C.** Confocal images of IF stainings of tubuloids at day 7 using anti-Ki67 (fuchsia) antibody and lectins LTL (green) (scale bar, 10 µm). Blue: DAPI. Dex was added from day 3. **D.** Quantification of LTL-positive cells and LTL mislocalization. Dex was added from day 3. **E.** Quantification of Ki67- positive cells. Dex was added from day1 (left) or day 3 (right). veh, vehicle; dex, dexamethasone.

6.2.5 Dexamethasone treatment inhibits the formation of human tubuloids

To test whether dex treatment could affect epithelial plasticity of human renal epithelia, the culture of human kidney organoids (tubuloids) from adult patient-derived kidney tissue was established. Single cells were then dissociated from passaged human tubuloids and re-seeded back to matrigel to re-establish tubuloids. Dex (100 nM or 1 µM) treatment was added at the day after seeding (Fig. 10 A), and tubuloid numbers were quantified after 2 weeks (Fig. 10 B). Indeed, dex treatment inhibited the formation of human tubuloids. This phenotype was stronger than in mouse tubuloids, in which formation of tubuloids was delayed by dex, but not reduced.

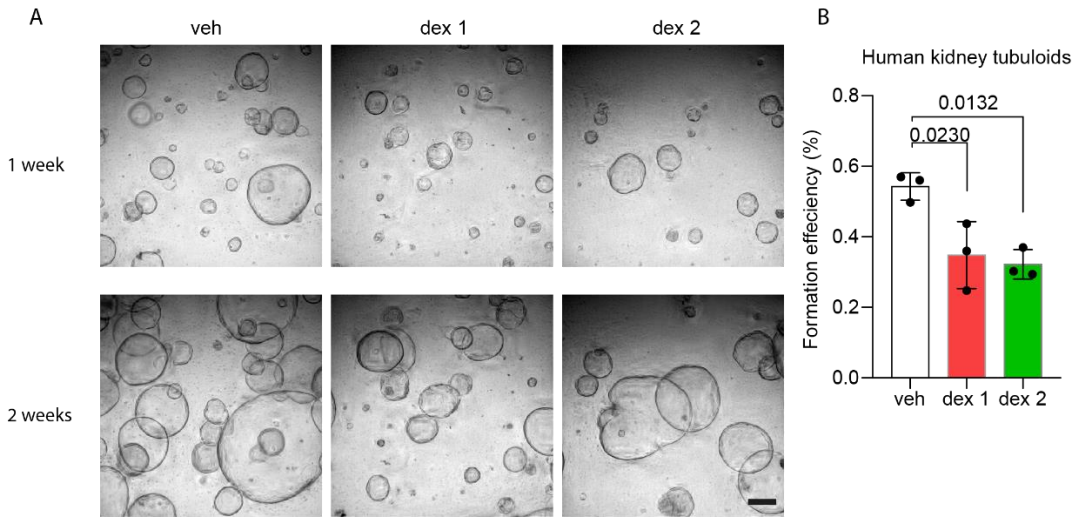

Fig. 10. Dexamethasone treatment inhibits the formation of human tubuloids. A. BF images of human tubuloids after 1 week and 2 weeks of culture. Dex (dex 1 and dex 2 represent 100nM and 1 µM of dex treatment, respectively) treatment was started the day after seeding. Scale bar, 100 µm. **B.** Quantifications of tubuloid formation 2 weeks after

beginning the culture (mean ± SD; One-way ANOVA, Tukey test). veh, vehicle; dex, dexamethasone.

6.3 Dexamethasone aggravates myoglobin-induced injury of tubuloids

6.3.1 Dexamethasone treatment aggravates damage of mouse tubuloids

It has been postulated that a progenitor-like phenotype renders TECs more resistant to stressors such as ischemia (Bonventre et al., 2011; Tata et al., 2016). To induce damage, myoglobin ("myo") (20 mg/ml) was added to passaged mouse tubuloids for 3 days, and the tubuloid damage score was analyzed based on the PI staining. To test the effect of dex on tubuloid damage, the tubuloids were also treated with or without dex (100 nM) starting from the beginning of myo treatment. While slightly increasing damage already under basal conditions, dex strongly aggravated myo-induced tubular injury (Fig. 11)

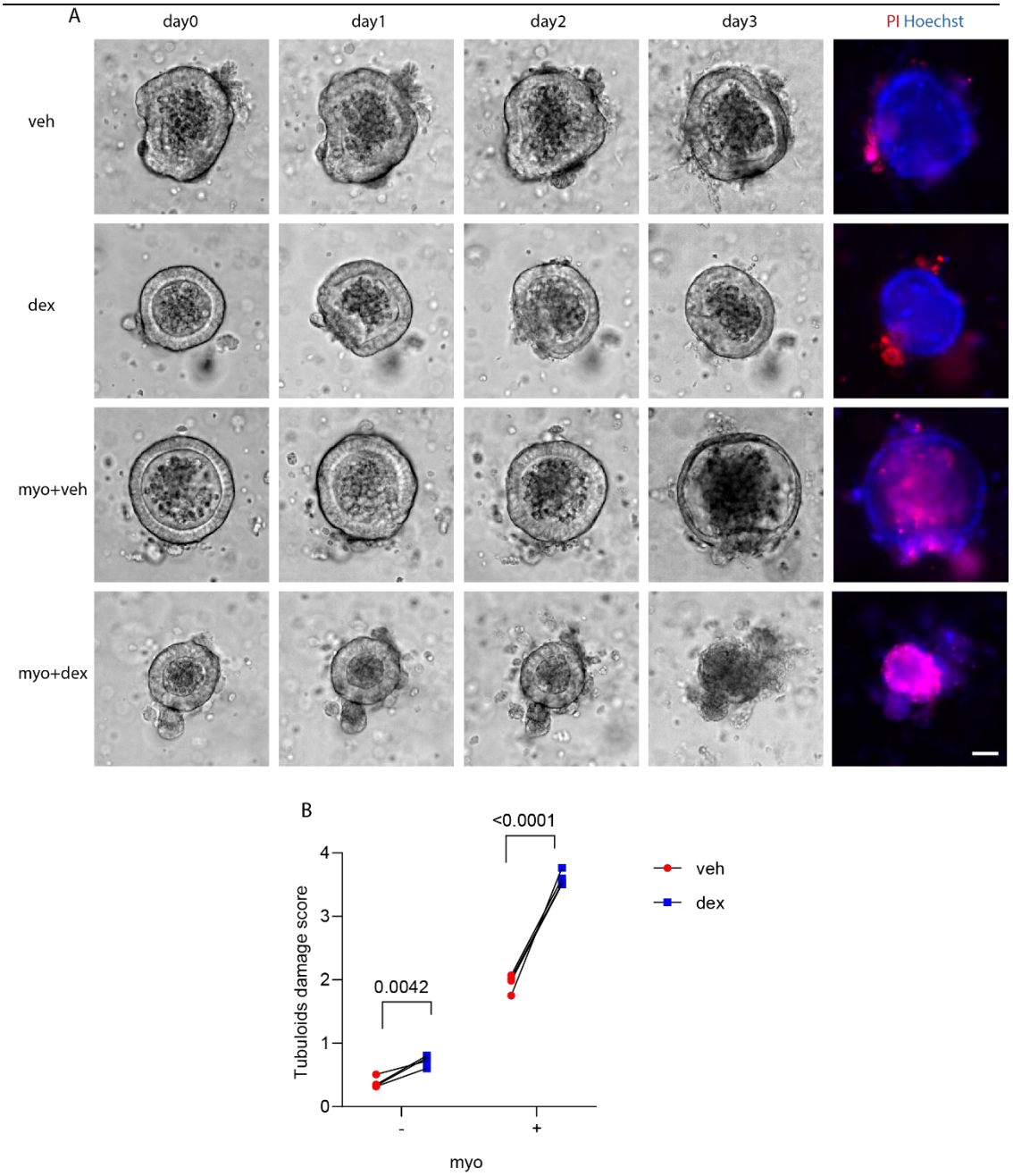

Fig. 11. Dexamethasone treatment aggravates the damage of mouse tubuloids. A. Representative BF and fluorescence images of mouse tubuloids. Tubuloids were treated with myo (20 mg/ml) and/or dex (100 nM) as indicated. Myo treatment was for 3 days. PI/Hoechst staining was performed at day 3 of myo treatment (Scale bar, 10 µm). **B.** Quantifications of tubuloid damage score (mean ± SD; One-way ANOVA, Tukey test). veh, vehicle; dex, dexamethasone; myo, myoglobin.

6.3.2 Dexamethasone treatment aggravates the damage of human tubuloids

An experiment, analogous to the experiment described in 6.3.1 for mouse tubuloids, was also performed with passaged human tubuloids. The results were highly similar to

those observed for mouse tubuloids (Fig. 12).

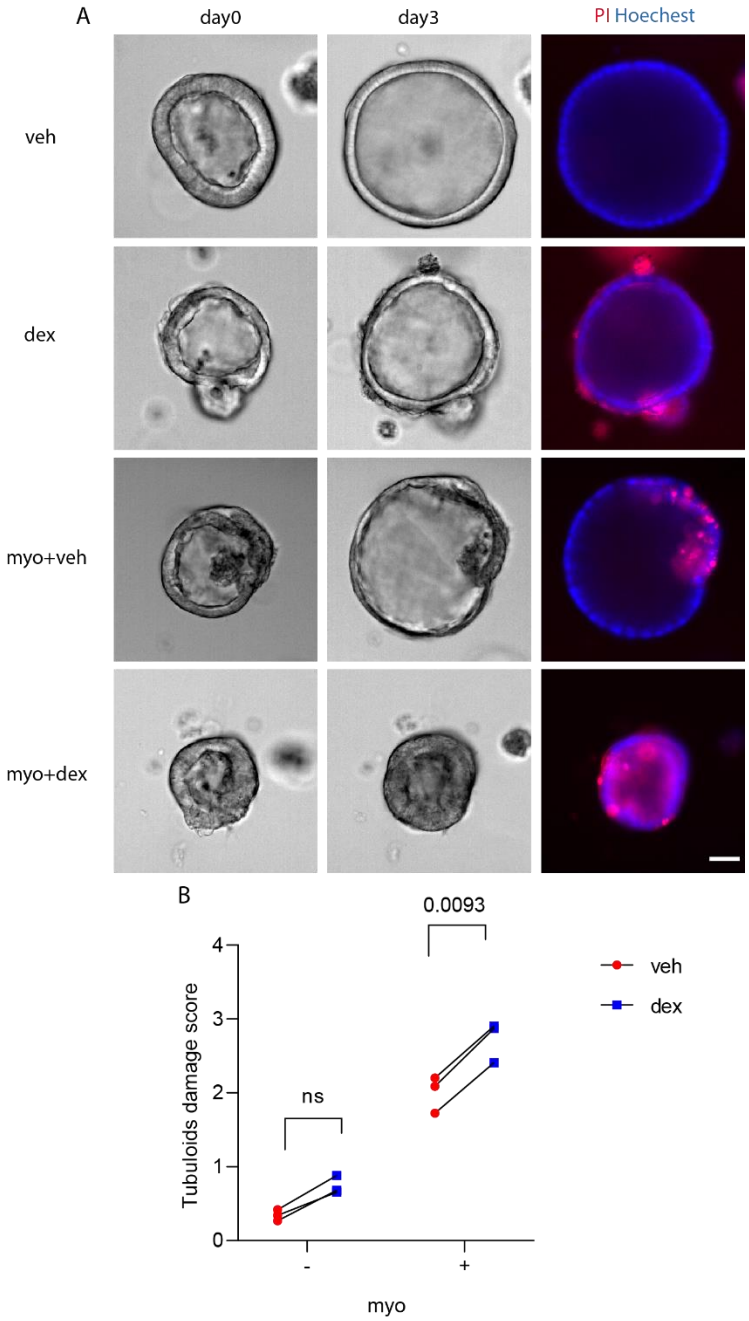

Fig. 12. Dexamethasone treatment aggravates the damage of human tubuloids. A. Representative BF and fluorescence images of tubuloids, treated with myo (20 mg/ml) and dex (100 nM) as indicated. Myo was added for 3 days. PI/Hoechst staining was performed at day 3 of myo treatment (Scale bar, 50 µm). **B.** Quantifications of the tubuloid damage score (mean ± SD; One-way ANOVA, Tukey test). veh, vehicle; dex, dexamethasone; myo, myoglobin.

6.3.3 Glucocorticoid receptor deficiency promotes mitochondrial respiration of

tubuloids.

To directly assess the role of the GR in tubuloids, tubuloid cultures from mice lacking the GR specifically in rTECs were generated (termed here “GR KO”). Tubuloids from mice carrying floxed alleles of the GR-encoding gene (Nr3c1) served as controls. qPCR analyses validated the loss of Nr3c1 gene expression in tubuloids (Fig. 13 A). It is known that the GR can control metabolic functions of cells (Weikum et al., 2017) and alterations of metabolic pathways or metabolites are involved in epithelial cell differentiation (Ju et al., 2021; Martínez-Reyes et al., 2020). It was therefore hypothesized that the GR could modulate epithelial plasticity in tubuloids through a regulation of cellular metabolism. Bioenergetic analyses (Seahorse) of tubuloids indeed showed that GR deficiency led to significantly increased basal and maximal oxygen consumption rates (OCR), a measure for mitochondrial function (Fig. 13 B, D). There was also a trend towards an increased extracellular acidification rate (ECAR) and OCR/ECAR ratio; however, this was not statistically significant (Fig. 13 C, E, F). In light of the elevated mitochondrial respiration in tubuloids lacking the GR, a higher ATP production rate was postulated for these tubuloids. This hypothesis could be experimentally confirmed (Fig. 13 G).

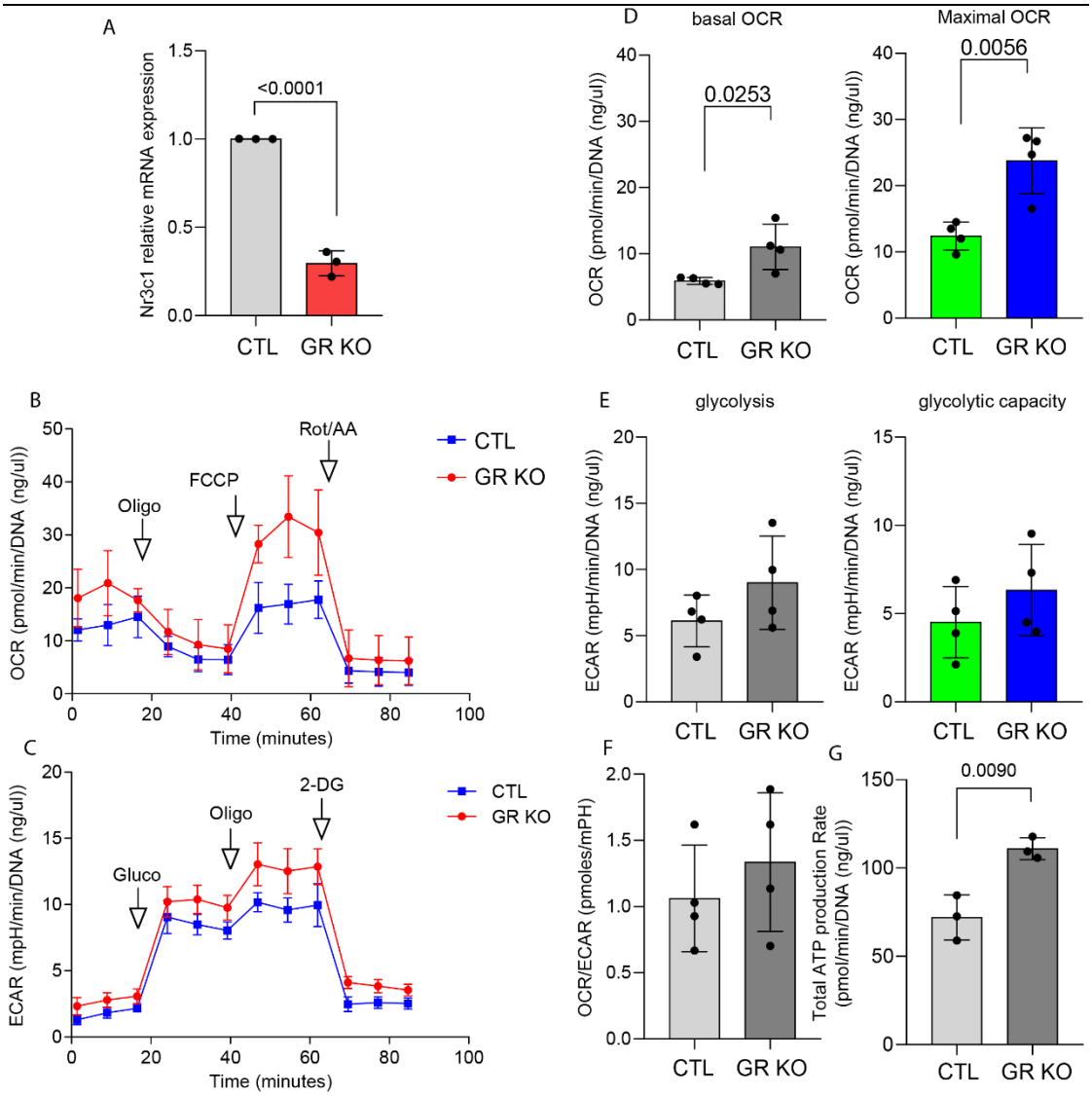

Fig. 13. Knockout of the glucocorticoid receptor promotes mitochondrial respiration of tubuloids. A. Relative mRNA expression of Nr3c1 in CTL and GR KO tubuloids (mean ± SD; unpaired t-test). **B.** Effect of GR KO on basal and maximal OCR in tubuloids. **C.** Effect of GR KO on ECAR in tubuloids. **D.** Quantification of basal and maximal OCR values in CTL and GR KO tubuloids (mean ± SD; unpaired t-test). **E.** Quantification of glycolysis and glycolytic capacity values in CTL and GR KO tubuloids (mean ± SD; unpaired t-test). **F.** Effect of GR KO on the basal OCR/ECAR ratio in tubuloids (mean ± SD; unpaired t-test). **G.** Total cellular ATP production in CTL and GR KO tubuloids (mean ± SD; unpaired t-test). CTL, control tubuloids; GR KO, GR-deficient tubuloids; OCR, oxygen consumption rate; ECAR, extracellular acidification rate.

6.3.4 Deficiency of glucocorticoid receptor promotes the expression of enzymes of respiration of tubuloids.

In line with the findings in 6.3.3, GR deficiency increased the expression of several enzymes known to be involved in oxidative phosphorylation (OXPHOS), such as

NDUFB6 (Fig. 14 A), and of mitochondrial biogenesis markers, such as PGC-1α and PGC-1β (Fig. 14 C). In addition, some of the enzymes involved in glycolysis were also found to be increased in GR-deficient tubuloids (Fig. 14 B). In summary these results indicate an important role of the GR in tubuloid metabolism, particularly in mitochondrial respiration.

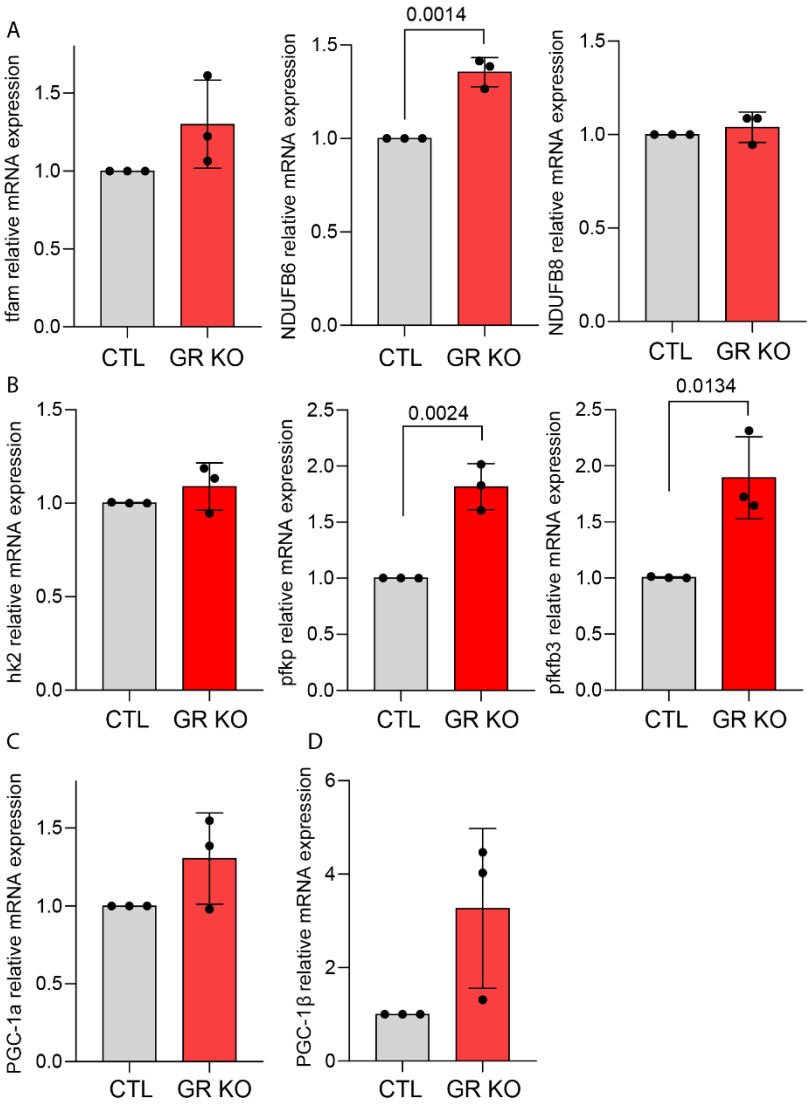

Fig. 14. Deficiency of glucocorticoid receptor promotes the expression of enzymes of respiration in tubuloids. A. Relative mRNA expression of oxidative phosphorylation enyzmes in CTL and GR KO tubuloids (mean ± SD; unpaired t-test). **B.** Relative mRNA expression of glycolytic enyzmes in CTL and GR KO tubuloids (mean ± SD; unpaired t-test). **C. and D.** Relative mRNA expression of PGC-1α and PGC-1β in CTL and GR KO tubuloids (mean ± SD; unpaired t-test). CTL, control tubuloids; GR KO, GR-deficient tubuloids; tfam, transcription factor A, mitochondrial; NDUFB6, oxidoreductase subunit B6; NDUFB8, oxidoreductase subunit B8; hk2, hexokinase 2; pfkp, phosphofructokinase, platelet; pfkfb3, 6-phosphofructo-2-kinase/fructose-2,6-biphosphatase 3; PGC-1α, peroxisome proliferative activated receptor, gamma (PPARG), coactivator 1 alpha; PGC-1β, PPARG coactivator beta.

6.3.5 Deficiency of glucocorticoid receptor alterates the mitochondrial membrane potential in tubuloids

To further investigate the connection between the GR and mitochondrial function, the mitochondrial membrane potential of control and GR-deficient tubuloids was measured using MitoTracker DeepRed dyes (R. Zhou et al., 2011). Using this approach, the mitochondrial membrane potential was found to be elevated in GR KO tubuloids as compared to CTL tubuloids at day 4 of culture (Fig. 15) (work flow of Fig. 6 A).

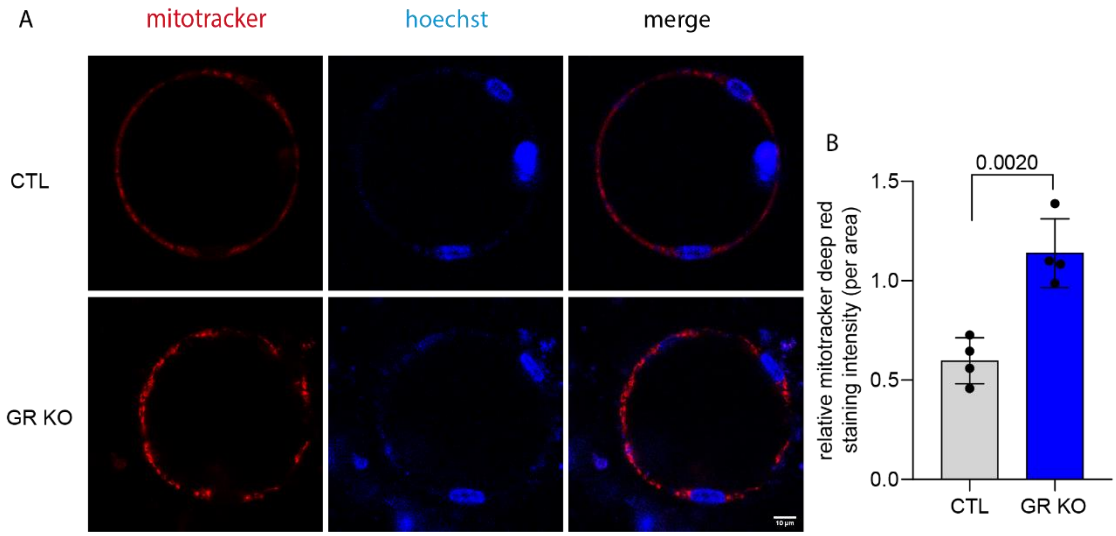

Fig. 15. Knockout of glucocorticoid receptor alters the mitochondrial membrane potential in tubuloids. A. Representative confocal images of MitoTracker DeepRed dye staining of CTL and GR KO tubuloids. Blue: Hoechst 33342 (Scale bar, 10 µm). **B.** Quantification of relative mitotracker deep red staining intensity in CTL and GR KO tubuloids (mean ± SD; unpaired t-test). CTL, control tubuloids; GR KO, GR-deficient tubuloids.

6.3.6 Inhibition of glycolysis has no major impact on the viability of GR-deficient tubuloids

In a next step, a potential causal relationship between GR-regulated metabolism and viability was tested. To do so, control and GR-deficient tubuloids were exposed to 2-Deoxy-D-glucose (2-DG), an inhibitor of glycolysis. Under basal conditions, i.e. without myo-induced injury, GR-deficient tubuloids were less sensitive to 2-DG treatment as compared to control tubuloids, indicating that the surviving of GR-deficient tubuloids relied less on glycolysis than on mitochondrial function (Fig. 16). This was fully consistent with the results obtained in 6.3.3, showing a shift of GR-deficient tubuloids towards increased mitochondrial respiration. After combined myo and 2-DG treatment,

both CTL tubuloids as well as tubuloids lacking the GR were largely dead (score 4); this impaired a valid interpretation of the role of GR-regulated metabolism after injury.

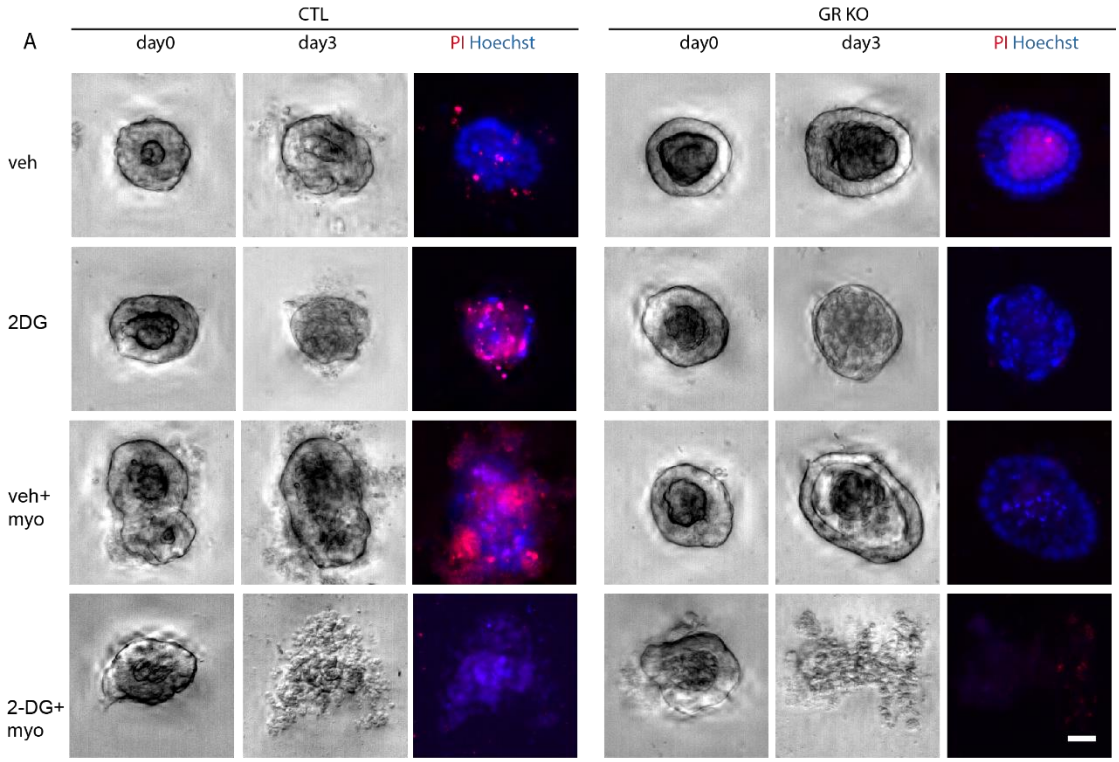

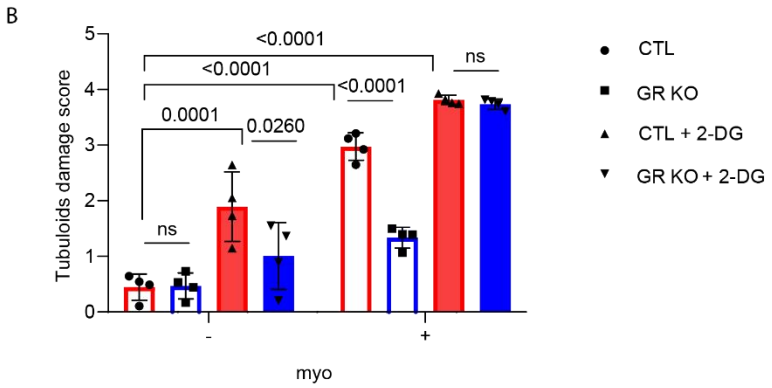

Fig. 16. Inhibition of glycolysis has no major impact on the viability of GR-deficient tubuloids. A. Representative BF and fluorescence images of vehicle, 2-DG (20 µM) and myo (30 mg/ml) treated CTL and GR KO tubuloids. Myo and 2-DG were added for 3 days. PI/Hoechst staining was performed after 3 days of myo treatment (Scale bar, 10 µm). **B.** Quantifications of tubuloid damage scores (mean ± SD; One-way ANOVA, Tukey test). 2DG, 2-Deoxy-D-glucose; myo, myoglobin; CTL, control tubuloids; GR KO, GR-deficient tubuloids.

6.3.7 Inhibition of oxidative phosphorylation lowers viability of GR-deficient tubuloids

OXPHOS can be blocked by oligomycin (oligo), an inhibitor of the mitochondrial ATP synthase (complex V). Interestingly, oligo blunted the protective effect of GR deficiency on tubuloid viability under basal conditions (Fig. 17). This increased sensitivity of GR KO tubuloids to oligo was fully in line with the findings in 6.3.3, which had shown elevated mitochondrial respiration of GR-deficient tubuloids. In summary, these data show that the protective effects of the GR on tubuloid viability are, at least in part, mediated by promoting mitochondrial respiration.

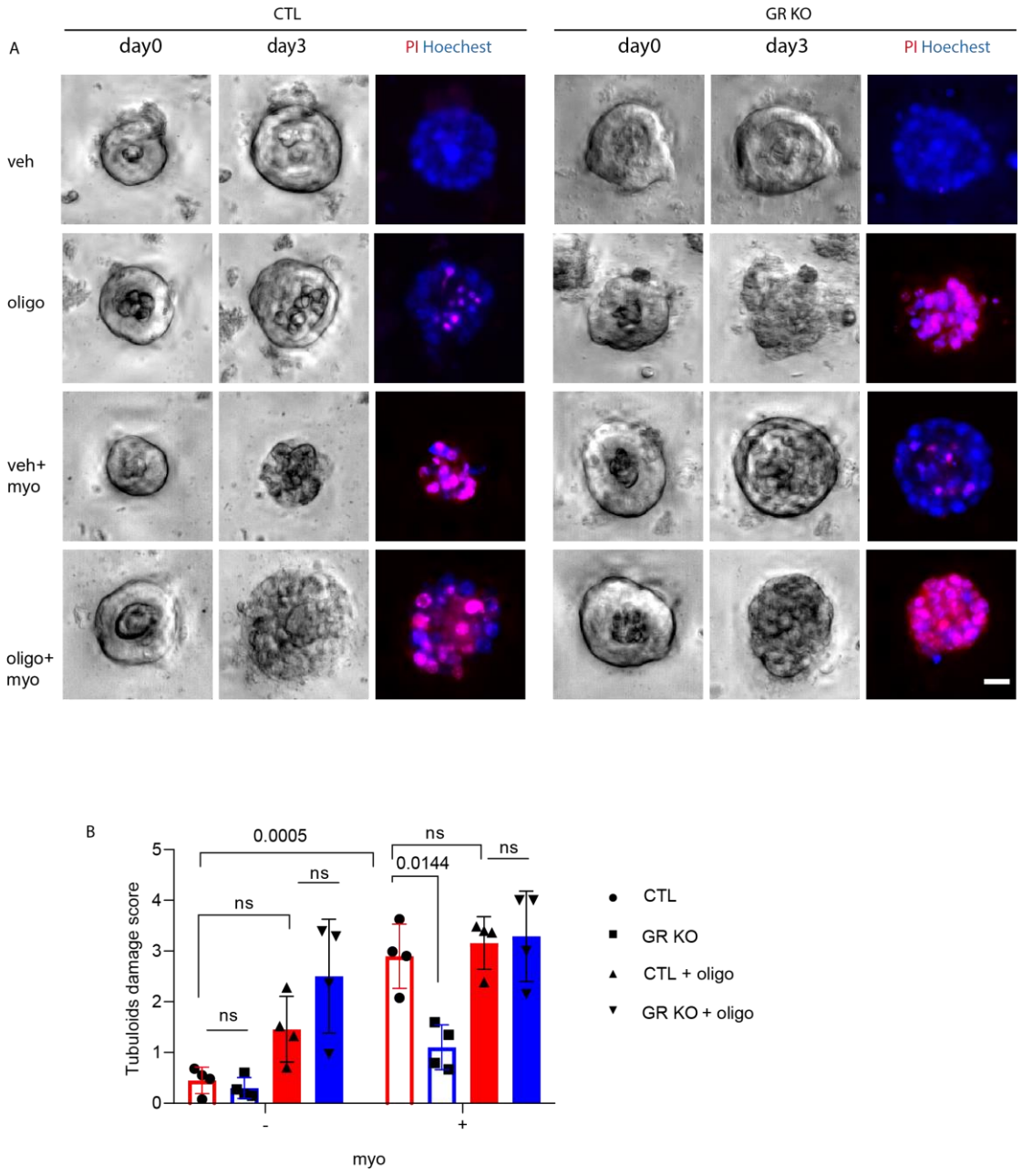

Fig. 17. Inhibition of oxidative phosphorylation lowers viability of GR-deficient tubuloids. A. Representative BF and fluorescence images of veh, oligo (0.1 µg/ml) and myo (30 mg/ml) treated CTL and GR KO tubuloids. Myo, veh and oligo were added for 3 days.

PI/Hoechst staining was performed at day3 of myoglobin treatment. (scale bar, 10 µm). **B**. Quantifications of tubuloids damage score of A (mean ± SD; One-way ANOVA, Tukey test). veh, vehicle; oligo, oligomycin; myo, myoglobin; CTL, control tubuloids; GR KO, GR-deficient tubuloids.

6.4 The regulation of the mTOR pathway by GR is functionally relevant for tubuloid injury

6.4.1 Dexamethasone potentially inhibits the mTOR pathway activity in kidney cell lines

The mTOR pathway is central to the control of cellular metabolism (Brugarolas et al., 2004) (Efeyan et al., 2013; Kalender et al., 2010). It was therefore hypothesized that the GR could modulate cellular metabolism through a regulation of mTOR signaling. To test this hypothesis, firstly two renal epithelial cell lines, mIMCD-3 and HK2, were treated with dex (1 µM) for 24 hours, and total mTOR and phosphorylated mTOR (p-mTOR) levels were detected by Western blotting. As shown in Fig. 18, a decrease of p-mTOR was detected in both of the cell lines however, also total mTOR protein expression showed a significant decrease in the HK2 cell line.

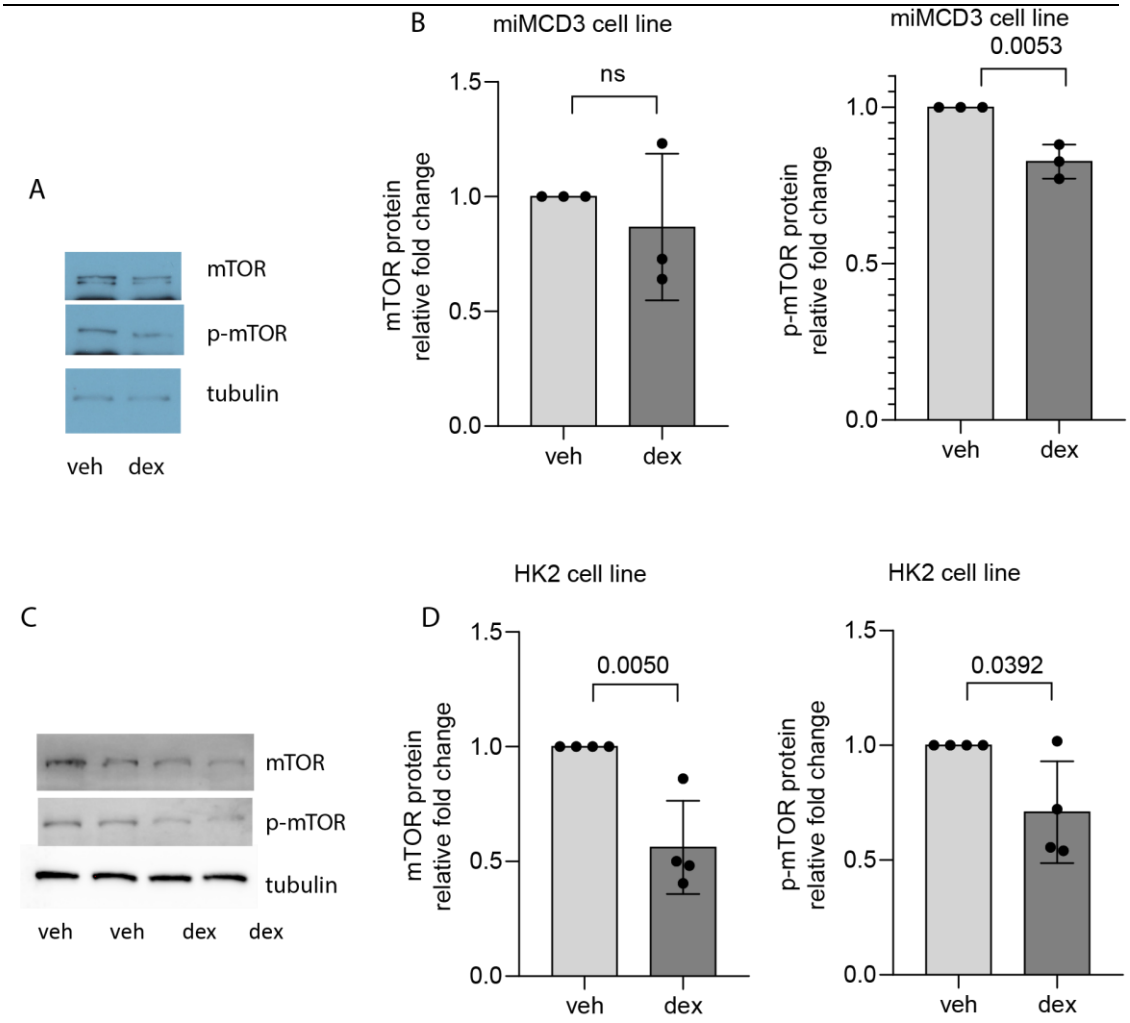

Fig. 18. Dexamethasone potentially inhibits mTOR pathway activity in kidney cell lines. **A.** Western blotting results for mTOR and p-mTOR in the mIMCD-3 cell line, which was treated with veh or dex (1 µM) for 24 hours. **B.** Quantifications of mTOR and p-mTOR levels (fold change) of A, normalized to tubulin (mean ± SD; n=3; unpaired t-test). **C.** Western blotting results for mTOR and p-mTOR in the HK2 cell line, which was treated with veh or dex (1 µM) for 24 hours. **D.** Quantifications of mTOR and p-mTOR protein levels (fold change) of C, normalized to tubulin (mean ± SD; n=4; unpaired t-test). veh, vehicle; dex, dexamethasone.

6.4.2 Glucocorticoid receptor deficiency promotes the activation of the mTOR pathway

As a next step after analyzing the effect of a pharmacological activation of the GR on mTOR, the effect of an siRNA-mediated knockdown of the GR on mTOR was examined in the mIMCD-3 cell line. As shown in Fig. 19, a significant increase of mTOR phosphorylation was detected by Western blotting. Taken together with the results in 6.4.1, the data suggest that the activation of GR with dex inhibits mTOR activity in rTECs.

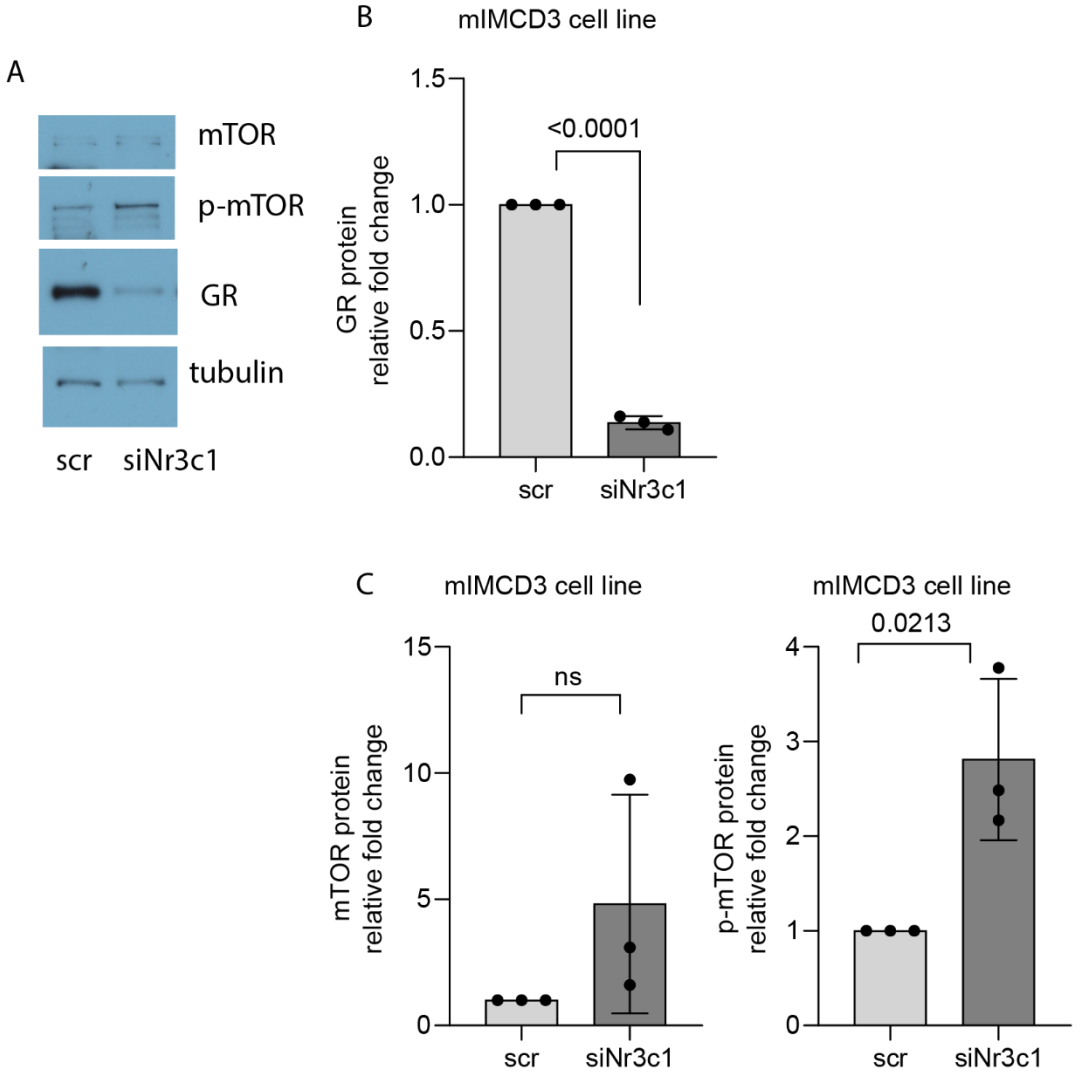

Fig. 19. Deficiency of glucocorticoid receptor promotes the activation of the mTOR pathway. A. Western blotting results of mIMCD-3 cells using anti-GR, anti-mTOR and anti-p-mTOR after knockdown of Nr3c1 expression (encoding GR) by siRNA. **B.** Quantification of GR protein expression (fold change), normalized to tubulin (mean ± SD; n=3; unpaired t-test). **C.** Quantifications of mTOR and p-mTOR levels (fold change), normalized to tubulin (mean ± SD; n=3; unpaired t-test). Veh, vehicle; scr, scrambled RNA; siNr3c1, siRNA of Nr3c1 (coding GR).

6.4.3 mTOR activation in GR-deficient tubuloids is crucial for resistance to injury

Next, it was studied in tubuloids whether a regulation of mTOR activity by the GR was functionally relevant for susceptibility to injury and injury-induced dedifferentiation of epithelial cells. Rapamycin (rapa) was used as mTOR inhibitor. Under basal conditions, i.e. without myoglobin-induced injury, rapa treatment had no significant

effect on tubuloid morphology and viability (Fig. 20). Similarly, rapa did also not significantly influence the susceptibility of control tubuloids to myoglobin-induced injury. In contrast, the protective effect of a loss of GR on myglobin-induced tubuloid injury was blunted by rapamycin treatment (Fig. 20).

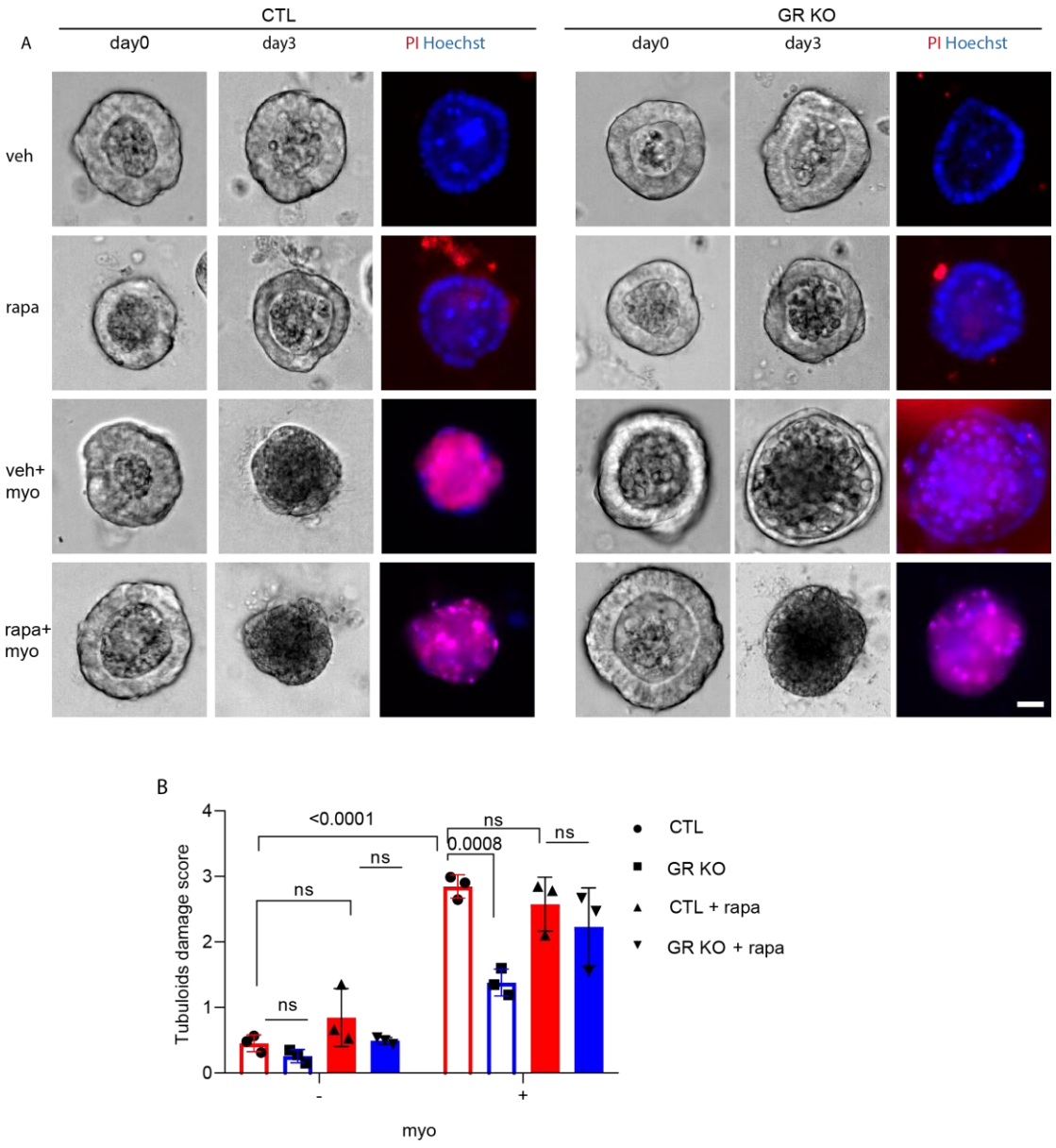

Fig. 20. mTOR activation in GR-deficient tubuloids is crucial for resistance to injury. **A.** Representative BF and fluorescence images of veh, rapa (10 µM) and myo (30 mg/ml) treated CTL and GR KO tubuloids. Myo, veh and rapa were treated for 3 days. PI/Hoechst staining was performed after 3 days of these treatments (Scale bar, 10 µm). **B.** Quantifications of tubuloid damage scores of the experiment depicted in A. (mean ± SD; n=3; One-way ANOVA, Tukey test). Veh, vehicle; rapa, rapamycin; myo, myoglobin; CTL, control tubuloids; GR KO, GR-deficient tubuloids.

6.5 GR signaling suppresses epithelial plasticity by inhibition of the Wnt/β-catenin pathway

6.5.1 Activation of the Wnt pathway rescues the suppressive effect of dexamethasone on tubuloid formation

The Wnt pathway is crucial in the development and regeneration of the epithelium in multiple organs, including, for example, the intestine and the kidney (Bastakoty et al., 2016; Sprangers et al., 2021; Westendorf et al., 2004). The key effector of the canonical Wnt pathway is β-catenin (Nelson et al., 2004). Dysregulation of the Wnt/β-catenin pathway has been implicated in various disesases such as cancer (tumorigenesis, tumor progression) and osteoporosis (Westendorf et al., 2004; White et al., 2012; Zhan et al., 2017). However, the role of the Wnt/β-catenin pathway in plasticity of rTECs and the link between GR and Wnt signaling are still open questions. To test for a potential connection between GR and Wnt/β-catenin signaling in rTECs, the formation of tubuloids was analyzed in the presence of dex (GR agonist) and CHIR, a widely used GSK-3 inhibitor that activates the Wnt pathway by suppressing β-catenin degradation (Tran et al., 2017; Z. Xu et al., 2016). As already described above (section 6.2.1), dex treatment delayed the sequence of morphological changes during tubuloid formation and decreased tubuloid numbers. Interestingly, application of CHIR could partially rescue these dex-induced effects, i.e. CHIR increased tubuloid numbers (Fig. 21 A-C) and promoted a cuboidal tubuloid morphology (Fig. 21 D, E).

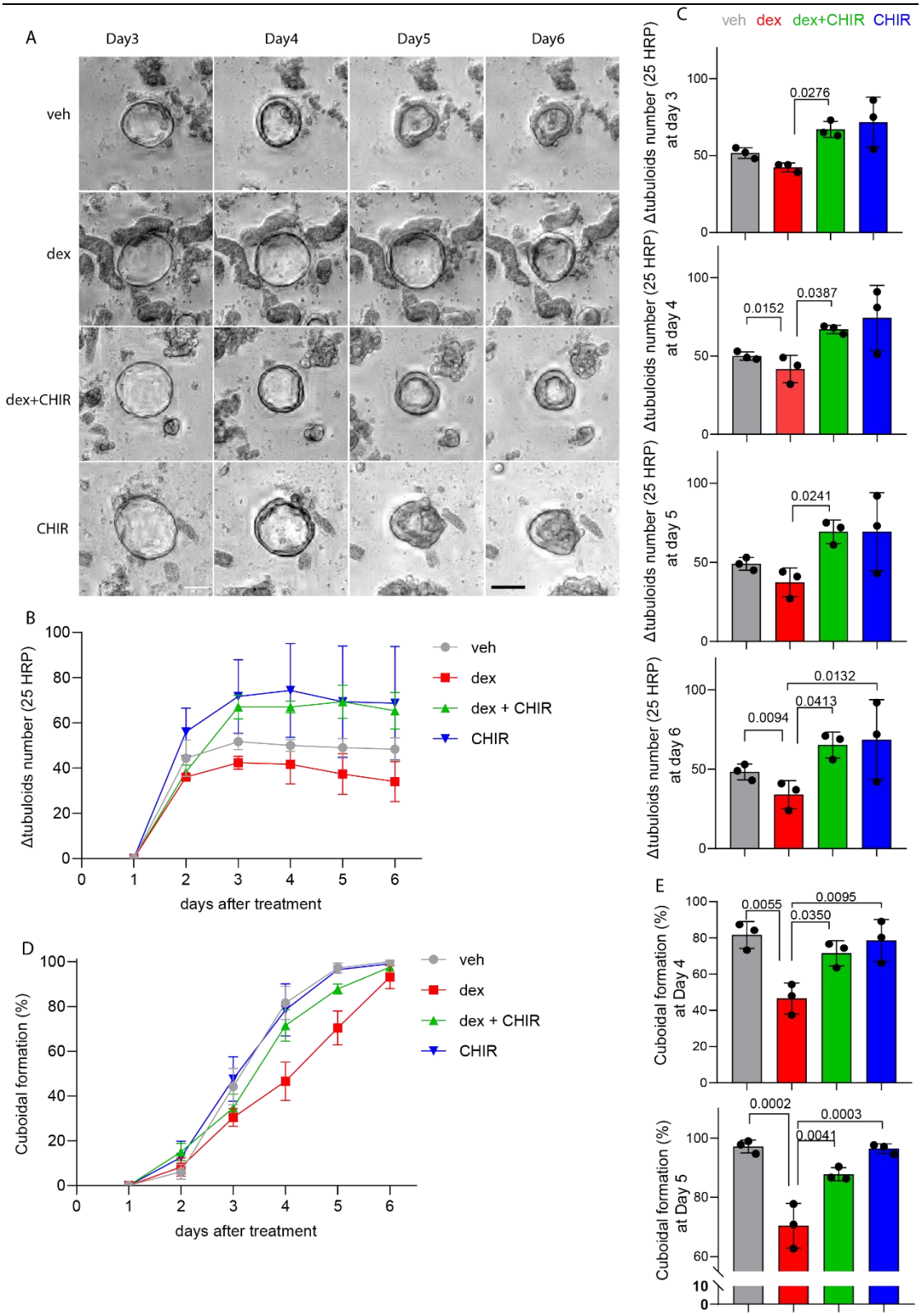

Fig. 21. Activation of the Wnt pathway rescues the suppressive effect of dexamethasone on tubuloid formation. A. Representative BF images of vehicle-, dex- (1 µM) and CHIR- (2 µM) treated tubuloids (same work flow as shown in Fig. 6 A.). All of the

treatments were started from day 1 onwards (scale bar, 50 µm). **B.** Quantification of tubuloid numbers. Tubuloid numbers were normalized (shown with Δ, see section 5.7.1.3) to day1 (mean ± SD; n=3). **C.** Quantifications of tubuloid numbers on different days of culture (mean ± SD; n=3; One-way ANOVA, Tukey test). Tubuloid numbers were normalized (shown with Δ, see section 5.7.1.3) to the number of day1. **D.** Quantification of the percentage of tubuloids with cuboidal cells (mean ± SD; n=3.). **E.** Quantification of cuboidal tubuloid formation on day 4 and day 5 of culture (mean ± SD; n=3; One-way ANOVA, Tukey test). veh, vehicle; dex, dexamethasone; CHIR, CHIR99021.

6.5.2 Dexamethasone treatment suppresses the Wnt/β-catenin pathway

To further test the connection between GR signaling and Wnt/β-catenin pathway, the expression of target genes of the Wnt/β-catenin pathway (AXIN2, TCF4, CD44, CCND1, CDH1, BCL9L) in the HK2 cell line was analyzed with or without dex (1 µM) and CHIR (2 µM) treatment. At basal conditions, dex treatment decreased the mRNA expression of AXIN2 (Fig. 22 A) and CD44 (Fig. 22 E). With CHIR treatment, relative mRNA expression level of AXIN2 (Fig. 22 A) and CCND1 (Fig. 22 C) were significantly upregulated in comparison to basal conditions. In CHIR-treated cells, dex treatment decreased the mRNA expression of AXIN2 (Fig. 22 A), TCF4 (Fig. 22 B), CCND1 (Fig. 22 C) and CD44 (Fig. 22 E), although statistical significance was not reached.

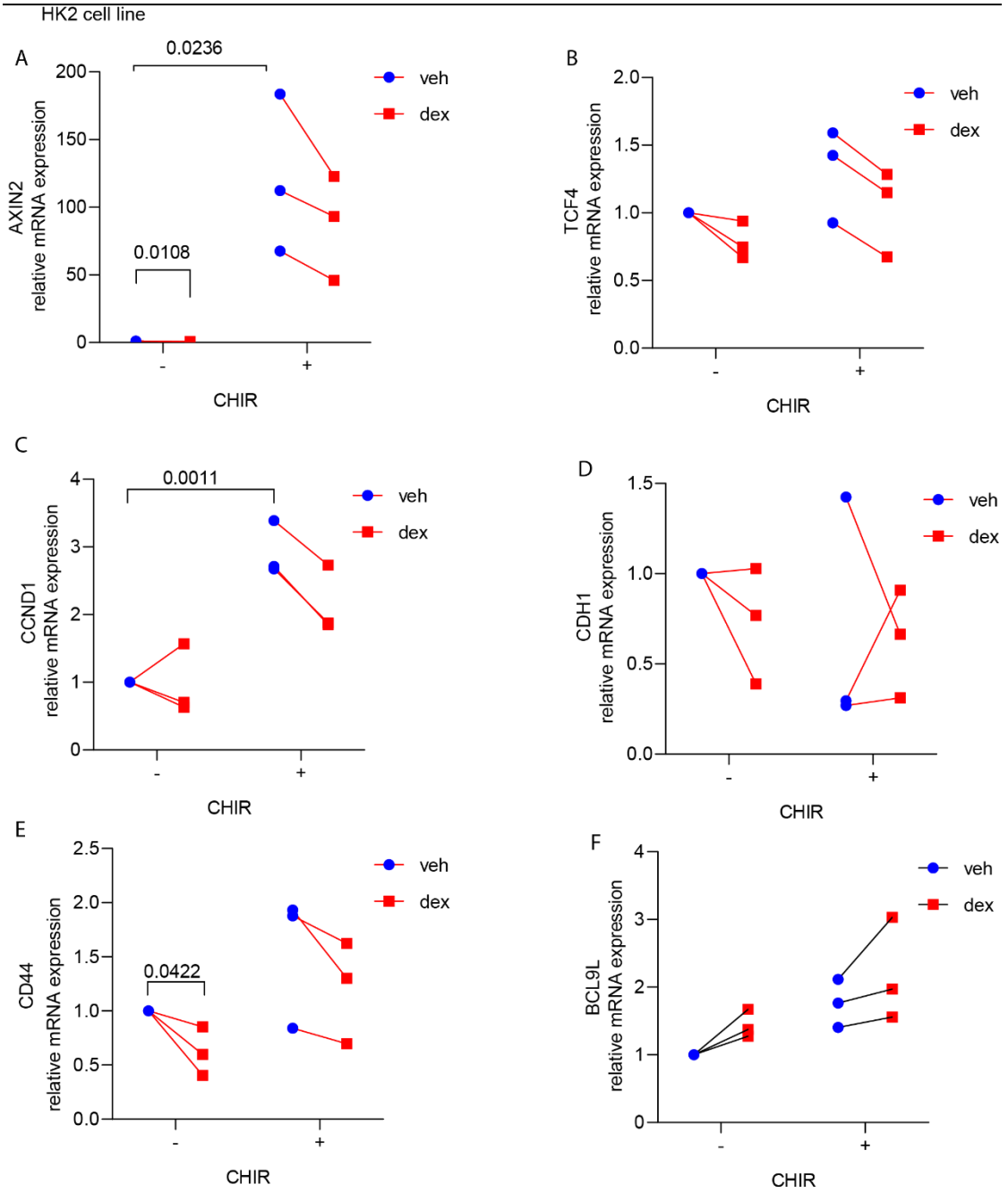

Fig. 22 Dexamethasone treatment partially inhibits CHIR-induced activation of the Wnt/β-catenin pathway. Relative mRNA expression of Wnt/β-catenin pathway target genes, including AXIN2 (**A**), TCF4 (**B**), CCND1 (**C**), CDH1 (**D**), CD44 (**E**), BCL9l (**F**), in HK2 cells with or without dex treatment (1 µM) and CHIR (2 µM) (mean ± SD; One-way ANOVA, Tukey test). veh, vehicle; dex, dexamethasone; CHIR, CHIR99021; TCF4, transcription factor 4; CCND1, cyclin D1; CDH1, cadherin 1; BCL9L, BCL9-like.

Secondly, to assess the level of the Wnt signaling pathway affected by GR signaling, the impact of dex on the activation of the Wnt/β-catenin pathway by Wnt3a was tested.

At basal conditions, dex treatment significantly downregulated the the expression level of CD44 (Fig. 23 E). In Wnt3a-stimulated cells, dex treatment decreased the mRNA expression of AXIN2 (Fig. 23 A) and CD44 (Fig. 23 E).

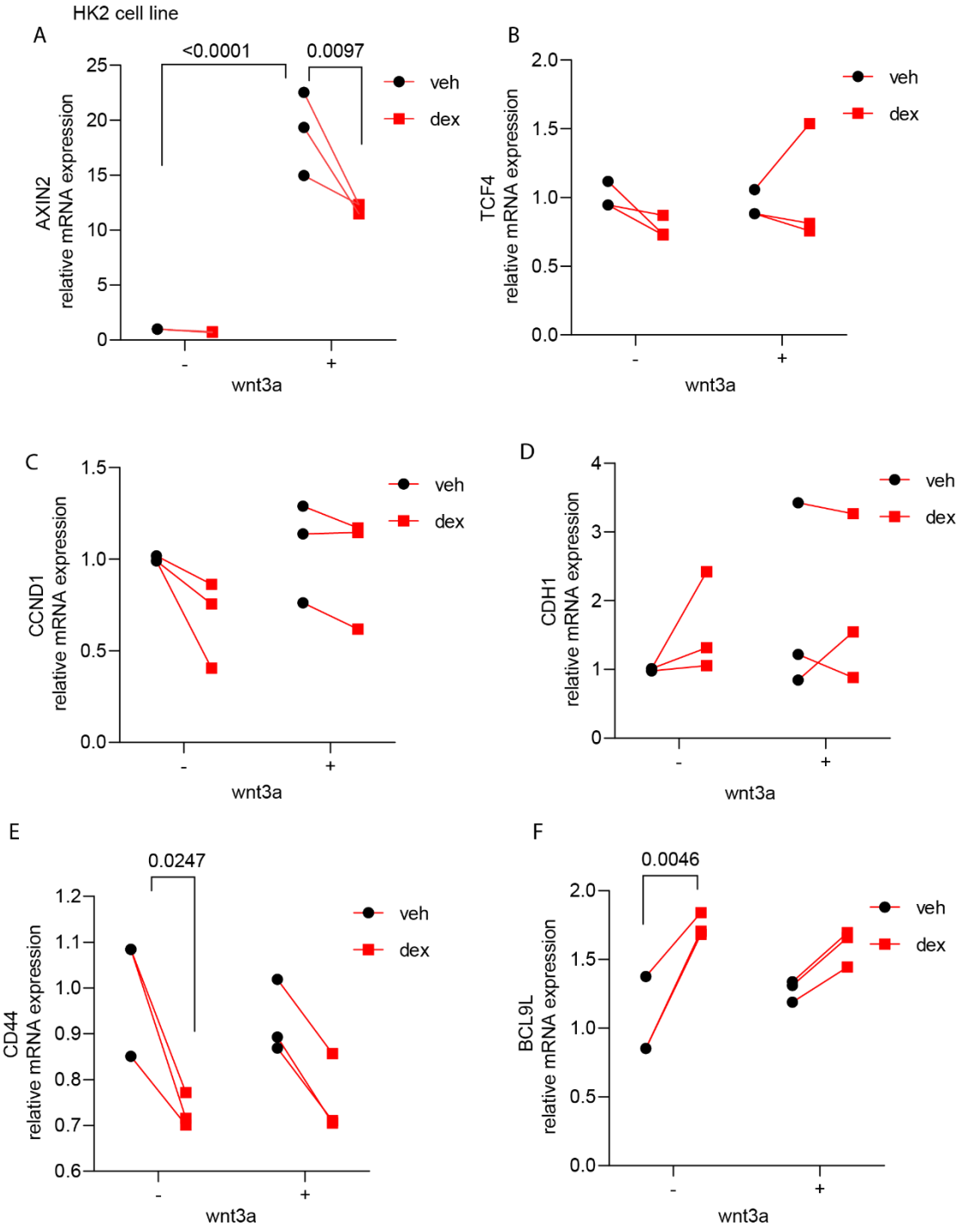

Fig. 23. Dexamethasone treatment partially suppresses Wnt3a-induced activation of the Wnt/β-catenin pathway. Relative mRNA expression levels of Wnt/β-catenin pathway target genes, including AXIN2 (**A**), TCF4 (**B**), CCND1 (**C**), CDH1 (**D**), CD44 (**E**), BCL9L (**F**),

in HK2 cells treated with or without dex (1 µM) and Wnt3a conditioned medium (40%) (mean ± SD; One-way ANOVA, Tukey test). veh, vehicle; dex, dexamethasone. TCF4, transcription factor 4; CCND1, cyclin D1; CDH1, cadherin 1; BCL9L, BCL9-like.

Moreover, the effect of dex on protein expression levels of total β-catenin was tested. As shown in Fig. 24, dex treatment tendenitially lowered the expression of β-catenin. However, these trends were not statistically significant.

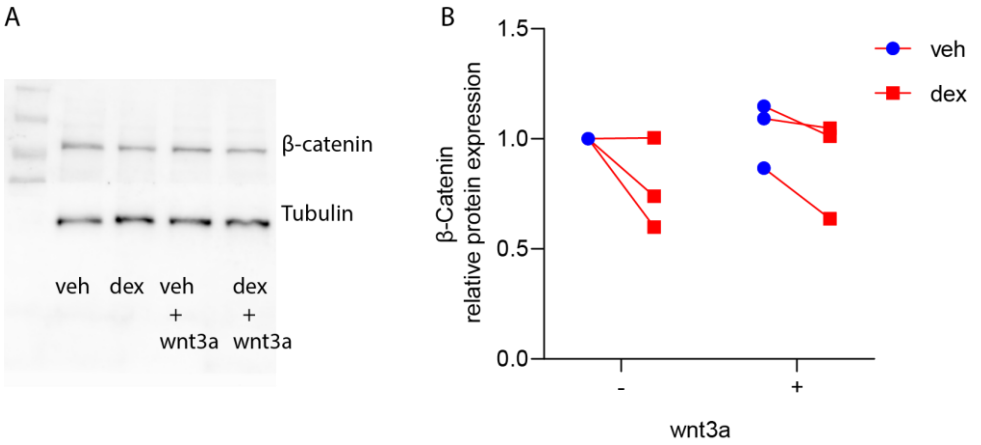

Fig. 24. Dexamethasone treatment might reduce protein expression of β-catenin. A. Representative western blots for β-catenin and tubulin of lysates from HK2 cells treated with veh, dex (1 µM) and/or wnt3a conditioned medium (40%) as indicated. **B**. Quantification of the results (mean ± SD; One-way ANOVA, Tukey test). veh, vehicle; dex, dexamethasone.

6.5.3 CHIR treatment promotes the expression of dedifferentiation marker of tubuloids

To investigate the connection between GR signaling, wnt/β-catenin pathway and dedifferentiation of rTECs, the tubuloids were treated with or without CHIR (2 µM) and dex (1 µM) from day 1 onwards for 24 hours (work flow of Fig. 6 A), the most important period for dedifferentiation of tubuloids as investigated previously (see sesion 6.2.1). At basal conditions, no difference of expression of vimentin between veh and dex treatment was observed (Fig. 25). With CHIR treatment, the expression of vimentin in tubuloids was significantly increased (Fig. 25). However, dex treatment significantly blocked the effect of CHIR and significantly down-regulated the expression of vimentin (Fig. 25). These results suggest that CHIR treatment promotes the dedifferentiation of tubuloids, while GR activation by dex partly blocks this effect of CHIR, and inhibits the dedifferentiation of rTECs after kidney injury.

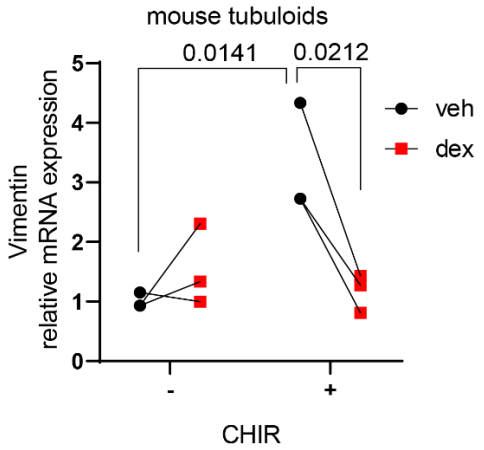

Fig. 25. CHIR treatment promotes the expression of dedifferentiation marker of tubuloids. Relative mRNA expression of vimentin in tubuloids at day1. Vehicle, dex (1 µM), CHIR (2 µM) treatment were added from day1 for 24 hours (mean ± SD; n=3; One-way ANOVA, Tukey test). veh, vehicle; dex, dexamethasone.

6.5.4 CHIR treatment promotes redifferentiation of tubuloids

To further test whether the Wnt signaling pathway plays an opposing role to the GR signaling pathway in the redifferentiation of tubuloids, IF stainings for LTL were performed on tubuloids at day7 (work flow of Fig. 6 A). This time point represents a late stage of tubuloid formation when cells have started to redifferentiate and re-express maturation markers. While under control conditions, around 20% of rTECs in tubuloids re-expressed LTL, CHIR treatment (added from day1 (Fig. 26) or day3 (Fig. 27), work flow of Fig. 6 A) increased LTL-positivity to 50%~60% of all rTECs, suggesting that CHIR can promote redifferentiation of tubuloids. In contrast, dex treatment (100 nM or 1 µM) partially decreased the LTL positivity of rTECs in tubuloids (Fig. 26, 27). Interestingly, a mislocation of LTL was observed in most of the dex-treated tubuloids (Fig. 26, 27). In these tubuloids, LTL was not located at the apical membrane of rTECs (Fig. 26 A, Fig. 27 A). To test the role of GR and Wnt pathway to the proliferation of rTECs, Ki67 IF staining was also performed at day7 (work flow of Fig. 6 A). No difference in the percentage of Ki67 positive cells was observed between veh and dex treatment groups (Figures 26 and 27). However, treating tubuloids with CHIR starting at day1 significantly increased the percentage of Ki67 positive cells (Fig. 26 B right), while CHIR treatment from day 3 onwards did not result in higher proliferative activity (Fig. 27 B right).

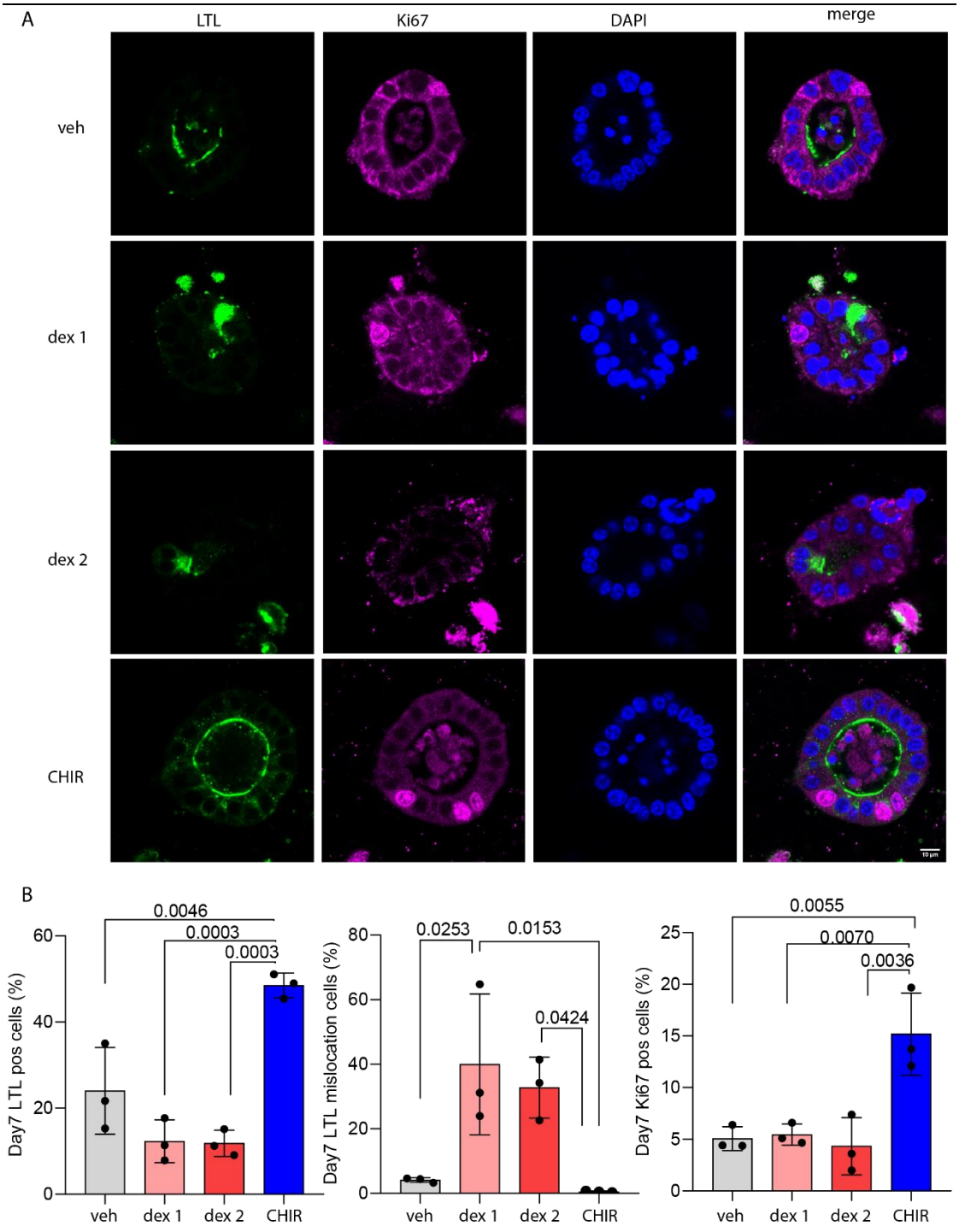

Fig. 26. CHIR treatment from day 1 onwards promotes redifferentiation of tubuloids. A. Representative confocal images of veh, dex 1 (100nM), dex2 (1 µM) and CHIR (2 µM) treated mouse tubuloids at day7 (work flow of Fig. 6 A) using the lectin LTL (green) (scale bar, 10 µm). Blue: DAPI. Dex, veh and CHIR treatment were started at day 1. **B**. Quantification of the percentage of LTL-positive cells, and quantification of the percentage of cells with a mislocation of LTL in the LTL-positive cells (mean ± SD; One-way ANOVA, Tukey test). veh, vehicle; dex, dexamethasone; CHIR, CHIR99021.

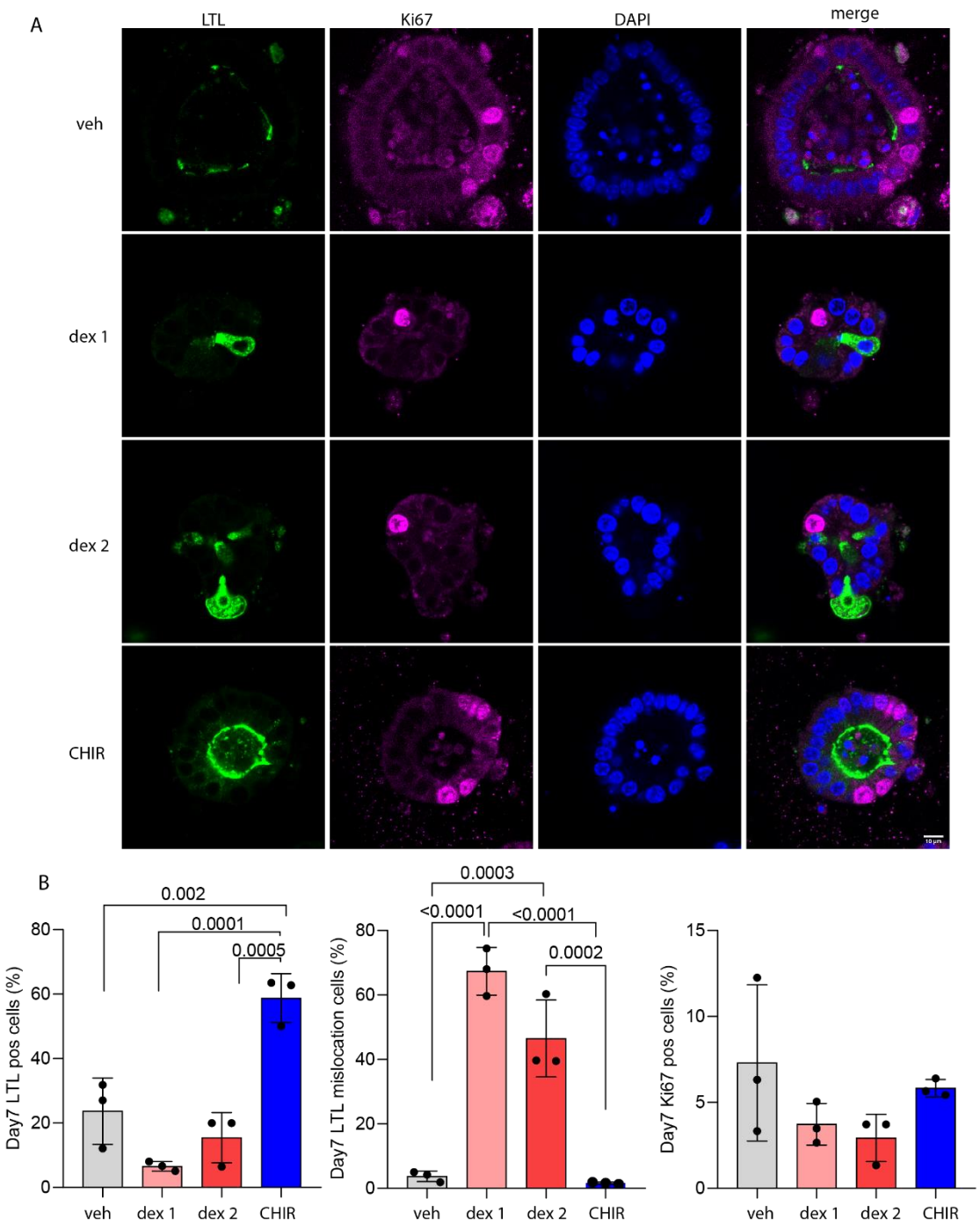

Fig. 27. CHIR treatment from day3 increases redifferentiation of tubuloids. A. Representative confocal images of vehicle, dex 1 (100nM), dex2 (1 µM) and CHIR (2 µM) treated mice tubuloids at day7 (work flow of Fig. 6 A) using the lectin LTL (green) (scale bar, 10 µm). Blue: DAPI. Dex, veh and CHIR treatment were started from day 3 onwards. **B**. Quantification of the percentage of LTL-positive cells, and quantification of the percentage of cells with a mislocation of LTL in the LTL-positive cells (mean ± SD; One-way ANOVA, Tukey test). Veh, vehicle; dex, dexamethasone; CHIR, CHIR99021.

7 DISCUSSION

After injury, the renal epithelium has a high regenerative capacity. Questions as to which cells are responsible for the regeneration of rTECs after injury and as to how the plasticity of rTECS is regulated on a molecular level have been unclear for decades. As a master transcription factor, the GR was addressed in this study due to its role as a central component of the cellular stress response.

7.1 Origin of regenerating tubular epithelial cells after acute kidney injury

7.1.1 Regeneration by surviving tubular epithelial cells

The cellular sources of renal regeneration after AKI are still controversial. Most of the studies propose that regeneration by surviving TECs after AKI is the predominant mechanism of repair after tubular injury in the adult mammalian kidney (Berger et al., 2014; Humphreys et al., 2011; Humphreys et al., 2008; Kusaba & Humphreys, 2014; Kusaba, Lalli, et al., 2014). However, some groups postulate that so-called scattered progenitor epithelial cells in the kidney are the source of regeneration of damaged rTECs, especially in the human kidney (Bussolati et al., 2005; K. Kim et al., 2008).

To test whether the surviving rTECs are the origin of regenerating TECs after AKI, firstly, the morphological and molecular characteristics of these surviving rTECs have been monitored. In this thesis, shifting of flat tubuloids to cuboidal tubuloids was observed during the formation of tubuloids. Consistent with the morphological changes, the expression of progenitor markers (including sox9 and vimentin) were increased at the early stage of the tubuloid formation (day1) and decreased at the late stage of tubuloid formation (day7). Interestingly, a peak of proliferative signals, depicted with Ki67 and bromodeoxyuridine (BrdU), have been observed 48 h after renal injury in studies previously, and regular epithelial morphology would be restored within 5–7 days (Humphreys et al., 2011; Little et al., 2017), i.e. within a time frame similar to that needed for the formation of tubuloids in this PhD thesis. Histological analysis of injured kidney tissue has shown that the surviving rTECs rapidly exihibit molecular changes. In rats only 15 min of ischemia induced an apical membrane enrichment of NaK-ATPase, which is normally located at the basolateral membrane (BLM) (Molitoris et al., 1988). Following ischemic injury (50 min), leucine aminopeptidase (LAP), which normally localizes to the apical domain of rTECs, could be detected within the cell and along the BLM (Molitoris et al., 1988). 24 hour after reperfusion, the BLM distribution of LAP was further enhanced (Molitoris et al., 1988). With cellular recovery from ischemic injury (5 days), LAP was again only visualized in the apical membrane (Molitoris et al., 1988). In addition, these surviving rTECs re-express progenitor markers, such as vimentin (Gröne et al., 1987; Kitamura et al., 2015; Kitamura et al., 2005;

Maeshima et al., 2006; Maeshima et al., 2003; Witzgall et al., 1994) and sox9 (Chang-Panesso et al., 2019; Kang et al., 2016). The process of regeneration by surviving TECs also exists in human kidney after injury. For example, the loss of brush border in surviving rTECs after injury also has been shown in human kidney (Solez et al., 1979). And, primary adult human kidney epithelial cells can quickly switch from quiescence to an active phenotype and re-express progenitor markers, including CD24, CD133 and NCAM1, once placed in culture (Buzhor et al., 2013). With lineage traced transgenic mice, Benjamin D. Humphreys, et al. (Humphreys et al., 2008) observed, that 2 days after IRI, 50.5% of outer medullary epithelial cells of mice coexpress Ki67 and red fluorescent protein, and no dilution of cell-fate marker, indicating that surviving differentiated rTECs undergo proliferative expansion. In another mouse experiment, similar results have been obtained by using an unbiased DNA analog-based approach to track multiple rounds of cell division in vivo, i.e. an approach that does not just rely on candidate markers (Humphreys et al., 2011). In this study, it has been observed that cell division was stochastic and enriched among cells that were injured and dedifferentiated (Humphreys et al., 2011). In addition, specialized populations of progenitors repeatedly divided in response to injury, suggesting that self-duplication of surviving cells could not be determined as the predominant mechanism of repair after tubular injury in the adult mouse kidney. Again, to address this controversy, another line of lineage tracing mice (SLC34a1-GFPCreERT2) was generated (Kusaba, Lalli, et al., 2014). With this mouse model, Kusaba T.et al.(Kusaba, Lalli, et al., 2014) observed that after IRI injury, labeled differentiated rTECs temporarily express the progenitor markers, including CD24, CD133, vimentin, and KIM-1. In addition, there was no dilution of fate markers when completely labeled kidneys were subjected to injury and repair (Kusaba, Lalli, et al., 2014), indicating that unlabeled progenitors do not contribute to kidney repair. Therefore, it was concluded that the predominant source of tubular repair in mouse kidney are differentiated rTECs. Hence, it would be interesting to test the cellular sorce of the sox9-GFP and vim-GFP cells sorted by flow cytometry.

7.1.2 Regeneration by scattered progenitor epithelial cells

In this thesis, progenitor markers (including sox9 and vimentin) were found to be temporarily expressed during the formation of tubuloids. In addition, cells that stabely express the progenitor markers have not been detected. However, in several reports it has been suggested that scattered progenitor cells in kidney constitute one source of kidney regeneration after injury (Duffield et al., 2011; Little et al., 2009; McCampbell et al., 2012; Reule et al., 2011). For example, in rat kidney, Maeshima et al.(Maeshima et al., 2003) have reported that progenitor cells were scattering among rTECs in “normal kidneys”. In

this study, they detected scattered progenitor epithelial cells in normal kidneys with in vivo bromodeoxyuridine (BrdU) labeling. During the recovery after renal ischemia, they observed that most of the BrdU positive cells underwent cell division and became positive for proliferating cell nuclear antigen (PCNA). In contrast, PCNA–positive, but BrdU-negative, tubular cells were rarely observed, suggesting that cells proliferating during tubular regeneration are essentially derived from these scattered progenitor epithelial cells. In another study, epithelial marker positive (such as Ecadherin positive or cytokeratin positive) and mesenchymal marker negative (vimentin negative) freshly isolated rTECs were seeded for three-dimensional culture and microinjected into the metanephric mouse kidney (Maeshima et al., 2006). Interestingly, only BrdU positive rTECs could form tubule-like or tubulocystic structures (Challen et al., 2006). These studies indicate that the epithelial cells which regain proliferative capacity can rebuilt tubules. In another study, a cell clone from the S3 segment of rat kidney was defined as the stem/progenitor (rKS56) cells (Kitamura et al., 2005). They found that rKS56 cells could differentiate to mature TECs with proper culture condition. Interestingly, rKS56 cells could also partially replace injured tubules and improve renal function when engrafted into injured rat kidney. These results suggest that rKS56 cells possess characters, such as self-renewal, multi-plasticity and capability of tissue repair, similar to stem cells. However, this model is not analogous to the majority of acute renal failures. Whether there is a niche of progenitor epithelial cells which always maintain a potential for differentiation and give rise to regenerating TECs after kidney injury has not been unequivocally proven by these experiments. The immunophenotype and the expression profile of kidney scattered progenitor epithelial cells has been described as distinct from bone marrow derived progenitor cells, suggesting that they may be a resident nonhematopoietic cell population (Challen et al., 2006). To go further, abundant studies committed to search for the permanentely existing progenitor epithelial cells in kidney. Bart Smeets, et al.(Smeets et al., 2013) characterized a special cell population in normal human kidney, which were CD24-, CD133-, and vimentin-positive and scattered throughout the proximal tubules. They observed, compared to 'normal' proximal tubular cells, that these CD24-positive cells contained less cytoplasm, fewer mitochondria, and no brush border. However, in healthy rat kidney, these CD24-positive cells could not be detected. After injury, they appeared de novo – arguing against the notion that these cells represent a pre-existing progenitor cell population. In addition, these scattered progenitor epithelial cells coexpressed vimentin, while not expressing differentiation markers, such as E-cadherin (Piepenhagen et al., 1995). These features are very similar with the dedifferentiation-redifferentiation transition of rTECs during the regeneration after kidney injury. Maybe these so-called scattered progenitor epithelial cells

are just a transient state of surviving rTECs which dedifferentiated to the progenitor state during the regeneration of rTECs after kidney injury. It can be argued that in the adult kidney cell senescence and replacement by neighbouring cells take place stochastically and that these latter cells are defined as progenitor cells disposed for proliferation but nonetheless stemming from regular TECs. In addition, the model surmises that cells are replaced in acute renal failure and are not sustained to regain differentiation, a process which is not probable for the majority of acute renal failure cases in humans.

7.2 Cellular plasticity of tubuloids

In this thesis, primary kidney tubular epithelial organoids, termed tubuloids, were cultured in matrigel following a previously published protocol (Schutgens et al., 2019). During the formation of tubuloids, , documented by live imaging in this thesis, a typical morphological transition from flat tubuloids to cuboidal tubuloids was observed, which was similar to phenotypes of dedifferentiation to redifferentiation in vivo (Chang-Panesso et al., 2019; Hansson et al., 2014; Smeets et al., 2013). However, maybe because this culture system for kidney tubular epithelial organoids is very new, there is no research that has claimed and verified that these flat tubuloids can represent the dedifferentiation state of rTECs, and cuboidal tubuloids can represent the redifferentiation state. To test whether the dedifferentiation-differentiation transition really existed in tubuloids, vimentin-reporter-GFP mouse (Vim-GFP) and sox9-reporter-GFP mouse lines (sox9-GFP) were taken to clearly observe transitions from dedifferentiation to differentiation. Primary kidney tubular epithelium fragments were isolated from Vim-GFP and sox9-GFP mouse line, and vim- and sox9- GFP positive cells percentage were analyzed. Indeed, a peak of vim- as well as sox9- GFP positive cells percentage was observed during the formation of tubuloids. Interestingly, consistent with in vivo research (Chang-Panesso et al., 2019), vim-GFP positive cell percentages of tubuloids inceased and decreased earlier in comparison with sox9-GFP. In addition, we checked the IF staining of vimentin and LTL of tubuloids at day1 and day3: the flat tubuloids were vimentin-positive and LTL-negative, while cuboidal tubuloids were vimentin-negative and LTL-positive. These results demonstrated a dedifferentiation-differentiation transition in tubuloids.

Then, to investigate whether the tubuloids can be a model to study regeneration of rTECs, a damage model was generated. To mimic glycerol or myoglobinuria induced AKI, myoglobin was administrated to the tubuloids (Lazzeri et al., 2018). After myoglobin stimulation, death of rTECs was observed with a destruction of the overall structure combined with PI/Hoechst staining of tubuloids. Surviving rTECs changed shape from cuboidal structure to flat structure, and rebuilt the cuboidal phenotype again. This

documents that tubuloids could be a model to study regeneration of rTECs after injury in vitro.

7.3 Role of glucocorticoid receptor in acute kidney injury

This thesis provides evidence that dex treatment of tubuloids, i.e. both mouse tubuloids as well as human tubuloids, worsened injury of TECs after myoglobin treatment. It has been established that glycerol-induced AKI in mice can dramatically increase plasma and urinary cortisol levels as well as the cyclin kinase inhibitor p21 (which can induce cell cycle arrest and may exert cytoprotective effects) expression level in the renal cortices (Zager et al., 2019). However, mifepristone treatment (GR antagonist) blocks glycerol-induced p21 mRNA and protein accumulation, while dex treatment (GR agonists) markedly increases p21 protein and mRNA in both normal and glycerol-treated mice. In a rat study, H Horiguchi, et al.(Horiguchi et al., 2001) observed that pre-treatment of dex (1mg/kg) exacerbated kidney functuion of cadmium-induced AKI. A clinical case reported by Minami Nakajima, et al.(Nakajima et al., 2015) showed that intravenous therapy with dex for severe asthma attack induced AKI-like symptoms. Thus, GCs administration after AKI may worse the damage of the kidney, potentially by increasing cell stress in the epithelium.

This thesis also provides evidence that dex treatment induces the mislocation of lectins LTL, a marker of cell polarity of TECs. It has been established that polarity of rTECs is essential for the normal function of renal epithelium (Eymael et al., 2016). Therefore, testing whether cells with LTL mislocalization have normal function could further verify the inhibitiory effect of dex treatment on the differentiation of tubuloids. Furthermore, it would be an interesting direction to explore the mechanism between GR signaling and polarity of rTECs.

7.4 Role of metabolism in cellular plasticity of renal epithelial cells

In this thesis, genetic inactivation of the GR rendered kidney organoids more resistant to myoglobin treatment. A similar improvement of myoglobinuric renal failure has also been seen in vivo in mice with tubule-specific deletion of the GR (results not shown). In addition, deficiency of the GR promotes mitochondrial respiration of tubuloids, and inhibition of OXPHOS lowers the viability of GR-deficient tubuloids. Interestingly, the GR has previously been shown to play versatile roles in modulating energy balance and metabolism in cells (Mcmaster et al., 2008). And, it has been established that proper energy metabolism of rTECs is essential for surviving and repair of rTECs after injury (Legouis et al., 2020). One could therefore hypothesize that the protective effects of GR

deficiency on rTECs against renal-toxic factors might be a result of mitochondrial protection, which may rely on genomic signaling or nongenomic signaling of the GR. In a genome-wide binding analysis of the dominant transcription factors of AKI, Julia Wilflingseder, et al.(Wilflingseder et al., 2020) observed GR binding to the regulatory element next to Havcr1 (encoding KIM1) before injury. Interestingly, this binding is reduced after IRI (Fig. 28). This study indicates that GR may have a repressive function on expression of kidney injury markers before injury (Wilflingseder et al., 2020).

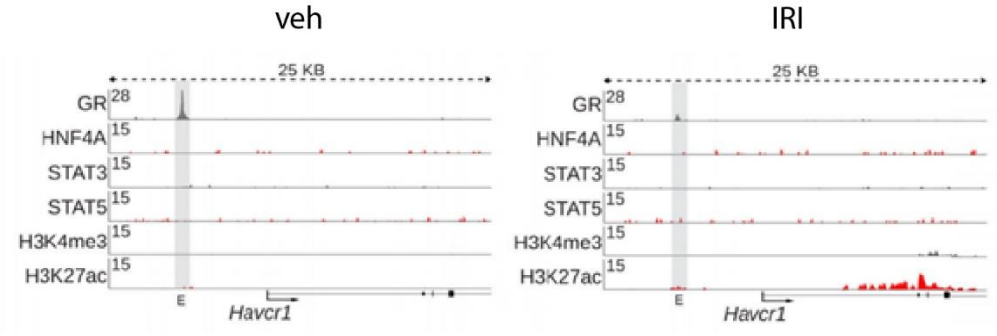

Fig. 28. Binding of glucocorticoid receptors to the regulatory element next to Havcr1 is modulated by injury. With high quality ChIP-seq profiles, researchers analyzed the binding of GR with the regulatory elements of Havcr1 (encoding KIM-1). They observed GR binding before injury and reduced GR binding after IRI, indicating GR may has a repressive function on kidney injury markers before injury. Veh, vehicle; IRI, ischemia reperfusion injury; GR, glucocorticoid receptor (Wilflingseder et al., 2020).

This thesis provides evidence that GR deficiency promotes the respiration of tubuloids by upregulating expression of associated respiration enzymes. Interestingly, GR-deficient tubuloids were less sensitive to inhibition of glycolysis (2-DG treatment) while more sensitive to inhibition of OXPHOS (oligo treatment) as compared to control tubuloids, indicating that the surviving of GR-deficient tubuloids relied mainly on mitochondrial respiratorion. It has been established that the immense transport functions of rTECs (only 1% of 180l of filtered primary urine are excreted), especially proximal TECs, require a high turnover of ATP, derived almost totally via mitochondrial OXPHOS (Guder et al., 1984; Hall et al., 2007; Weinberg et al., 2009). Interestingly, after injury, the number of mitochondria in flat epithelial cells can be temporarily reduced (Kempczinski et al., 1968; Ormos et al., 1973; Venkatachalam et al., 1978), which may suggest that the dedifferentiation state of survival rTECs protects them temporarily from damage in adequate oxygen radical formation by inadequately active mitochondria. In addition, alterations of energy metabolism occur in models of AKI, including diminished fatty acid oxidation during folic acid nephropathy (Kang et al., 2015), increased glycolysis after mercuric chloride AKI (Ash et al., 1970), increased lactate release into kidney interstitium

after ischemic AKI (Eklund et al., 1991), and elevated pyruvate kinase in kidney homogenates after IRI (Bonventre et al., 2003). Redifferentiation during tubular recovery requires substantial mitochondrial biogenesis (Weinberg, 2011). The proximal tubules fail to redifferentiate and become atrophic if mitochondria do not increase in number (Lan et al., 2012). In such tubules, mitochondria are greatly reduced in number and of smaller size with round profiles, unlike tubules that recovered normally (Lan et al., 2016). These evidences indicate that mitochondrial function and energy cosuming processes are needed for regeneraration.

What is the connection between the cellular metabolism and the differentiation state during regeneration? It has been shown in cancer cells that increased nitric oxide can trigger the shift of the metabolic phenotype of the cell from OXPHOS to glycolysis, which can induce a differentiation to dedifferentiation switch (Warburg, 1956; Warburg et al., 1927). Differentiation changes are involved in dynamic epigenetic, transcriptional, and metabolic remodeling (Trefely et al., 2018). Metabolic changes (mainly mitochondrial OXPHOS and glycolysis) may not only result from differentiation but also control the cellular differentiation state (Agostini et al., 2016; Drehmer et al., 2016; Folmes et al., 2012). In several types of AKI mouse models, elevated expression levels of glycolytic enzymes correlate with the repair after AKI (Ash et al., 1970; Lan et al., 2016; Semenza, 2011; Semenza et al., 1994; Smith et al., 2014). For example, ischemic AKI induces an increase in renal pyruvate, lactate and the glycolytic enzymes activation, including hexokinase 2 (hk2), phosphofructokinase platelet isoform (PFKP), 6-phosphofructo-2-kinase/fructose-2,6-bisphosphatase 3 (PFKFB3), and pyruvate kinase M2 (PKM2; or called M2-PK), these enzymes are mainly regulated by hypoxia-inducible factor 1a (HIF 1a) (Lan et al., 2016; Semenza, 2011; Semenza et al., 1994). A specific and rapid increase in these glycolytic enzymes activity of kidney cortex and outer medulla homogenises of mice were observed 2 days after IRI(Lan et al., 2016). However, there is no direct evidence to show a connection between regeneration of TECs and glycolysis. Also, whether inhibition of OXPHOs and fatty acid metabolism can modulate the regeneration of TECs has not been studied. Hence, it should be very interesting to test whether the modulation of metabolism state can lead to the transition of the dedifferentiation-differentiation state of the tubuloids. In addition, what the precise role of the GR in the transition of dedifferentiation-differentiation state via control of metabolism requires further investigation.

7.5 Connection between mTOR pathway and GR signaling in renal epithelial cells

This thesis provides evidence, that GR silencing promotes mTOR activity in in vitro cell experiments. In addition, GR deficiency promotes the energy production of TECs and

protects the TECs against myoglobin-induced damage in tubuloid experiments. It has been shown that the atypical serine/threonine kinase mTOR, a master modulator of the metabolism of cells, promotes anabolic processes such as ribosome biogenesis and protein, nucleotide, fatty acid and lipid synthesis and inhibits catabolic processes (Saxton et al., 2017). It consists of two structurally and functionally distinct complexes, mTOR complex 1 (mTORC1) and mTORC2. mTORC1 contains mTOR, regulatory-associated protein of mTOR (RAPTOR) and mammalian lethal with sec-13 protein 8 (mLST8) and is rapamycin sensitive (Saxton et al., 2017). mTORC2 contains mTOR, rapamycin-insensitive companion of mTOR (RICTOR), mammalian stress-activated MAPK-interacting protein 1 (mSIN1; also known as MAPKAP1) and mLST8 and is insensitive to acute rapamycin treatment (Saxton et al., 2017). mTORC1 can also directly respond to intracellular and environmental stresses that are incompatible with growth such as low ATP levels, hypoxia, or DNA damage. A reduction in cellular energy charge, for example during glucose deprivation, can activate the stress responsive metabolic regulator AMPK, which inhibits mTORC1 both indirectly through phosphorylation and activation of TSC2 as well as directly through the phosphorylation of Raptor (Gwinn et al., 2008; Inoki et al., 2003; Shah et al., 2004). Interestingly, hypoxia inhibits mTORC1 in part through AMPK activation, but also through the induction of REDD1 (one of the target genes of GR signaling), which activates TSC (Brugarolas et al., 2004).

How could GR signaling modulate the activation of the mTOR pathway? In this thesis, treatment by rapamycin reverses the the protective effects of GR deficiency against myoglobin treatment in tubuloids. It has been established that inhibition of the mTOR pathway with rapamycin or Torin1 could override the anti-inflammatory potency of GCs both in human monocytes and myeloid dendritic cells by modulating the activation of nuclear factor-κB and c-Jun N-terminal kinase (JNK) pathway, the expression of proinflammatory cytokines, and the promotion of T helper 1 cells responses (Weichhart et al., 2011). In human neuroblastoma SH-SY5Y cells, Gee E. C. et al.(G. E. Choi et al., 2018) showed that cortisol can promote the translocation of HSP70-bound GR into mitochondria, triggering GR-Bcl-2 interaction and Ca^{2+} influx in mitochondria, which triggered mTOR activation (G. E. Choi et al., 2018). In keratinocytes and lymphoid cells, rapamycin treatment inhibits GR phosphorylation, nuclear translocation, and loading on GREs in REDD1 promoter (Lesovaya et al., 2018). In addition, rapamycin treatment surpresses activation of GR target genes and through its repressive functionm enhanced the repression of pro-proliferative and pro-inflammatory genes (Lesovaya et al., 2018). Thus, GR may exert its catabolic activity and anti OXPHOS activity partly through mTOR pathway.

7.6 Connection between Wnt/β-catenin pathway and GR signaling in renal epithelial cells

In this thesis, dex (an agonist of GR) treatment resulted in the inhibition of the dedifferentiation-redifferentiation sequence of tubuloids. CHIR (a Wnt activator) could partly rescue this inhibititory effect of dex. The canonical Wnt/β-catenin pathway, which is involved in regulating the nuclear and nonnuclear activities of GR, controls the proliferation and differentiation of many differentiated tissues (Bastakoty et al., 2016; Mulholland et al., 2005; Sprangers et al., 2021). Interestingly, it has been shown in GR-positive bladder cancer cells that dex treatment significantly reduced the expression of β-catenin and its downstream genes, including C-MYC, Snail, and OCT-4 (C. Xu et al., 2020). On the contrary, GR silencing with siRNA transfection showed the opposite effects and promoted the expression of β-catenin. It has been established that Wnt-dependent activation and GR-mediated repression of cell cycle regulator genes are functionally coupled (He et al., 1998; Takayama et al., 2006; Tetsu et al., 1999). Moreover, GR can directly bind β-catenin in vitro, indicating that GR signaling pathways and Wnt pathways could communicate directly through their effectors (Takayama et al., 2006). In human U2OS/GR osteosarcoma cells, activation of the GR repressed the expression of cyclin D1 (a potent cell cycle regulator) by inhibiting the activity of Tcf-β-catenin without changing the nuclear localization of β-catenin (Takayama et al., 2006). These data strongly suggest a close and direct connection between GR signaling and Wnt/β-catenin pathway.

How could the GR modulate the differentiation of cells via Wnt/β-catenin pathway? In this thesis, interestingly, treating tubuloids with CHIR starting from day1 significantly increased the percentage of Ki67 positive cells and LTL positive cells, while CHIR treatment from day3 onwards did not result in higher proliferative activity but only led to higher redifferentiation of tubuloids. However, dex treatment, no matter when started, had no effect neither on the number of Ki67 positive cells nor LTL positive cells. Some studies have shown that dex treatment can recruit β-catenin to the cell membrane and modulate the integrity of E-cadherin/β-catenin complex via regulating the expression of fascin, an actin-bundling protein that also interacts with the adherens junction component beta-catenin (Guan et al., 2004; Wong et al., 1999). In rat mammary epithelial tumor cells, binding of GCs and GR results in the up-regulated fascin, it promotes the formation of E-cadherin and β-catenin complexes (Wong et al., 1999), the enhancement of tight and adherens junctions (Buse, Woo, Alexander, Cha, et al., 1995; Buse, Woo, Alexander, Reza, et al., 1995; Zettl et al., 1992) and triggers the differentiation of mammary tumor epithelium. In addition, a rescent study showed that conditional medium of GR-deficient-endothelial cells promoted the activation of Wnt/β-catenin pathway in TECs and

accelerated the kidney fibrosis of diabetic nephropathy (Srivastava et al., 2021). On the contrary, this thesis provides exidence that activation of Wnt (with CHIR) triggers the redifferentiation of rTECs. This suggests that cell type-specific differences of GR signaling may exist between endothelial cells, tumor cells and epithelial cells.

In summary, the results of this thesis establish kidney organoids as a model system to study cellular plasticity of the renal tubular epithelium. Moreover, the data of this thesis identify the GR as a master negative regulator of injury-induced plasticity of rTECs via suppressing the Wnt/β-catenin and mTOR pathways as well as cellular energy production.

8 REFERENCES

Abbate, M., Brown, D., & Bonventre, J. V. (1999). Expression of NCAM recapitulates tubulogenic development in kidneys recovering from acute ischemia. Am J Physiol, 277(3), F454-463.

Abbinante-Nissen, J. M., Simpson, L. G., & Leikauf, G. D. (1995). Corticosteroids increase secretory leukocyte protease inhibitor transcript levels in airway epithelial cells. Am J Physiol, 268(4 Pt 1), L601-606.

Agostini, M., Romeo, F., Inoue, S., Niklison-Chirou, M. V., Elia, A. J., Dinsdale, D., . . . Melino, G. (2016). Metabolic reprogramming during neuronal differentiation. Cell Death Differ, 23(9), 1502-1514.

Almlöf, T., Gustafsson, J. A., & Wright, A. P. (1997). Role of hydrophobic amino acid clusters in the transactivation activity of the human glucocorticoid receptor. Mol Cell Biol, 17(2), 934-945.

Almlöf, T., Wallberg, A. E., Gustafsson, J. A., & Wright, A. P. (1998). Role of important hydrophobic amino acids in the interaction between the glucocorticoid receptor tau 1-core activation domain and target factors. Biochemistry, 37(26), 9586-9594.

Alt, S. R., Turner, J. D., Klok, M. D., Meijer, O. C., Lakke, E. A. J. F., DeRijk, R. H., & Muller, C. P. (2010). Differential expression of glucocorticoid receptor transcripts in major depressive disorder is not epigenetically programmed. Psychoneuroendocrinology, 35(4), 544-556.

Angelotti, M. L., Ronconi, E., Ballerini, L., Peired, A., Mazzinghi, B., Sagrinati, C., . . . Romagnani, P. (2012). Characterization of renal progenitors committed toward tubular lineage and their regenerative potential in renal tubular injury. Stem Cells, 30(8), 1714-1725.

Arsenault, P., & Ménard, D. (1985). Influence of hydrocortisone on human fetal small intestine in organ culture. J Pediatr Gastroenterol Nutr, 4(6), 893-901.

Ash, S. R., & Cuppage, F. E. (1970). Shift toward anaerobic glycolysis in the regenerating rat kidney. Am J Pathol, 60(3), 385-402.

Atsuta, J., Plitt, J., Bochner, B. S., & Schleimer, R. P. (1999). Inhibition of VCAM-1 Expression in Human Bronchial Epithelial Cells by Glucocorticoids. American Journal of Respiratory Cell and Molecular Biology, 20(4), 643-650.

Ballegeer, M., Van Looveren, K., Timmermans, S., Eggermont, M., Vandevyver, S., Thery, F., . . . Libert, C. (2018). Glucocorticoid receptor dimers control intestinal STAT1 and TNF-induced inflammation in mice. J Clin Invest, 128(8), 3265-3279.

Bamberger, C. M., Bamberger, A. M., de Castro, M., & Chrousos, G. P. (1995). Glucocorticoid receptor beta, a potential endogenous inhibitor of glucocorticoid action in humans. J Clin Invest, 95(6), 2435-2441.

Bancos, I., Hazeldine, J., Chortis, V., Hampson, P., Taylor, A. E., Lord, J. M., & Arlt, W. (2017). Primary adrenal insufficiency is associated with impaired natural killer cell function: a potential link to increased mortality. Eur J Endocrinol, 176(4), 471-480.

Barnes, P. J. (2011). Glucocorticosteroids: current and future directions. Br J Pharmacol, 163(1), 29-43.

Bastakoty, D., & Young, P. P. (2016). Wnt/β-catenin pathway in tissue injury: roles in pathology and therapeutic opportunities for regeneration. FASEB journal : official publication of the Federation of American Societies for Experimental Biology, 30(10), 3271-3284.

Bauer, C. R., Morrison, J. C., Poole, W. K., Korones, S. B., Boehm, J. J., Rigatto, H., & Zachman, R. D. (1984). A decreased incidence of necrotizing enterocolitis after prenatal glucocorticoid therapy. Pediatrics, 73(5), 682-688.

Baumgart, D. C., & Sandborn, W. J. (2007). Inflammatory bowel disease: clinical aspects and established and evolving therapies. Lancet, 369(9573), 1641-1657.

Beck, I. M. E., Vanden Berghe, W., Vermeulen, L., Yamamoto, K. R., Haegeman, G., & De Bosscher, K. (2009). Crosstalk in Inflammation: The Interplay of Glucocorticoid Receptor-Based Mechanisms and Kinases and Phosphatases. Endocrine Reviews, 30(7), 830-882.

Benecke, A., Chambon, P., & Gronemeyer, H. (2000). Synergy between estrogen receptor alpha activation functions AF1 and AF2 mediated by transcription intermediary factor TIF2. EMBO Rep, 1(2), 151-157.

Berger, K., Bangen, J. M., Hammerich, L., Liedtke, C., Floege, J., Smeets, B., & Moeller, M. J. (2014). Origin of regenerating tubular cells after acute kidney injury. Proc Natl Acad Sci U S A, 111(4), 1533-1538.

Bertram, C., Trowern, A. R., Copin, N., Jackson, A. A., & Whorwood, C. B. (2001). The maternal diet during pregnancy programs altered expression of the glucocorticoid receptor and type 2 11beta-hydroxysteroid dehydrogenase: potential molecular mechanisms underlying the programming of hypertension in utero. Endocrinology, 142(7), 2841-2853.

Biol-N'garagba M, C., Niepceron, E., Mathian, B., & Louisot, P. (2003). Glucocorticoid-induced maturation of glycoprotein galactosylation and fucosylation processes in the rat small intestine. The Journal of steroid biochemistry and molecular biology, 84(4), 411-422.

Bird, A. D., Tan, K. H., Olsson, P. F., Zieba, M., Flecknoe, S. J., Liddicoat, D. R., . . . Cole, T. J. (2007). Identification of glucocorticoid-regulated genes that control cell proliferation during murine respiratory development. J Physiol, 585(Pt 1), 187-201.

Bledsoe, R. K., Montana, V. G., Stanley, T. B., Delves, C. J., Apolito, C. J., McKee, D. D., . . . Xu, H. E. (2002). Crystal structure of the glucocorticoid receptor ligand binding domain reveals a novel mode of receptor dimerization and coactivator recognition. Cell, 110(1), 93-105.

Bonventre, J. V. (2003). Dedifferentiation and proliferation of surviving epithelial cells in acute renal failure. Journal of the American Society of Nephrology : JASN, 14 Suppl 1, S55-61.

Bonventre, J. V., & Weinberg, J. M. (2003). Recent advances in the pathophysiology of ischemic acute renal failure. Journal of the American Society of Nephrology : JASN, 14(8), 2199-2210.

Bonventre, J. V., & Yang, L. (2011). Cellular pathophysiology of ischemic acute kidney injury. J Clin Invest, 121(11), 4210-4221.

Bouchard, M., Souabni, A., Mandler, M., Neubüser, A., & Busslinger, M. (2002). Nephric lineage specification by Pax2 and Pax8. Genes Dev, 16(22), 2958-2970.

Breslau, N., Chilcoat, H., DelDotto, J., Andreski, P., & Brown, G. (1996). Low birth weight and neurocognitive status at six years of age. Biol Psychiatry, 40(5), 389-397.

Brewer, J. A., Kanagawa, O., Sleckman, B. P., & Muglia, L. J. (2002). Thymocyte apoptosis induced by T cell activation is mediated by glucocorticoids in vivo. J Immunol, 169(4), 1837-1843.

Brown, H. M., Storey, G., & George, W. H. (1972). Beclomethasone dipropionate: a new steroid aerosol for the treatment of allergic asthma. Br Med J, 1(5800), 585-590.

Brugarolas, J., Lei, K., Hurley, R. L., Manning, B. D., Reiling, J. H., Hafen, E., . . . Kaelin, W. G., Jr. (2004). Regulation of mTOR function in response to hypoxia by REDD1 and the TSC1/TSC2 tumor suppressor complex. Genes Dev, 18(23), 2893-2904.

Buse, P., Woo, P. L., Alexander, D. B., Cha, H. H., Reza, A., Sirota, N. D., & Firestone, G. L. (1995). Transforming growth factor-alpha abrogates glucocorticoid-stimulated tight junction formation and growth suppression in rat mammary epithelial tumor cells. J Biol Chem, 270(12), 6505-6514.

Buse, P., Woo, P. L., Alexander, D. B., Reza, A., & Firestone, G. L. (1995). Glucocorticoid-induced functional polarity of growth factor responsiveness regulates tight junction dynamics in transformed mammary epithelial tumor cells. J Biol Chem, 270(47), 28223-28227.

Busillo, J. M., & Cidlowski, J. A. (2013). The five Rs of glucocorticoid action during inflammation: ready, reinforce, repress, resolve, and restore. Trends in Endocrinology & Metabolism, 24(3), 109-119.

Bussolati, B., Bruno, S., Grange, C., Buttiglieri, S., Deregibus, M. C., Cantino, D., & Camussi, G. (2005). Isolation of renal progenitor cells from adult human kidney. Am J Pathol, 166(2), 545-555.

Buzhor, E., Omer, D., Harari-Steinberg, O., Dotan, Z., Vax, E., Pri-Chen, S., . . . Dekel, B. (2013). Reactivation of NCAM1 defines a subpopulation of human adult kidney epithelial cells with clonogenic and stem/progenitor properties. Am J Pathol, 183(5), 1621-1633.

Bywaters, E. G. L., & Stead, J. K. (1942). The production of renal failure following injection of solutions containing myohaemoglobin. Q J Exp Physiol, 33(1), 53–70.

Cain, D. W., & Cidlowski, J. A. (2017). Immune regulation by glucocorticoids. Nature Reviews Immunology, 17(4), 233-247.

Celsi, G., Kistner, A., Aizman, R., Eklöf, A. C., Ceccatelli, S., de Santiago, A., & Jacobson, S. H. (1998). Prenatal dexamethasone causes oligonephronia, sodium retention, and higher blood pressure in the offspring. Pediatr Res, 44(3), 317-322.

Challen, G. A., Bertoncello, I., Deane, J. A., Ricardo, S. D., & Little, M. H. (2006). Kidney side population reveals multilineage potential and renal functional capacity but also cellular heterogeneity. Journal of the American Society of Nephrology : JASN, 17(7), 1896-1912.

Chang-Panesso, M., & Humphreys, B. D. (2017). Cellular plasticity in kidney injury and repair. Nat Rev Nephrol, 13(1), 39-46.

Chang-Panesso, M., Kadyrov, F. F., Lalli, M., Wu, H., Ikeda, S., Kefaloyianni, E., . . . Humphreys, B. D. (2019). FOXM1 drives proximal tubule proliferation during repair from acute ischemic kidney injury. J Clin Invest, 129(12), 5501-5517.

Choi, G. E., Oh, J. Y., Lee, H. J., Chae, C. W., Kim, J. S., Jung, Y. H., & Han, H. J. (2018). Glucocorticoid-mediated ER-mitochondria contacts reduce AMPA receptor and mitochondria trafficking into cell terminus via microtubule destabilization. Cell Death Dis, 9(11), 1137.

Choi, H. M., Jo, S. K., Kim, S. H., Lee, J. W., Cho, E., Hyun, Y. Y., . . . Kim, H. K. (2013). Glucocorticoids attenuate septic acute kidney injury. Biochem Biophys Res Commun, 435(4), 678-684.

Chrousos, G. P., & Kino, T. (2005). Intracellular glucocorticoid signaling: a formerly simple system turns stochastic. Sci STKE, 2005(304), pe48.

Clark, A. R., & Belvisi, M. G. (2012). Maps and legends: The quest for dissociated ligands of the glucocorticoid receptor. Pharmacology & Therapeutics, 134(1), 54-67.

Clark, T. J. (1972). Effect of beclomethasone dipropionate delivered by aerosol in patients with asthma. Lancet, 1(7765), 1361-1364.

Coe, C. L., & Lubach, G. R. (2005). Developmental consequences of antenatal dexamethasone treatment in nonhuman primates. Neurosci Biobehav Rev, 29(2), 227-235.

Cole, T. J., Blendy, J. A., Monaghan, A. P., Krieglstein, K., Schmid, W., Aguzzi, A., . . . Schütz, G. (1995). Targeted disruption of the glucocorticoid receptor gene blocks adrenergic chromaffin cell development and severely retards lung maturation. Genes Dev, 9(13), 1608-1621.

Cole, T. J., Solomon, N. M., Van Driel, R., Monk, J. A., Bird, D., Richardson, S. J., . . . Hooper, S. B. (2004). Altered epithelial cell proportions in the fetal lung of glucocorticoid

receptor null mice. Am J Respir Cell Mol Biol, 30(5), 613-619.

Cronstein, B. N., Kimmel, S. C., Levin, R. I., Martiniuk, F., & Weissmann, G. (1992). A mechanism for the antiinflammatory effects of corticosteroids: the glucocorticoid receptor regulates leukocyte adhesion to endothelial cells and expression of endothelial-leukocyte adhesion molecule 1 and intercellular adhesion molecule 1. Proceedings of the National Academy of Sciences, 89(21), 9991.

Cruz-Topete, D., He, B., Xu, X., & Cidlowski, J. A. (2016). Krüppel-like Factor 13 Is a Major Mediator of Glucocorticoid Receptor Signaling in Cardiomyocytes and Protects These Cells from DNA Damage and Death. J Biol Chem, 291(37), 19374-19386.

Dammann, O., Walther, H., Allers, B., Schroder, M., Drescher, J., Lutz, D., . . . Schulte, F. J. (1996). Development of a regional cohort of very-low-birthweight children at six years: cognitive abilities are associated with neurological disability and social background. Dev Med Child Neurol, 38(2), 97-106.

de Kloet, E. R., Joels, M., & Holsboer, F. (2005). Stress and the brain: from adaptation to disease. Nat Rev Neurosci, 6(6), 463-475.

Diaz, R., Fuxe, K., & Ogren, S. O. (1997). Prenatal corticosterone treatment induces long-term changes in spontaneous and apomorphine-mediated motor activity in male and female rats. Neuroscience, 81(1), 129-140.

Draper, N., & Stewart, P. M. (2005). 11beta-hydroxysteroid dehydrogenase and the pre-receptor regulation of corticosteroid hormone action. J Endocrinol, 186(2), 251-271.

Drehmer, D. L., de Aguiar, A. M., Brandt, A. P., Petiz, L., Cadena, S. M., Rebelatto, C. K., . . . Abud, A. P. (2016). Metabolic switches during the first steps of adipogenic stem cells differentiation. Stem Cell Res, 17(2), 413-421.

Duffield, J. S., & Humphreys, B. D. (2011). Origin of new cells in the adult kidney: results from genetic labeling techniques. Kidney Int, 79(5), 494-501.

Efeyan, A., Zoncu, R., Chang, S., Gumper, I., Snitkin, H., Wolfson, R. L., . . . Sabatini, D. M. (2013). Regulation of mTORC1 by the Rag GTPases is necessary for neonatal autophagy and survival. Nature, 493(7434), 679-683.

Ehrchen, J., Steinmüller, L., Barczyk, K., Tenbrock, K., Nacken, W., Eisenacher, M., . . . Roth, J. (2006). Glucocorticoids induce differentiation of a specifically activated, anti-inflammatory subtype of human monocytes. Blood, 109(3), 1265-1274.

Eiby, Y. A., Lumbers, E. R., Headrick, J. P., & Lingwood, B. E. (2012). Left ventricular output and aortic blood flow in response to changes in preload and afterload in the preterm piglet heart. American journal of physiology. Regulatory, integrative and comparative physiology, 303(7), R769-777.

Eklund, T., Wahlberg, J., Ungerstedt, U., & Hillered, L. (1991). Interstitial lactate, inosine and hypoxanthine in rat kidney during normothermic ischaemia and recirculation. Acta Physiol Scand, 143(3), 279-286.

Eymael, J., & Smeets, B. (2016). Origin and fate of the regenerating cells of the kidney. Eur J Pharmacol, 790, 62-73.

Felinski, E. A., Cox, A. E., Phillips, B. E., & Antonetti, D. A. (2008). Glucocorticoids induce transactivation of tight junction genes occludin and claudin-5 in retinal endothelial cells via a novel cis-element. Exp Eye Res, 86(6), 867-878.

Fischer, A., Stuckas, H., Gluth, M., Russell, T. D., Rudolph, M. C., Beeman, N. E., . . . Theuring, F. (2007). Impaired tight junction sealing and precocious involution in mammary glands of PKN1 transgenic mice. J Cell Sci, 120(Pt 13), 2272-2283.

Flecknoe, S. J., Boland, R. E., Wallace, M. J., Harding, R., & Hooper, S. B. (2004). Regulation of alveolar epithelial cell phenotypes in fetal sheep: roles of cortisol and lung expansion. Am J Physiol Lung Cell Mol Physiol, 287(6), L1207-1214.

Folmes, C. D., Dzeja, P. P., Nelson, T. J., & Terzic, A. (2012). Metabolic plasticity in stem cell homeostasis and differentiation. Cell Stem Cell, 11(5), 596-606.

Gandelman, R., & Rosenthal, C. (1981). Deleterious effects of prenatal prednisolone exposure upon morphological and behavioral development of mice. Teratology, 24(3), 293-301.

Gay, M. S., Li, Y., Xiong, F., Lin, T., & Zhang, L. (2015). Dexamethasone Treatment of Newborn Rats Decreases Cardiomyocyte Endowment in the Developing Heart through Epigenetic Modifications. PloS one, 10(4), e0125033. doi:10.1371/journal.pone.0125033

Gelfand, M. L. (1951). Administration of cortisone by the aerosol method in the treatment of bronchial asthma. N Engl J Med, 245(8), 293-294.

Giles, K. M., Ross, K., Rossi, A. G., Hotchin, N. A., Haslett, C., & Dransfield, I. (2001). Glucocorticoid Augmentation of Macrophage Capacity for Phagocytosis of Apoptotic Cells Is Associated with Reduced p130Cas Expression, Loss of Paxillin/pyk2 Phosphorylation, and High Levels of Active Rac. The Journal of Immunology, 167(2), 976-986.

Goldenberg, R. L., DuBard, M. B., Cliver, S. P., Nelson, K. G., Blankson, K., Ramey, S. L., & Herman, A. (1996). Pregnancy outcome and intelligence at age five years. Am J Obstet Gynecol, 175(6), 1511-1515.

Gong, S., Zheng, C., Doughty, M. L., Losos, K., Didkovsky, N., Schambra, U. B., . . . Heintz, N. (2003). A gene expression atlas of the central nervous system based on bacterial artificial chromosomes. Nature, 425(6961), 917-925.

Goodwin, J. E., & Geller, D. S. (2012). Glucocorticoid-induced hypertension. Pediatric nephrology (Berlin, Germany), 27(7), 1059-1066.

Goodwin, J. E., Zhang, J., & Geller, D. S. (2008). A critical role for vascular smooth muscle in acute glucocorticoid-induced hypertension. Journal of the American Society of Nephrology : JASN, 19(7), 1291-1299.

Goodwin, J. E., Zhang, J., Gonzalez, D., Albinsson, S., & Geller, D. S. (2011). Knockout of the vascular endothelial glucocorticoid receptor abrogates dexamethasone-induced hypertension. Journal of hypertension, 29(7), 1347-1356.

Goodwin, J. E., Zhang, X., Rotllan, N., Feng, Y., Zhou, H., Fernández-Hernando, C., . . . Sessa, W. C. (2015). Endothelial Glucocorticoid Receptor Suppresses Atherogenesis—Brief Report. Arteriosclerosis, Thrombosis, and Vascular Biology, 35(4), 779-782.

Gould, E. (1994). The effects of adrenal steroids and excitatory input on neuronal birth and survival. Ann N Y Acad Sci, 743, 73-92; discussion 92-73.

Gould, E., Woolley, C. S., & McEwen, B. S. (1991). Adrenal steroids regulate postnatal development of the rat dentate gyrus: I. Effects of glucocorticoids on cell death. J Comp Neurol, 313(3), 479-485.

Gröne, H. J., Weber, K., Gröne, E., Helmchen, U., & Osborn, M. (1987). Coexpression of keratin and vimentin in damaged and regenerating tubular epithelia of the kidney. Am J Pathol, 129(1), 1-8.

Guan, Y., Rubenstein, N. M., Failor, K. L., Woo, P. L., & Firestone, G. L. (2004). Glucocorticoids control beta-catenin protein expression and localization through distinct pathways that can be uncoupled by disruption of signaling events required for tight junction formation in rat mammary epithelial tumor cells. Mol Endocrinol, 18(1), 214-227.

Guder, W. G., & Ross, B. D. (1984). Enzyme distribution along the nephron. Kidney Int, 26(2), 101-111.

Gwinn, D. M., Shackelford, D. B., Egan, D. F., Mihaylova, M. M., Mery, A., Vasquez, D. S., . . . Shaw, R. J. (2008). AMPK phosphorylation of raptor mediates a metabolic checkpoint. Mol Cell, 30(2), 214-226.

Halac, E., Halac, J., Bégué, E. F., Casañas, J. M., Indiveri, D. R., Petit, J. F., . . . et al.

(1990). Prenatal and postnatal corticosteroid therapy to prevent neonatal necrotizing enterocolitis: a controlled trial. J Pediatr, 117(1 Pt 1), 132-138.

Hall, A. M., & Unwin, R. J. (2007). The not so 'mighty chondrion': emergence of renal diseases due to mitochondrial dysfunction. Nephron Physiol, 105(1), p1-10.

Hallman, M., Peltoniemi, O., & Kari, M. A. (2010). Enhancing functional maturity before preterm birth. Neonatology, 97(4), 373-378.

Hallman, M. A., Zhuang, S., & Schnellmann, R. G. (2008). Regulation of dedifferentiation and redifferentiation in renal proximal tubular cells by the epidermal growth factor receptor. J Pharmacol Exp Ther, 325(2), 520-528.

Hansson, J., Hultenby, K., Cramnert, C., Pontén, F., Jansson, H., Lindgren, D., . . . Johansson, M. E. (2014). Evidence for a morphologically distinct and functionally robust cell type in the proximal tubules of human kidney. Hum Pathol, 45(2), 382-393.

Hasenmajer, V., Sbardella, E., Sciarra, F., Minnetti, M., Isidori, A. M., & Venneri, M. A. (2020). The Immune System in Cushing's Syndrome. Trends Endocrinol Metab, 31(9), 655-669.

He, T. C., Sparks, A. B., Rago, C., Hermeking, H., Zawel, L., da Costa, L. T., . . . Kinzler, K. W. (1998). Identification of c-MYC as a target of the APC pathway. Science, 281(5382), 1509-1512.

Henrik, O., Etienne, C., Volker, O., Emanuela, A., Ronald, D. K. E., Derk-Jan, D., . . . Eve, V. C. (2017). The Functional and Clinical Significance of the 24-Hour Rhythm of Circulating Glucocorticoids. Endocrine Reviews(1), 3-45.

Hollenberg, S. M., Weinberger, C., Ong, E. S., Cerelli, G., Oro, A., Lebo, R., . . . Evans, R. M. (1985). Primary structure and expression of a functional human glucocorticoid receptor cDNA. Nature, 318(6047), 635-641.

Holmes, M. C., Kotelevtsev, Y., Mullins, J. J., & Seckl, J. R. (2001). Phenotypic analysis of mice bearing targeted deletions of 11beta-hydroxysteroid dehydrogenases 1 and 2 genes. Mol Cell Endocrinol, 171(1-2), 15-20.

Holson, R. R., Gough, B., Sullivan, P., Badger, T., & Sheehan, D. M. (1995). Prenatal dexamethasone or stress but not ACTH or corticosterone alter sexual behavior in male rats. Neurotoxicol Teratol, 17(4), 393-401.

Horiguchi, H., Oguma, E., Kayama, F., Sato, M., & Fukushima, M. (2001). Dexamethasone prevents acute cadmium-induced hepatic injury but exacerbates kidney dysfunction in rabbits. Toxicol Appl Pharmacol, 174(3), 225-234.

Huling, J., & Yoo, J. J. (2017). Comparing adult renal stem cell identification, characterization and applications. J Biomed Sci, 24(1), 32.

Humphreys, B. D., Czerniak, S., DiRocco, D. P., Hasnain, W., Cheema, R., & Bonventre, J. V. (2011). Repair of injured proximal tubule does not involve specialized progenitors. Proc Natl Acad Sci U S A, 108(22), 9226-9231.

Humphreys, B. D., Valerius, M. T., Kobayashi, A., Mugford, J. W., Soeung, S., Duffield, J. S., . . . Bonventre, J. V. (2008). Intrinsic epithelial cells repair the kidney after injury. Cell Stem Cell, 2(3), 284-291.

Inoki, K., Li, Y., Xu, T., & Guan, K. L. (2003). Rheb GTPase is a direct target of TSC2 GAP activity and regulates mTOR signaling. Genes Dev, 17(15), 1829-1834.

Ishmael, F. T., Fang, X., Houser, K. R., Pearce, K., Abdelmohsen, K., Zhan, M., . . . Stellato, C. (2011). The Human Glucocorticoid Receptor as an RNA-Binding Protein: Global Analysis of Glucocorticoid Receptor-Associated Transcripts and Identification of a Target RNA Motif. The Journal of Immunology, 186(2), 1189-1198.

Ismaili, N., & Garabedian, M. J. (2004). Modulation of glucocorticoid receptor function via phosphorylation. Ann N Y Acad Sci, 1024, 86-101.

Ito, K., Chung, K. F., & Adcock, I. M. (2006). Update on glucocorticoid action and resistance. J Allergy Clin Immunol, 117(3), 522-543.

Jobe, A. H., & Soll, R. F. (2004). Choice and dose of corticosteroid for antenatal treatments. Am J Obstet Gynecol, 190(4), 878-881.

Johnston, A. P., Yuzwa, S. A., Carr, M. J., Mahmud, N., Storer, M. A., Krause, M. P., . . . Miller, F. D. (2016). Dedifferentiated Schwann Cell Precursors Secreting Paracrine Factors Are Required for Regeneration of the Mammalian Digit Tip. Cell Stem Cell, 19(4), 433-448.

Ju, Z., Shao, J., Zhou, M., Jin, J., Pan, H., Ding, P., & Huang, R. (2021). Transcriptomic and metabolomic profiling reveal the p53-dependent benzeneacetic acid attenuation of silica-induced epithelial-mesenchymal transition in human bronchial epithelial cells. Cell Biosci, 11(1), 30.

Kadmiel, M., & Cidlowski, J. A. (2013). Glucocorticoid receptor signaling in health and disease. Trends Pharmacol Sci, 34(9), 518-530.

Kalender, A., Selvaraj, A., Kim, S. Y., Gulati, P., Brûlé, S., Viollet, B., . . . Thomas, G. (2010). Metformin, independent of AMPK, inhibits mTORC1 in a rag GTPase-dependent manner. Cell Metab, 11(5), 390-401.

Kang, H. M., Ahn, S. H., Choi, P., Ko, Y. A., Han, S. H., Chinga, F., . . . Susztak, K. (2015). Defective fatty acid oxidation in renal tubular epithelial cells has a key role in kidney fibrosis development. Nat Med, 21(1), 37-46.

Kang, H. M., Huang, S., Reidy, K., Han, S. H., Chinga, F., & Susztak, K. (2016). Sox9-Positive Progenitor Cells Play a Key Role in Renal Tubule Epithelial Regeneration in Mice. Cell Rep, 14(4), 861-871.

Kapoor, A., Dunn, E., Kostaki, A., Andrews, M. H., & Matthews, S. G. (2006). Fetal programming of hypothalamo-pituitary-adrenal function: prenatal stress and glucocorticoids. J Physiol, 572(Pt 1), 31-44.

Kellum, J. A., Romagnani, P., Ashuntantang, G., Ronco, C., Zarbock, A., & Anders, H. J. (2021). Acute kidney injury. Nat Rev Dis Primers, 7(1), 52.

Kempczinski, R. F., & Caulfield, J. B. (1968). A light and electron microscopic study of renal tubular regeneration. Nephron, 5(4), 249-264.

Khan, S. H., Awasthi, S., Guo, C., Goswami, D., Ling, J., Griffin, P. R., . . . Kumar, R. (2012). Binding of the N-terminal region of coactivator TIF2 to the intrinsically disordered AF1 domain of the glucocorticoid receptor is accompanied by conformational reorganizations. J Biol Chem, 287(53), 44546-44560.

Kim, K., Lee, K. M., Han, D. J., Yu, E., & Cho, Y. M. (2008). Adult stem cell-like tubular cells reside in the corticomedullary junction of the kidney. Int J Clin Exp Pathol, 1(3), 232-241.

Kim, M. Y., Eiby, Y. A., Lumbers, E. R., Wright, L. L., Gibson, K. J., Barnett, A. C., & Lingwood, B. E. (2014). Effects of glucocorticoid exposure on growth and structural maturation of the heart of the preterm piglet. PloS one, 9(3), e93407. doi:10.1371/journal.pone.0093407

Kim, S.-W., Rhee, H. J., Ko, J., Kim, Y. J., Kim, H. G., Yang, J. M., . . . Na, D. S. (2001). Inhibition of Cytosolic Phospholipase A2 by Annexin I

SPECIFIC INTERACTION MODEL AND MAPPING OF THE INTERACTION SITE. Journal of Biological Chemistry, 276(19), 15712-15719.

Kitamura, S., Sakurai, H., & Makino, H. (2015). Single adult kidney stem/progenitor cells reconstitute three-dimensional nephron structures in vitro. Stem Cells, 33(3), 774-784.

Kitamura, S., Yamasaki, Y., Kinomura, M., Sugaya, T., Sugiyama, H., Maeshima, Y., & Makino, H. (2005). Establishment and characterization of renal progenitor like cells from S3 segment of nephron in rat adult kidney. FASEB journal : official publication of the

Federation of American Societies for Experimental Biology, 19(13), 1789-1797.

Kornel, L., Nelson, W. A., Manisundaram, B., Chigurupati, R., & Hayashi, T. (1993). Mechanism of the effects of glucocorticoids and mineralocorticoids on vascular smooth muscle contractility. Steroids, 58(12), 580-587.

Kumar, R., Volk, D. E., Li, J., Lee, J. C., Gorenstein, D. G., & Thompson, E. B. (2004). TATA box binding protein induces structure in the recombinant glucocorticoid receptor AF1 domain. Proc Natl Acad Sci U S A, 101(47), 16425-16430.

Kuppe, C., Ibrahim, M. M., Kranz, J., Zhang, X., Ziegler, S., Perales-Patón, J., . . . Kramann, R. (2021). Decoding myofibroblast origins in human kidney fibrosis. Nature, 589(7841), 281-286.

Kuppe, C., van Roeyen, C., Leuchtle, K., Kabgani, N., Vogt, M., Van Zandvoort, M., . . . Moeller, M. J. (2017). Investigations of Glucocorticoid Action in GN. Journal of the American Society of Nephrology : JASN, 28(5), 1408-1420.

Kusaba, T., & Humphreys, B. D. (2014). Controversies on the origin of proliferating epithelial cells after kidney injury. Pediatric nephrology (Berlin, Germany), 29(4), 673-679.

Kusaba, T., Lalli, M., Kramann, R., Kobayashi, A., & Humphreys, B. D. (2014). Differentiated kidney epithelial cells repair injured proximal tubule. Proc Natl Acad Sci U S A, 111(4), 1527-1532.

Lan, R., Geng, H., Polichnowski, A. J., Singha, P. K., Saikumar, P., McEwen, D. G., . . . Venkatachalam, M. A. (2012). PTEN loss defines a TGF-β-induced tubule phenotype of failed differentiation and JNK signaling during renal fibrosis. Am J Physiol Renal Physiol, 302(9), F1210-1223.

Lan, R., Geng, H., Singha, P. K., Saikumar, P., Bottinger, E. P., Weinberg, J. M., & Venkatachalam, M. A. (2016). Mitochondrial Pathology and Glycolytic Shift during Proximal Tubule Atrophy after Ischemic AKI. Journal of the American Society of Nephrology : JASN, 27(11), 3356-3367.

Lasa, M., Abraham, S. M., Boucheron, C., Saklatvala, J., & Clark, A. R. (2002). Dexamethasone causes sustained expression of mitogen-activated protein kinase (MAPK) phosphatase 1 and phosphatase-mediated inhibition of MAPK p38. Mol Cell Biol, 22(22), 7802-7811.

Lazzeri, E., Angelotti, M. L., Peired, A., Conte, C., Marschner, J. A., Maggi, L., . . . Romagnani, P. (2018). Endocycle-related tubular cell hypertrophy and progenitor proliferation recover renal function after acute kidney injury. Nat Commun, 9(1), 1344.

Legouis, D., Ricksten, S. E., Faivre, A., Verissimo, T., Gariani, K., Verney, C., . . . de Seigneux, S. (2020). Altered proximal tubular cell glucose metabolism during acute kidney injury is associated with mortality. Nat Metab, 2(8), 732-743.

Lesovaya, E., Agarwal, S., Readhead, B., Vinokour, E., Baida, G., Bhalla, P., . . . Budunova, I. (2018). Rapamycin Modulates Glucocorticoid Receptor Function, Blocks Atrophogene REDD1, and Protects Skin from Steroid Atrophy. J Invest Dermatol, 138(9), 1935-1944.

Li, Y., Yang, J., Luo, J. H., Dedhar, S., & Liu, Y. (2007). Tubular epithelial cell dedifferentiation is driven by the helix-loop-helix transcriptional inhibitor Id1. Journal of the American Society of Nephrology : JASN, 18(2), 449-460.

Liggins, G. C., & Howie, R. N. (1972). A controlled trial of antepartum glucocorticoid treatment for prevention of the respiratory distress syndrome in premature infants. Pediatrics, 50(4), 515-525.

Little, M. H., & Bertram, J. F. (2009). Is there such a thing as a renal stem cell? Journal of the American Society of Nephrology : JASN, 20(10), 2112-2117.

Little, M. H., & Kairath, P. (2017). Does Renal Repair Recapitulate Kidney Development?

Journal of the American Society of Nephrology : JASN, 28(1), 34-46.

Liu, Y., Cousin, J. M., Hughes, J., Van Damme, J., Seckl, J. R., Haslett, C., . . . Rossi, A. G. (1999). Glucocorticoids Promote Nonphlogistic Phagocytosis of Apoptotic Leukocytes. The Journal of Immunology, 162(6), 3639-3646.

Lombardi, D., Becherucci, F., & Romagnani, P. (2016). How much can the tubule regenerate and who does it? An open question. Nephrol Dial Transplant, 31(8), 1243-1250.

Lyons, C. A., & Garite, T. J. (2002). Corticosteroids and fetal pulmonary maturity. Clin Obstet Gynecol, 45(1), 35-41.

MacArthur, B. A., Howie, R. N., Dezoete, J. A., & Elkins, J. (1981). Cognitive and psychosocial development of 4-year-old children whose mothers were treated antenatally with betamethasone. Pediatrics, 68(5), 638-643.

MacArthur, B. A., Howie, R. N., Dezoete, J. A., & Elkins, J. (1982). School progress and cognitive development of 6-year-old children whose mothers were treated antenatally with betamethasone. Pediatrics, 70(1), 99-105.

Maeshima, A., Sakurai, H., & Nigam, S. K. (2006). Adult kidney tubular cell population showing phenotypic plasticity, tubulogenic capacity, and integration capability into developing kidney. Journal of the American Society of Nephrology : JASN, 17(1), 188-198.

Maeshima, A., Yamashita, S., & Nojima, Y. (2003). Identification of renal progenitor-like tubular cells that participate in the regeneration processes of the kidney. Journal of the American Society of Nephrology : JASN, 14(12), 3138-3146.

Manwani, N., Gagnon, S., Post, M., Joza, S., Muglia, L., Cornejo, S., . . . Sweezey, N. B. (2010). Reduced viability of mice with lung epithelial-specific knockout of glucocorticoid receptor. Am J Respir Cell Mol Biol, 43(5), 599-606.

Martínez-Reyes, I., & Chandel, N. S. (2020). Mitochondrial TCA cycle metabolites control physiology and disease. Nat Commun, 11(1), 102.

Martinez, F. O., Sica, A., Mantovani, A., & Locati, M. (2008). Macrophage activation and polarization. Frontiers in bioscience : a journal and virtual library, 13, 453-461. doi:10.2741/2692

Matthews, S. G. (2000). Antenatal glucocorticoids and programming of the developing CNS. Pediatr Res, 47(3), 291-300.

McCampbell, K. K., & Wingert, R. A. (2012). Renal stem cells: fact or science fiction? Biochem J, 444(2), 153-168.

McCarton, C. M., Wallace, I. F., Divon, M., & Vaughan, H. G., Jr. (1996). Cognitive and neurologic development of the premature, small for gestational age infant through age 6: comparison by birth weight and gestational age. Pediatrics, 98(6 Pt 1), 1167-1178.

Mcmaster, A., & Ray, D. W. (2008). Drug Insight: selective agonists and antagonists of the glucocorticoid receptor. Nature Clinical Practice Endocrinology & Metabolism, 4(2), 91-101.

Mittelstadt, P. R., Monteiro, J. P., & Ashwell, J. D. (2012). Thymocyte responsiveness to endogenous glucocorticoids is required for immunological fitness. J Clin Invest, 122(7), 2384-2394.

Miyata, T., Minai, Y., & Haga, M. (2008). Impaired growth of small intestinal epithelium by adrenalectomy in weaning rats. Acta Histochem Cytochem, 41(4), 83-88.

Molitoris, B. A., Hoilien, C. A., Dahl, R., Ahnen, D. J., Wilson, P. D., & Kim, J. (1988). Characterization of ischemia-induced loss of epithelial polarity. J Membr Biol, 106(3), 233-242.

Mulholland, D. J., Dedhar, S., Coetzee, G. A., & Nelson, C. C. (2005). Interaction of nuclear receptors with the Wnt/beta-catenin/Tcf signaling axis: Wnt you like to know? Endocr Rev,

26(7), 898-915.

Nakajima, M., Inoue, T., Kato, H., & Nangaku, M. (2015). Pseudo-acute kidney injury secondary to intravenous dexamethasone. Am J Kidney Dis, 65(2), 344.

Nelson, W. J., & Nusse, R. (2004). Convergence of Wnt, beta-catenin, and cadherin pathways. Science, 303(5663), 1483-1487.

Nicolaides, N. C., Chrousos, G., & Kino, T. (2000). Glucocorticoid Receptor. In K. R. Feingold, B. Anawalt, A. Boyce, G. Chrousos, W. W. de Herder, K. Dhatariya, K. Dungan, J. M. Hershman, J. Hofland, S. Kalra, G. Kaltsas, C. Koch, P. Kopp, M. Korbonits, C. S. Kovacs, W. Kuohung, B. Laferrère, M. Levy, E. A. McGee, R. McLachlan, J. E. Morley, M. New, J. Purnell, R. Sahay, F. Singer, M. A. Sperling, C. A. Stratakis, D. L. Trence & D. P. Wilson (Eds.), Endotext. South Dartmouth (MA): MDText.com, Inc.

Copyright © 2000-2021, MDText.com, Inc.

Oakley, R. H., & Cidlowski, J. A. (2013). The biology of the glucocorticoid receptor: new signaling mechanisms in health and disease. J Allergy Clin Immunol, 132(5), 1033-1044.

Oakley, R. H., Cruz-Topete, D., He, B., Foley, J. F., Myers, P. H., Xu, X., . . . Cidlowski, J. A. (2019). Cardiomyocyte glucocorticoid and mineralocorticoid receptors directly and antagonistically regulate heart disease in mice. Science signaling, 12(577). doi:10.1126/scisignal.aau9685

Oakley, R. H., Ren, R., Cruz-Topete, D., Bird, G. S., Myers, P. H., Boyle, M. C., . . . Cidlowski, J. A. (2013). Essential role of stress hormone signaling in cardiomyocytes for the prevention of heart disease. Proceedings of the National Academy of Sciences, 110(42), 17035-17040.

Oakley, R. H., Sar, M., & Cidlowski, J. A. (1996). The Human Glucocorticoid Receptor Isoform EXPRESSION, BIOCHEMICAL PROPERTIES, AND PUTATIVE FUNCTION. Journal of Biological Chemistry, 271(16), 9550.

Oppong, E., Flink, N., & Cato, A. C. B. (2013). Molecular mechanisms of glucocorticoid action in mast cells. Molecular and Cellular Endocrinology, 380(1), 119-126.

Ormos, J., Elemér, G., & Csapó, Z. (1973). Ultrastructure of the proximal convoluted tubules during repair following hormonally induced necrosis in rat kidney. Virchows Arch B Cell Pathol, 13(1), 1-13.

Ortí, E., Hu, L. M., & Munck, A. (1993). Kinetics of glucocorticoid receptor phosphorylation in intact cells. Evidence for hormone-induced hyperphosphorylation after activation and recycling of hyperphosphorylated receptors. J Biol Chem, 268(11), 7779-7784.

Pácha, J., Vagnerová, R., & Bryndová, J. (2003). Carbenoxolone accelerates maturation of rat intestine. Pediatr Res, 53(5), 808-813.

Patel, R., Williams-Dautovich, J., & Cummins, C. L. (2014). Minireview: new molecular mediators of glucocorticoid receptor activity in metabolic tissues. Mol Endocrinol, 28(7), 999-1011.

Patrick, G. (2013). History of Cortisone and Related Compounds: John Wiley & Sons Ltd.

PERRETTI, M., & AHLUWALIA, A. (2000). The Microcirculation and Inflammation: Site of Action for Glucocorticoids. Microcirculation, 7(3), 147-161.

Perretti, M., Chiang, N., La, M., Fierro, I. M., Marullo, S., Getting, S. J., . . . Serhan, C. N. (2002). Endogenous lipid- and peptide-derived anti-inflammatory pathways generated with glucocorticoid and aspirin treatment activate the lipoxin A4 receptor. Nature Medicine, 8(11), 1296-1302.

Perretti, M., & Flower, R. J. (2004). Annexin 1 and the biology of the neutrophil. Journal of Leukocyte Biology, 76(1), 25-29.

Picard, D., Khursheed, B., Garabedian, M. J., Fortin, M. G., Lindquist, S., & Yamamoto, K.

R. (1990). Reduced levels of hsp90 compromise steroid receptor action in vivo. Nature, 348(6297), 166-168.

Piepenhagen, P. A., Peters, L. L., Lux, S. E., & Nelson, W. J. (1995). Differential expression of Na(+)-K(+)-ATPase, ankyrin, fodrin, and E-cadherin along the kidney nephron. Am J Physiol, 269(6 Pt 1), C1417-1432.

Provencher, P. H., Saltis, J., & Funder, J. W. (1995). Glucocorticoids but not mineralocorticoids modulate endothelin-1 and angiotensin II binding in SHR vascular smooth muscle cells. The Journal of steroid biochemistry and molecular biology, 52(3), 219-225.

Psarra, A. M., & Sekeris, C. E. (2011). Glucocorticoids induce mitochondrial gene transcription in HepG2 cells: role of the mitochondrial glucocorticoid receptor. Biochim Biophys Acta, 1813(10), 1814-1821.

Quaroni, A., Tian, J. Q., Göke, M., & Podolsky, D. K. (1999). Glucocorticoids have pleiotropic effects on small intestinal crypt cells. Am J Physiol, 277(5), G1027-1040.

Quatrini, L., & Ugolini, S. (2021). New insights into the cell- and tissue-specificity of glucocorticoid actions. Cell Mol Immunol, 18(2), 269-278.

Quax, R. A., Manenschijn, L., Koper, J. W., Hazes, J. M., Lamberts, S. W. J., van Rossum, E. F. C., & Feelders, R. A. (2013). Glucocorticoid sensitivity in health and disease. Nature Reviews Endocrinology, 9(11), 670-686.

Rayburn, W. F., Christensen, H. D., & Gonzalez, C. L. (1997). A placebo-controlled comparison between betamethasone and dexamethasone for fetal maturation: differences in neurobehavioral development of mice offspring. Am J Obstet Gynecol, 176(4), 842-850; discussion 850-841.

Reul, J. M., & de Kloet, E. R. (1985). Two receptor systems for corticosterone in rat brain: microdistribution and differential occupation. Endocrinology, 117(6), 2505-2511.

Reule, S., & Gupta, S. (2011). Kidney regeneration and resident stem cells. Organogenesis, 7(2), 135-139.

Richardson, R. V., Rog-Zielinska, E. A., Thomson, A. J. W., Moran, C. M., Kenyon, C. J., Gray, G. A., & Chapman, K. E. (2014). Pathological cardiac remodeling caused by cardiomyocyte/vascular smooth muscle glucocorticoid receptor deficiency. Cardiovascular Research, 103.

Ridder, S., Chourbaji, S., Hellweg, R., Urani, A., Zacher, C., Schmid, W., . . . Gass, P. (2005). Mice with genetically altered glucocorticoid receptor expression show altered sensitivity for stress-induced depressive reactions. J Neurosci, 25(26), 6243-6250.

Rog-Zielinska, E. A., Craig, M. A., Manning, J. R., Richardson, R. V., Gowans, G. J., Dunbar, D. R., . . . Chapman, K. E. (2015). Glucocorticoids promote structural and functional maturation of foetal cardiomyocytes: a role for PGC-1α. Cell Death & Differentiation, 22(7), 1106-1116.

Rog-Zielinska, E. A., Thomson, A., Kenyon, C. J., Brownstein, D. G., Moran, C. M., Szumska, D., . . . Chapman, K. E. (2013). Glucocorticoid receptor is required for foetal heart maturation. Human Molecular Genetics, 22(16), 3269-3282.

Romero, I. A., Radewicz, K., Jubin, E., Michel, C. C., Greenwood, J., Couraud, P. O., & Adamson, P. (2003). Changes in cytoskeletal and tight junctional proteins correlate with decreased permeability induced by dexamethasone in cultured rat brain endothelial cells. Neurosci Lett, 344(2), 112-116.

Rompolas, P., Mesa, K. R., & Greco, V. (2013). Spatial organization within a niche as a determinant of stem-cell fate. Nature, 502(7472), 513-518.

Sainte-Marie, Y., Nguyen Dinh Cat, A., Perrier, R., Mangin, L., Soukaseum, C., Peuchmaur, M., . . . Jaisser, F. (2007). Conditional glucocorticoid receptor expression in

the heart induces atrio-ventricular block. FASEB journal : official publication of the Federation of American Societies for Experimental Biology, 21(12), 3133-3141.

Salokorpi, T., Sajaniemi, N., Hällback, H., Kari, A., Rita, H., & von Wendt, L. (1997). Randomized study of the effect of antenatal dexamethasone on growth and development of premature children at the corrected age of 2 years. Acta Paediatr, 86(3), 294-298.

Sato, A., Suzuki, H., Nakazato, Y., Shibata, H., Inagami, T., & Saruta, T. (1994). Increased expression of vascular angiotensin II type 1A receptor gene in glucocorticoid-induced hypertension. Journal of hypertension, 12(5), 511-516.

Saxton, R. A., & Sabatini, D. M. (2017). mTOR Signaling in Growth, Metabolism, and Disease. Cell, 169(2), 361-371.

Scheinman, R. I., Cogswell, P. C., Lofquist, A. K., & Baldwin, A. S. (1995). Role of Transcriptional Activation of IκBα in Mediation of Immunosuppression by Glucocorticoids. Science, 270(5234), 283-286.

Schutgens, F., Rookmaaker, M. B., Margaritis, T., Rios, A., Ammerlaan, C., Jansen, J., . . . Heitzer, E. (2019). Tubuloids derived from human adult kidney and urine for personalized disease modeling. Nat Biotechnol, 37(3), 303-313.

Semenza, G. L. (2011). Regulation of metabolism by hypoxia-inducible factor 1. Cold Spring Harb Symp Quant Biol, 76, 347-353.

Semenza, G. L., Roth, P. H., Fang, H. M., & Wang, G. L. (1994). Transcriptional regulation of genes encoding glycolytic enzymes by hypoxia-inducible factor 1. J Biol Chem, 269(38), 23757-23763.

Serhan, C. N., & Savill, J. (2005). Resolution of inflammation: the beginning programs the end. Nature Immunology, 6(12), 1191-1197.

Shah, O. J., Wang, Z., & Hunter, T. (2004). Inappropriate activation of the TSC/Rheb/mTOR/S6K cassette induces IRS1/2 depletion, insulin resistance, and cell survival deficiencies. Curr Biol, 14(18), 1650-1656.

Shipp, L. E., Lee, J. V., Yu, C. Y., Pufall, M., Zhang, P., Scott, D. K., & Wang, J. C. (2010). Transcriptional regulation of human dual specificity protein phosphatase 1 (DUSP1) gene by glucocorticoids. PloS one, 5(10), e13754.

Smeets, B., Boor, P., Dijkman, H., Sharma, S. V., Jirak, P., Mooren, F., . . . Moeller, M. J. (2013). Proximal tubular cells contain a phenotypically distinct, scattered cell population involved in tubular regeneration. J Pathol, 229(5), 645-659.

Smith, J. A., Stallons, L. J., & Schnellmann, R. G. (2014). Renal cortical hexokinase and pentose phosphate pathway activation through the EGFR/Akt signaling pathway in endotoxin-induced acute kidney injury. Am J Physiol Renal Physiol, 307(4), F435-444.

Smolders-de Haas, H., Neuvel, J., Schmand, B., Treffers, P. E., Koppe, J. G., & Hoeks, J. (1990). Physical development and medical history of children who were treated antenatally with corticosteroids to prevent respiratory distress syndrome: a 10- to 12-year follow-up. Pediatrics, 86(1), 65-70.

Solez, K., Morel-Maroger, L., & Sraer, J. D. (1979). The morphology of "acute tubular necrosis" in man: analysis of 57 renal biopsies and a comparison with the glycerol model. Medicine (Baltimore), 58(5), 362-376.

Sprangers, J., Zaalberg, I. C., & Maurice, M. M. (2021). Organoid-based modeling of intestinal development, regeneration, and repair. Cell Death Differ, 28(1), 95-107.

Srivastava, S. P., Zhou, H., Setia, O., Liu, B., Kanasaki, K., Koya, D., . . . Goodwin, J. (2021). Loss of endothelial glucocorticoid receptor accelerates diabetic nephropathy. Nat Commun, 12(1), 2368.

Stange, D. E., Koo, B. K., Huch, M., Sibbel, G., Basak, O., Lyubimova, A., . . . Clevers, H. (2013). Differentiated Troy+ chief cells act as reserve stem cells to generate all lineages of

the stomach epithelium. Cell, 155(2), 357-368.

Stewart, P. M., & Krozowski, Z. S. (1999). 11 beta-Hydroxysteroid dehydrogenase. Vitam Horm, 57, 249-324.

Stoloff, S. W., & Kelly, H. W. (2011). Updates on the use of inhaled corticosteroids in asthma. Curr Opin Allergy Clin Immunol, 11(4), 337-344.

Takayama, S., Rogatsky, I., Schwarcz, L. E., & Darimont, B. D. (2006). The glucocorticoid receptor represses cyclin D1 by targeting the Tcf-beta-catenin complex. J Biol Chem, 281(26), 17856-17863.

Talabér, G., Jondal, M., & Okret, S. (2013). Extra-adrenal glucocorticoid synthesis: immune regulation and aspects on local organ homeostasis. Mol Cell Endocrinol, 380(1-2), 89-98.

Tata, P. R., Mou, H., Pardo-Saganta, A., Zhao, R., Prabhu, M., Law, B. M., . . . Rajagopal, J. (2013). Dedifferentiation of committed epithelial cells into stem cells in vivo. Nature, 503(7475), 218-223.

Tata, P. R., & Rajagopal, J. (2016). Cellular plasticity: 1712 to the present day. Curr Opin Cell Biol, 43, 46-54.

Tetsu, O., & McCormick, F. (1999). Beta-catenin regulates expression of cyclin D1 in colon carcinoma cells. Nature, 398(6726), 422-426.

Tran, F. H., & Zheng, J. J. (2017). Modulating the wnt signaling pathway with small molecules. Protein Sci, 26(4), 650-661.

Trefely, S., & Wellen, K. E. (2018). Metabolite regulates differentiation. Science, 360(6389), 603-604.

Tsugita, M., Iwasaki, Y., Nishiyama, M., Taguchi, T., Shinahara, M., Taniguchi, Y., . . . Hashimoto, K. (2008). Differential regulation of 11β-hydroxysteroid dehydrogenase type-1 and -2 gene transcription by proinflammatory cytokines in vascular smooth muscle cells. Life Sciences, 83(11), 426-432.

Uno, H., Lohmiller, L., Thieme, C., Kemnitz, J. W., Engle, M. J., Roecker, E. B., & Farrell, P. M. (1990). Brain damage induced by prenatal exposure to dexamethasone in fetal rhesus macaques. I. Hippocampus. Brain Res Dev Brain Res, 53(2), 157-167.

van Es, J. H., Sato, T., van de Wetering, M., Lyubimova, A., Yee Nee, A. N., Gregorieff, A., . . . Clevers, H. (2012). Dll1+ secretory progenitor cells revert to stem cells upon crypt damage. Nat Cell Biol, 14(10), 1099-1104.

Vandevyver, S., Dejager, L., & Libert, C. (2014). Comprehensive overview of the structure and regulation of the glucocorticoid receptor. Endocr Rev, 35(4), 671-693.

Venkatachalam, M. A., Bernard, D. B., Donohoe, J. F., & Levinsky, N. G. (1978). Ischemic damage and repair in the rat proximal tubule: differences among the S1, S2, and S3 segments. Kidney Int, 14(1), 31-49.

Vielkind, U., Walencewicz, A., Levine, J. M., & Bohn, M. C. (1990). Type II glucocorticoid receptors are expressed in oligodendrocytes and astrocytes. J Neurosci Res, 27(3), 360-373.

Vogetseder, A., Karadeniz, A., Kaissling, B., & Le Hir, M. (2005). Tubular cell proliferation in the healthy rat kidney. Histochem Cell Biol, 124(2), 97-104.

Vogetseder, A., Picard, N., Gaspert, A., Walch, M., Kaissling, B., & Le Hir, M. (2008). Proliferation capacity of the renal proximal tubule involves the bulk of differentiated epithelial cells. Am J Physiol Cell Physiol, 294(1), C22-28.

Wärnmark, A., Gustafsson, J. A., & Wright, A. P. (2000). Architectural principles for the structure and function of the glucocorticoid receptor tau 1 core activation domain. J Biol Chem, 275(20), 15014-15018.

Wüst, S., van den Brandt, J., Tischner, D., Kleiman, A., Tuckermann, J. P., Gold, R., . . .

Reichardt, H. M. (2008). Peripheral T Cells Are the Therapeutic Targets of Glucocorticoids in Experimental Autoimmune Encephalomyelitis. The Journal of Immunology, 180(12), 8434-8443.

Wang, Q., Joels, M., Swaab, D. F., & Lucassen, P. J. (2012). Hippocampal GR expression is increased in elderly depressed females. Neuropharmacology, 62(1), 527-533.

Warburg, O. (1956). On the origin of cancer cells. Science, 123(3191), 309-314.

Warburg, O., Wind, F., & Negelein, E. (1927). THE METABOLISM OF TUMORS IN THE BODY. J Gen Physiol, 8(6), 519-530.

Webster, J. C., Oakley, R. H., Jewell, C. M., & Cidlowski, J. A. (2001). Proinflammatory cytokines regulate human glucocorticoid receptor gene expression and lead to the accumulation of the dominant negative beta isoform: a mechanism for the generation of glucocorticoid resistance. Proc Natl Acad Sci U S A, 98(12), 6865-6870.

Wei, Q., Hebda-Bauer, E. K., Pletsch, A., Luo, J., Hoversten, M. T., Osetek, A. J., . . . Akil, H. (2007). Overexpressing the Glucocorticoid Receptor in Forebrain Causes an Aging-Like Neuroendocrine Phenotype and Mild Cognitive Dysfunction. The Journal of Neuroscience, 27(33), 8836-8844.

Weichhart, T., Haidinger, M., Katholnig, K., Kopecky, C., Poglitsch, M., Lassnig, C., . . . Säemann, M. D. (2011). Inhibition of mTOR blocks the anti-inflammatory effects of glucocorticoids in myeloid immune cells. Blood, 117(16), 4273-4283.

Weikum, E. R., Knuesel, M. T., Ortlund, E. A., & Yamamoto, K. R. (2017). Glucocorticoid receptor control of transcription: precision and plasticity via allostery. Nat Rev Mol Cell Biol, 18(3), 159-174.

Weinberg, J. M. (2011). Mitochondrial biogenesis in kidney disease. Journal of the American Society of Nephrology : JASN, 22(3), 431-436.

Weinberg, J. M., & Molitoris, B. A. (2009). Illuminating mitochondrial function and dysfunction using multiphoton technology. Journal of the American Society of Nephrology : JASN, 20(6), 1164-1166.

Wepler, M., Preuss, J. M., Merz, T., McCook, O., Radermacher, P., Tuckermann, J. P., & Vettorazzi, S. (2020). Impact of downstream effects of glucocorticoid receptor dysfunction on organ function in critical illness-associated systemic inflammation. Intensive Care Med Exp, 8(Suppl 1), 37.

Westendorf, J. J., Kahler, R. A., & Schroeder, T. M. (2004). Wnt signaling in osteoblasts and bone diseases. Gene, 341, 19-39.

White, B. D., Chien, A. J., & Dawson, D. W. (2012). Dysregulation of Wnt/β-catenin signaling in gastrointestinal cancers. Gastroenterology, 142(2), 219-232.

Wild, G. E., Waschke, K. A., Bitton, A., & Thomson, A. B. (2003). The mechanisms of prednisone inhibition of inflammation in Crohn's disease involve changes in intestinal permeability, mucosal TNFalpha production and nuclear factor kappa B expression. Aliment Pharmacol Ther, 18(3), 309-317.

Wilflingseder, J., Willi, M., Lee, H. K., Olauson, H., Jankowski, J., Ichimura, T., . . . Bonventre, J. V. (2020). Enhancer and super-enhancer dynamics in repair after ischemic acute kidney injury. Nat Commun, 11(1), 3383.

Witzgall, R., Brown, D., Schwarz, C., & Bonventre, J. V. (1994). Localization of proliferating cell nuclear antigen, vimentin, c-Fos, and clusterin in the postischemic kidney. Evidence for a heterogenous genetic response among nephron segments, and a large pool of mitotically active and dedifferentiated cells. J Clin Invest, 93(5), 2175-2188.

Wong, V., Ching, D., McCrea, P. D., & Firestone, G. L. (1999). Glucocorticoid down-regulation of fascin protein expression is required for the steroid-induced formation of tight junctions and cell-cell interactions in rat mammary epithelial tumor cells. J Biol Chem,

274(9), 5443-5453.

Xiong, F., Lin, T., Song, M., Ma, Q., Martinez, S. R., Lv, J., . . . Zhang, L. (2016). Antenatal hypoxia induces epigenetic repression of glucocorticoid receptor and promotes ischemic-sensitive phenotype in the developing heart. Journal of molecular and cellular cardiology, 91, 160-171.

Xu, C., Sun, M., Zhang, X., Xu, Z., Miyamoto, H., & Zheng, Y. (2020). Activation of Glucocorticoid Receptor Inhibits the Stem-Like Properties of Bladder Cancer via Inactivating the β-Catenin Pathway. Front Oncol, 10, 1332.

Xu, Z., Robitaille, A. M., Berndt, J. D., Davidson, K. C., Fischer, K. A., Mathieu, J., . . . Moon, R. T. (2016). Wnt/β-catenin signaling promotes self-renewal and inhibits the primed state transition in naïve human embryonic stem cells. Proc Natl Acad Sci U S A, 113(42), E6382-e6390.

Yang, L., Guerrero, J., Hong, H., DeFranco, D. B., & Stallcup, M. R. (2000). Interaction of the tau2 transcriptional activation domain of glucocorticoid receptor with a novel steroid receptor coactivator, Hic-5, which localizes to both focal adhesions and the nuclear matrix. Mol Biol Cell, 11(6), 2007-2018.

Yang, S., & Zhang, L. (2004). Glucocorticoids and vascular reactivity. Current vascular pharmacology, 2(1), 1-12.

Zager, R. A., & Burkhart, K. (1997). Myoglobin toxicity in proximal human kidney cells: roles of Fe, Ca2+, H2O2, and terminal mitochondrial electron transport. Kidney Int, 51(3), 728-738.

Zager, R. A., & Foerder, C. A. (1992). Effects of inorganic iron and myoglobin on in vitro proximal tubular lipid peroxidation and cytotoxicity. J Clin Invest, 89(3), 989-995.

Zager, R. A., & Johnson, A. C. M. (2019). Acute kidney injury induces dramatic p21 upregulation via a novel, glucocorticoid-activated, pathway. Am J Physiol Renal Physiol, 316(4), F674-f681.

Zettl, K. S., Sjaastad, M. D., Riskin, P. M., Parry, G., Machen, T. E., & Firestone, G. L. (1992). Glucocorticoid-induced formation of tight junctions in mouse mammary epithelial cells in vitro. Proc Natl Acad Sci U S A, 89(19), 9069-9073.

Zhan, T., Rindtorff, N., & Boutros, M. (2017). Wnt signaling in cancer. Oncogene, 36(11), 1461-1473.

Zhou, H., Cooper, M. S., & Seibel, M. J. (2013). Endogenous Glucocorticoids and Bone. Bone Res, 1(2), 107-119.

Zhou, R., Yazdi, A. S., Menu, P., & Tschopp, J. (2011). A role for mitochondria in NLRP3 inflammasome activation. Nature, 469(7329), 221-225.

9 SUMMARY

Acute kidney injury (AKI) is a very frequent and challenging clinical problem associated with high morbidity and mortality, and can be triggered e.g. by hypoxic or toxic damage of the kidney. Other than dialysis, there is currently no therapeutic intervention to improve the survival of AKI patients. Therefore, there is an urgent medical need to identify novel therapeutic approaches for the treatment of AKI. In contrast to other epithelial organs such as the intestine or skin, the kidney lacks a functionally relevant stem cell compartment. Therefore, kidney repair after damage depends on surviving renal tubular epithelial cells (rTECs), which dedifferentiate, proliferate, replace lost cells, and finally re-differentiate to become mitotically quiescent again. This property of epithelial cells to tune their differentiation state is known as “cellular plasticity”. A targeted modulation of cellular plasticity could open new therapeutic avenues for AKI. However, the molecular mechanisms underlying cellular plasticity in the kidney have remained elusive.

The glucocorticoid receptor (GR) is an almost ubiquitously expressed receptor for cortisol and other glucocorticoids (GCs). Upon ligand binding, the GR translocates to the nucleus, where it acts as a transcription factor to regulate the expression of genes controlling immune responses and metabolism. Due to their immunosuppressive functions, GCs are frequently administered as a treatment of AKI. However, the direct effects of GCs on rTECs are largely unclear. In particular, it is unknown whether activation of the GR by GCs plays a role in cellular plasticity of the kidney tubular epithelium.

The elucidation of the molecular mechansisms controlling plasticity of rTECs has been hampered by the lack of biologically revelant in vitro systems amenable to experimental manipulation. Therefore, in this thesis, three-dimensional kidney organoids, so-called tubuloids, were generated from primary kidney tissue of mice and humans, and tested for their potential to serve as a model system for AKI-induced cellular plasticity. Indeed, following hypoxic or toxic damage, renal tubuloids underwent a dedifferentiation-redifferentiation sequence with characteristic morphological and molecular changes. This novel organoid model system was then employed to assess the significance of the GR for cellular plasticity. Pharmacological experiments showed that an activation of the GR by dexamethasone significantly delayed the dedifferentiation-redifferentiation sequence and aggravated cellular injury, while genetic inactivation of the GR rendered kidney organoids more resistant to stress. Mechanistically, this thesis provides evidence that GR signaling inhibits epithelial plasticity by suppressing the Wnt/β-catenin and mTOR pathways as well as cellular energy production.

In summary, the results of this thesis establish kidney organoids as a model system to

study cellular plasticity of the renal tubular epithelium. Moreover, the data of this thesis identify the glucocorticoid receptor as a central negative regulator of injury-induced plasticity of rTECs.

10 ZUSAMMENFASSUNG

Das akute Nierenversagen (acute kidney injury, AKI) ist eine sehr häufige klinische Problematik, die z.B. durch eine hypoxische oder toxische Nierenschädigung induziert werden kann, und die mit hoher Morbidität und Mortalität assoziiert ist. Außer der Dialyse gibt es derzeit keine therapeutische Intervention, um das Überleben der Patientinnen und Patienten zu verbessern. Es besteht daher der dringende Bedarf für neue Therapieansätze zur Behandlung des akuten Nierenversagens. Im Gegensatz zu anderen epithelialen Organen wie dem Darm oder der Haut fehlt der Niere ein funktionell relevantes Stammzellkompartiment. Daher hängt die Reparatur der Niere nach einer Schädigung von überlebenden renalen Tubulusepithelzellen ab, die dedifferenzieren, proliferieren, untergegangene Zellen ersetzen und sich schließlich wieder re-differenzieren. Diese Eigenschaft von Epithelzellen, ihren Differenzierungszustand verändern zu können, wird als „zelluläre Plastizität“ bezeichnet. Eine gezielte Modulation der zellulären Plastizität könnte neue therapeutische Ansätze beim akuten Nierenversagen eröffnen. Die molekularen Mechanismen, die der zellulären Plastizität in der Niere zugrunde liegen, sind bisher jedoch unklar.

Der Glukokortikoid-Rezeptor (GR) ist ein nahezu ubiquitär exprimierter Rezeptor für Cortisol und andere Glukokortikoide. Nach der Bindung eines Liganden transloziert der GR in den Zellkern, wo er als Transkriptionsfaktor wirkt, und die Expression von Genen reguliert, die Immunantworten und den Stoffwechsel kontrollieren. Aufgrund ihrer immunsuppressiven Funktion werden Glukokortikoide häufig zur Behandlung des akuten Nierenversages verabreicht. Die direkten Wirkungen von Glukokortikoiden auf renale Tubulusepithelzellen sind allerdings weitgehend unerforscht. Insbesondere ist nicht bekannt, ob die Aktivierung des GR durch Glukokortikoide eine Rolle bei der zellulären Plastizität der Niere spielt.

Die Aufklärung der molekularen Mechanismen, die die Plastizität von renalen tubulären Epithelzellen kontrollieren, wurde bisher durch das Fehlen biologisch relevanter in vitro-Systeme behindert, die einer experimentellen Manipulation zugänglich sind. Daher wurden in dieser Dissertation dreidimensionale Nierenorganoide, sogenannte Tubuloide, aus primärem Nierengewebe von Mäusen und Menschen generiert und auf ihr Potenzial als Modellsystem für zelluläre Plastizität getestet. Tatsächlich durchliefen Nierentubuloide nach hypoxischem oder toxischem Schaden eine Dedifferenzierungs-Redifferenzierungs-Sequenz mit charakteristischen morphologischen und molekularen Veränderungen. Dieses neuartige Organoid-Modellsystem wurde dann verwendet, um die Bedeutung des GR für die zelluläre Plastizität zu untersuchen. Pharmakologische Experimente zeigten, dass eine Aktivierung des GR durch Dexamethason die Dedifferenzierungs-

Redifferenzierungs-Sequenz signifikant verzögerte und die Zellschädigung verschlimmerte, während die genetische Inaktivierung des GR die Nierenorganoide stressresistenter machte. Mechanistisch liefert diese Dissertation starke Hinweise darauf, dass der GR die epitheliale Plastizität hemmt, indem er den Wnt/β-Catenin- und mTOR-Signalweg sowie die zelluläre Energieproduktion inhibiert.

Die Ergebnisse dieser Dissertation etablieren Nierenorganoide als Modellsystem zur Untersuchung der zellulären Plastizität des renalen Tubulusepithels. Darüber hinaus identifiziert sie den Glukokortikoid-Rezeptor als einen zentralen negativen Regulator der Plastizität von renalen Tubulusepithelzellen.

11 CURRICULUM VITAE

PERSONAL INFORMATION

Name	Luping Zhou
GENDER	Female
DATE OF BIRTH	27.08.1991
NATIONALITY	P. R. China
E-MAIL	lupingzhou718@163.com; luping.zhou@uni-marburg.de

EDUCATION

12/2018-now	PhD student Institute of Pharmacology Marburg, Germany
09/2015-06/2018	Master Internal Medicine Clinical medicine department of the Southwest Medical University, Sichuan, China
09/2010-06/2015	Bachelor Clinical Medicine Clinical medicine department of the Sichuan Medical University, Sichuan, China

12 LEBENSLAUF

Name	Luping Zhou
Geburtsdatum/-ort	27.08.1991/Luzhou
Nationalität	Chinesisch
Familienstand	verheiratet
Adresse	Fuchspaß 36, No. 223, 35039 Marburg
Telefon	015259916336
Email	lupingzhou718@163.com; luping.zhou@uni-marburg.de

Studien- und Ausbildungsgang

12/2018-Jetzt	**Doktorandin** in der Abteilung Pharmakologie Marburg
09/2015-06/2018	**Master** in der Innere Medizin Medizinische Universität Südwestliche, Sichuan, China
09/2010-06/2015	**Bachelor** in Klinische Medizin medizinische Universität Sichuan, Sichuan, China

13 AKADEMISCHE LEHRER

Prof. Dr. Thomas Worzfeld

Prof. Dr. Hermann-Josef Gröne

14 ACKNOWLEDGEMENTS

I would like to express my gratitude to those who helped to accomplish this study.

First of all, I want to express my sincere gratitude and respect to my supervisor Prof. Dr. Thomas Worzfeld, who has spent a lot of time and energy reading, thinking and discussing with me. He always responded my emails rapidly and in time with a lot of useful papers, protocols, useful sugggestions and comments. Whenever I met problems in work or in life, he was always very enthusiastic and polite to help me. There is a chinese proverb: “Be a teacher for one day, and be a father for life”. It is my honor to have such a supervisor for all my life.

Secondly, I want to thank Prof. Dr. Hermann-Josef Gröne for giving me this chance to know Thomas and have the chance to do my PhD project in Marburg. Thank him for enormous trust and giving me this chance to follow up on the project on the GR in the kidney. Prof. Gröne and his group have done a lot of preliminary work which helped me to better understand the background of this project and focused on the mechanism with peace of mind. I also want to thank the wife of Prof. Gröne, Mrs. Elisabeth Gröne, who always cared about me warmly and comforted me like a mother.

Thirdly, thanks to my colleagues and technicians in the Institute of Pharmacology of Marburg University. Thanks to Dr. Mark Schmitt, who gave me a lot of suggestions and nice ideas about my project. Thanks to Chen Jiang, who was a good brother in my life and scientific research. Thanks to Dr. Carola Meyer, who managed all of the experimental mice well. Thanks to Andrea Wüstenhagen, who gave me a big support in organoid cultures and RNA isolations. Thanks to Olga Ebers, who helped me to do the stanining of the organoids. Thanks to Marga Losekam, Pascal Ochs and Fatma Aktuna, who were responsible for the mouse genotyoings. Thanks to Svenja Estor, who properly arranged the administration of the lab. Thanks to Dr. Yun Jiang and Dandan Zhao. Thanks to so many friends in the lab.

I also want to thank our collaborators from DKFZ. Without the support of them, the project would have gone so much harder.

Then, I want to express my sincere appreciation and love to my husband Tao He and my son Zhouyang He, who always gave me the most tender love and spiritual support through the whole project. Before going abroad, I thought that having a baby at home would make my families miss me less. Facts have proven that my son cannot be my substitute, but there was one more person who missed me and the person I missed. Because of the corona virus, I have not been back to China for 2 years. Thanks my husband Tao, who took good care of the families and do a good job of logistic support for me.

Last, but certainly not least, I have to thank my parents and the parents of my husband.

Thanks them for enormous trust, love and support.

15 Ehrenwörtliche Erklärung

Ich erkläre ehrenwörtlich, dass ich die dem Fachbereich Medizin Marburg zur Promotionsprüfung eingereichte Arbeit mit dem Titel:

The glucocorticoid receptor regulates epithelial plasticity in the kidney

am Pharmakologischen Institut von Prof. Dr. Thomas Worzfeld ohne sonstige Hilfe selbst durchgeführt und bei der Abfassung der Arbeit keine anderen als die in der Dissertation aufgeführten Hilfsmittel benutzt habe. Ich habe bisher an keinem in- oder ausländischen Medizinischen Fachbereich ein Gesuch um Zulassung zur Promotion eingereicht, noch die vorliegende oder eine andere Arbeit als Dissertation vorgelegt.

Ich versichere, dass ich sämtliche wörtlichen oder sinngemäßen Übernahmen und Zitate kenntlich gemacht habe.

Mit dem Einsatz von Software zur Erkennung von Plagiaten bin ich einverstanden.

Die vorliegende Arbeit wurde noch nicht veröffentlicht. Im Rahmen der Arbeit entstand folgende Co-Autorenschaft[*1]:

Chen Jiang, Ahsan Javed, Laura Kaiser, Michele M. Nava, Rui Xu, Dominique T. Brandt, Dandan Zhao, Benjamin Mayer, Javier Fernández-Baldovinos, **Luping Zhou**, Carsten Höß, Kovilen Sawmynaden, Arkadiusz Oleksy, David Matthews, Lee S. Weinstein, Heidi Hahn, Hermann-Josef Gröne, Peter L. Graumann, Carien M. Niessen, Stefan Offermanns, Sara A. Wickström & Thomas Worzfeld. Mechanochemical control of epidermal stem cell divisions by B-plexins. Nature Communications. (2021)12: 1308.

Ort, Datum, Unterschrift Doktorandin/Doktorand

„Die Hinweise zur Erkennung von Plagiaten habe ich zur Kenntnis genommen.“**[*2]**

Ort, Datum, Unterschrift Referentin/Referent

[*1] Hier sind Publikationen/Abstracts aufzuführen, die aus der Dissertation entstanden sind bzw. eingereicht oder angenommen wurden. Für jedes DIN A4 Exemplar ist eine Kopie beizufügen.

[*2] Die „Hinweise zur Erkennung von Plagiaten“ sind auf unserer Homepage hinterlegt.